Mathematical Modeling of Synaptic Transmission at Chemical Synapses

Philipp Blandfort

Master's Thesis
Supervised by Prof. Dr. Sven O. Krumke[1]
Co-supervised by Prof. Dr. Christina Surulescu[2]

AG Optimierung,
Technische Universität Kaiserslautern

2015

[1]AG Optimierung, Fachbereich Mathematik, TU Kaiserslautern
[2]Biomathematics Group, Fachbereich Mathematik, TU Kaiserslautern

Hiermit versichere ich an Eides statt, dass ich die vorliegende Masterarbeit selbstständig verfasst und keine anderen als die angegebenen Quellen und Hilfsmittel benutzt habe. Die Arbeit hat in gleicher oder ähnlicher Form noch keiner Prüfungsbehörde vorgelegen.

Philipp Blandfort
Kaiserslautern, 1. April 2015

Contents

Introduction

Synapses are connections between different nerve cells that form an essential link in neural signal transmission. It is generally distinguished between electrical and chemical synapses, where chemical synapses are more common in the human brain and are also the type we deal with in this work.

In chemical synapses, small container-like objects called *vesicles* fill with neurotransmitter and expel them from the cell during synaptic transmission. This process is vital for communication between neurons. However, to the best of our knowledge no mathematical models that actually take different filling states of the vesicles into account have been developed yet.[3]

In this thesis we propose a novel mathematical model for modeling synaptic transmission at chemical synapses that includes the description of vesicles of different filling states. This model was originally formulated by Prof. Dr. Surulescu and slightly modified by me. It consists of a transport equation (for the vesicle growth process) plus three ODEs and focuses on the presynapse and synaptic cleft.

The well-posedness is proved in detail for this PDE system. We also propose a few different variations and related models. In particular, an ODE system is derived and a DDE system is formulated. We then use nonlinear optimization methods for data fitting to test some of the models on data made available by the group of Prof. Dr. Eckhard Friauf, TU Kaiserslautern.

This thesis is written as self-contained as possible. So most mathematical statements are either proved in detail or can be found in the appendix. The appendix also includes abbreviations and the not so common notations that are used throughout this work. Also, some supplementary figures that could be valuable for further analysis of the models are provided.

The contents of this work are divided into 8 sections:

(1) First the biological background is covered. This includes details about synaptic transmission but also some basic knowledge of neuroscience and an outline of the modeling of the rest of neural signal transmission.

    This section is a bit more comprehensive to facilitate understanding of the experimental data we work with and to allow for catching a glimpse of the whole picture of neural signal processing. Also, for future work on this or related models it is clearly better to know a bit more than what is essential to understand the models.

    Most of the information in this section comes from [KSJ$^+$13], [GKNP14] or [PAF$^+$04] and virtually no biological knowledge is assumed. Prof. Dr. Surulescu and Alexander Fischer[4] both greatly contributed to this part by summarizing most relevant facts for me and providing me with additional specific literature.

(2) In the next section the main PDE model is introduced. The model is formulated, explained and implicit assumptions are briefly discussed. Also, we address some modeling details that are based on discussions I had with Prof. Dr. Surulescu.

(3) Then we prove the well-posedness (in the sense of Hadamard) of the main PDE model. So it is shown that under certain assumptions there exists a unique solution to the PDE system and that this solution depends continuously on the given data.

[3] For some existing models of synaptic transmission, see [BK08], [BK12], [AG04] and [GKNP14, p. 58ff].

[4] PhD student at the biological department, AG Friauf – Tierphysiologie, TU Kaiserslautern

For existence and uniqueness, a fixed-point approach is used which was suggested by Prof. Dr. Surulescu. I figured out most of the details and added the proof for the continuous dependence, all with assistance of Prof. Dr. Krumke.

(4) After that, new similar models are proposed.

Most important is the derived ODE system which makes it possible to easily test our modeling approach on experimental data. Because of that, the derivation is given in detail.

We also suggest other models that could be useful for further research. These models are discussed shortly and short sketches of the well-posedness proofs are provided.

The ODE system was proposed by Prof. Dr. Surulescu. The other related systems were created by me, partly because of Fischer's suggestion that featuring two vesicle pools could be beneficial.

(5) Next we take a close look at the experimental data used for testing the models in later sections. All data come from one particular synapse and was provided by Alexander Fischer, who also took the time to explain to me the special properties of this synapse, the experimental procedure that was used for data acquisition and various characteristics of the data.

These points are all summarized and we see what kind of preprocessing is required.[5] Afterwards we elaborate on the specific preprocessing methods I developed for making the data suitable for the testing of our models.

(6) Subsequently, we formulate the abstract optimization problem that has to be solved in the context of model evaluation.

We start by stating a very general form of the problem and then see which assumptions can be made in order to make things manageable for our purposes. However, we do not choose any specific model in this section, so everything is formulated in a rather generic way.

These abstract problems were determined by Prof. Dr. Krumke and me.

(7) The description of the general optimization problem is followed by a report of the optimization experiments that have been performed for model evaluation. This includes the mentioning of concrete parameter choices and assumptions and a description of the specific optimization routines that have been used.

The codes for these experiments were written in Python and run under the use of IPython notebook. I designed the specific experiments, did the implementation and performed the tests mostly on my own with some assistance of Prof. Dr. Krumke.

(8) The thesis is completed by a short discussion. There, some results of the experiments are reviewed and interpreted and a few ideas for future research are given.

The figures in this work were either taken from books, are (modified) public domain pictures or were created by the use of IPython ([PG07]) together with matplotlib ([Hun07]).

Acknowledgements. First of all, I would like to thank Prof. Dr. Sven O. Krumke for being willing to supervise this thesis and giving me much freedom for making my own decisions while always helping me out when there was any need for discussion. Our numerous discussions often lead to new interesting insights and quickly resolved many issues.

[5] Details can be found in the master's thesis of Dennis Bakker. See [Bak13].

Next, I want to thank Prof. Dr. Christina Surulescu for providing me with a suitable model and co-supervising my work. In particular, all modeling- and PDE-related questions I asked were at all times answered quickly and concisely and our conversations at the very beginning of the writing process greatly eased access to this complex field.

Also, I thank Alexander Fischer for sharing the experimental data, providing helpful literature and for his great patience and readiness to provide additional assistance. Our conversations clearly helped me to understand the whole subject much better and saved me lots of time.

And again, thank-you to the three of you for taking part in the creation of this work and hereby making it possible for me to pursue my research interests.

1. Biological background

1.1. **Neurons.** In the nervous system, there are essentially two classes of cells: *Neurons*, or *nerve cells*, and *glia*, or *glial cells*. Neurons are the signaling units of the nervous system whereas the role of glial cells is more diversified. However, the different functions of glia are currently still under debate and they seem to play only a minor role in synaptic transmission. (Cf. [KSJ+13, p. 24–27].) Hence, glial cells will be neglected from now on and we focus on the study of neurons.

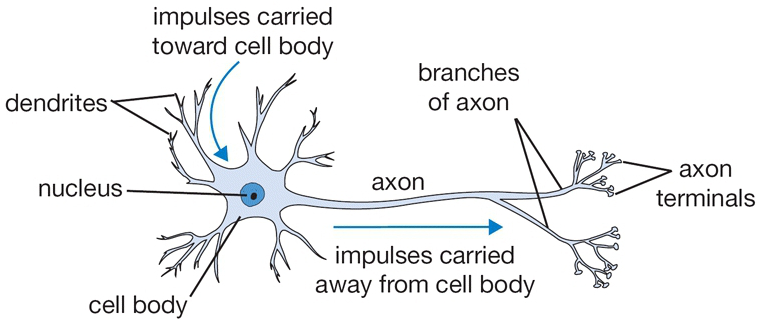

Figure 1. Basic structure of a typical neuron. (Public domain picture taken from http://www.wpclipart.com.)

A neuron consists of four different parts:[6]

(1) The *soma*, or *cell body*, is the metabolic center of the cell. It contains the nucleus, the endoplasmatic reticulum and other specialized organelles and supplies the other parts of the cell with various substances like proteins for example.
(2) *Dendrites* are processes spreading out from the cell body and serving as signal receivers.
(3) The *axon* has its origin at the cell body and is structurally similar to a dendrite but carries signals away from the cell body to other neurons and has special endings designed for signal transmission. A neuron has only one axon but in general many dendrites.
(4) *Presynaptic terminals* are the endings of axons. Here signals are communicated to other neurons by means of release of chemical substances called *neurotransmitters*.

Moreover, the interior of neurons is separated from the extracellular space by the *cell membrane*.

The (one-way) connections between neurons are called *synapses*. The axon terminal of a sending neuron is connected to some part (usually a dendrite) of the receiving neuron. In this context, the sending neuron is called *presynaptic neuron* and the receiving neuron *postsynaptic neuron*. It is distinguished between two types of synapses:

- Electrical synapses: The presynaptic neuron is directly connected to the postsynaptic neuron by so-called *gap junctions* which allow ions to freely move from one neuron to the other.
- Chemical synapses: There is a small gap, called *synaptic cleft*, between the *presynaptic terminal* and the *postsynaptic neuron*. The presynaptic cell releases NTs into the synaptic cleft which then move to postsynaptic receptors to cause a response.

[6]Cf. [KSJ+13, p. 22–24].

Chemical synapses are more complex but also more common in the vertebrate brain than electrical synapses. From now on we will consider synaptic transmission at chemical synapses only.

We will later have a closer look at the structure of chemical synapses. But first, we will examine neural signal transmission in general. The different parts of neural signaling share many common principles.

Signal transmission typically includes the following steps:

(1) The dendrites receive inputs from other neurons and transport them to the soma.
(2) At the soma, different inputs come together and are integrated.
(3) At the *trigger zone* (which is usually located at the junction between axon and soma) *action potentials* might be triggered, depending on the received inputs.[7]
(4) Action potentials are propagated down the axons to the presynaptic terminals.
(5) At the presynaptic terminals, synaptic release is triggered and usually causes a postsynaptic response of some sort. (This step is what we model below.)

To understand how exactly signals are propagated in neurons, we need to take a closer look at the cell membrane and the ion concentrations. (See below.)

1.2. **The cell membrane.** The cell membrane mainly consists of a bilayer of lipids which is impermeable to ions.

In addition to lipids, the membrane contains proteins that serve various purposes. Most relevant for our studies are ion pumps and ion channels, which are both transmembrane proteins and actively or passively transport special sorts of charged particles from one side of the membrane to the other.

- *Ion channels* can easily be passed (if they are open) by certain types of ions but not by others. Which ions are able to pass the channel depends on the particular type of the channel. There are many different kinds of channels, some of them being voltage-gated (i.e. their state depends on the membrane potential) and others receptor-gated (i.e. they open if certain particles bind to a associated receptors).[8] Transport through channels is passive, i.e. it only works along gradients. (Cf. [KSJ$^+$13, p. 100–109].)
- *Ion pumps* or *ion transporters* actively transport certain types of ions across the membrane against their electrochemical gradients. This process requires energy and is much slower than passive transport via ion channels. (Cf. [KSJ$^+$13, p. 119].)

The constant transport of ions across the membrane by ion pumps causes the ion concentrations inside resting neurons to differ significantly from extracellular ion concentrations. Typical values for the most important ion species are given in table 1.

These gradients in concentration are important for signal transmission to work since transmission is mainly based on opening and closing of ion channels.

We will now first analyze local membrane potentials and then see how signals spread from one neuron to another.

---

[7] An action potential is a characteristic sudden change in membrane potential. We will later see how action potentials are created and what causes their characteristic shape.

[8] There are also channels which employ phosphorylation gating or stretch or pressure gating. But these two types of gating are not relevant for this thesis.

ion species	intracellular conc.	extracellular conc.
Potassium (K^+)	140 mM	5 mM
Sodium (Na^+)	10 mM	145 mM
Chloride (Cl^-)	4-30 mM	110 mM
Calcium (Ca^{2+})	0.0001 mM	1-2 mM

TABLE 1. Approximate ion concentrations in mammalian neurons. Values taken from [PAF+04, p. 40].

1.3. **Local membrane potentials.** Assume for the moment that there is only one species of ions and consider a short piece of membrane. We have just mentioned that the ion concentration inside nerve cells differs from the ion concentration in the extracellular fluid. (See table 1.) Since ions are charged particles, this difference in concentration generates an electrical potential across the membrane:

Lemma 1.1 (Nernst potential)

$$\Delta u = \frac{kT}{q} \ln \frac{n_2}{n_1},$$

where k denotes the Boltzmann constant, T the temperature, q the charge of an ion, n_1 the intracellular and n_2 the extracellular ion concentration and Δu the potential for which there is no flux of ions given the ion concentrations n_1 and n_2 and assuming that ions can move freely through the membrane.

Proof. Based on thermodynamics, see e.g. [GKNP14, p. 29]. □

This formula actually describes an equilibrium state and if ions can move freely, it also works the other way around: If some potential is given, ion densities will adjust in order to reach the balanced state described by the Nernst potential.

Note that these observations imply that the Nernst potential can be used to determine the direction of ion flow in case of channel opening, given the current voltage across the membrane. Since this direction of flow changes at the potential Δu (given fixed ion concentrations), this value is also called *reversal potential*.

Example 1.2 (Nernst potential for sodium)
The charge of a sodium ion is $q = 1.6 \cdot 10^{-19} C$ and the Boltzmann constant is $k = 1.4 \cdot 10^{-23} J/K$.[9] Assuming a typical body temperature of 37°C ($310.15K$), an intracellular ion concentration of $10mM$ and an extracellular ion concentration of $145mM$, we obtain that

$$\Delta u \approx 72.6mV.$$

Hence, if sodium channels open, sodium ions will start flowing into the cell if the membrane potential is below $72.6mV$. (Given that the membrane potential at rest is around $-70mV$, this is the usual case.)

It is also possible to take multiple ion species into account and in this way calculate a reversal potential for the membrane in the presence of different sorts of ions. The formula for doing this is called *Goldman equation* and is similar to the formula for the Nernst potential.

None of these two equations, however, describes how the equilibrium states are reached. This is where the Hodgkin-Huxley model comes into play.

[9]The values for these constants are taken from [GKNP14, p. 30].

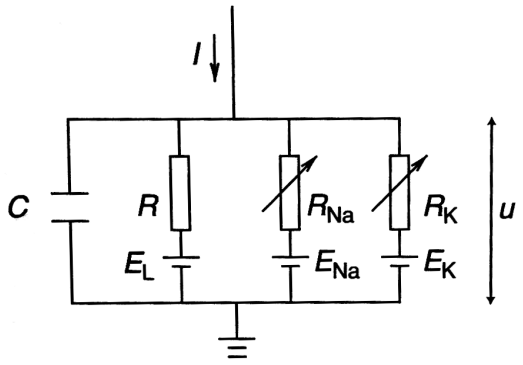

FIGURE 2. Diagram for the Hodgkin-Huxley model. Taken from [GKNP14, p. 31].

1.3.1. *The Hodgkin-Huxley model.* Based on experiments on the giant axon of the squid, Hodgkin and Huxley developed a model that describes the local reaction of the neural membrane potential to stimulus in form of an injected current. (See [HH52].)

The model can be represented by a circuit diagram which is depicted in figure 2.

- A capacitor with capacity C models the bilipid part of the membrane that separates the interior of the cell from the extracellular area and is considered impermeable to ions.
- Some current I is injected. The injected current might charge the capacitor or it flows through any of the three resistors.
- Three kinds of currents might flow through the membrane: Sodium, potassium or a "leak current" (which is introduced to represent all other currents — chloride being the most important one).
- The variable resistances account for the different states (e.g. open or closed) of the channels.
- The batteries account for the gradients in ion concentration, so the battery voltages E_L, E_{Na} and E_K are equal to the respective Nernst potentials.
- The membrane potential is denoted by u.

This electrical circuit can be converted into the following mathematical setting:

$$C\frac{du}{dt} = -\sum_{k\in\{Na,K,L\}} I_k(t) + I(t),$$

with

$$\begin{aligned} I_L(t) &= g_L \cdot (u(t) - E_L), \\ I_{Na}(t) &= g_{Na} m^3(t) h(t) \cdot (u(t) - E_{Na}), \\ I_K(t) &= g_K n^4(t) \cdot (u(t) - E_K), \end{aligned}$$

where g_L, g_{Na} and g_K denote the maximum conductances of the respective channels and the functions m, n and h are "gating variables" which account for the different states of the channels and are each described by a differential equation of the form

$$\frac{dx}{dt} = -\frac{1}{\tau_x(u(t))}(x - x_0(u(t))).$$

(So for a given voltage u, x approaches $x_0(u)$ with some time constant $\tau_x(u)$.)

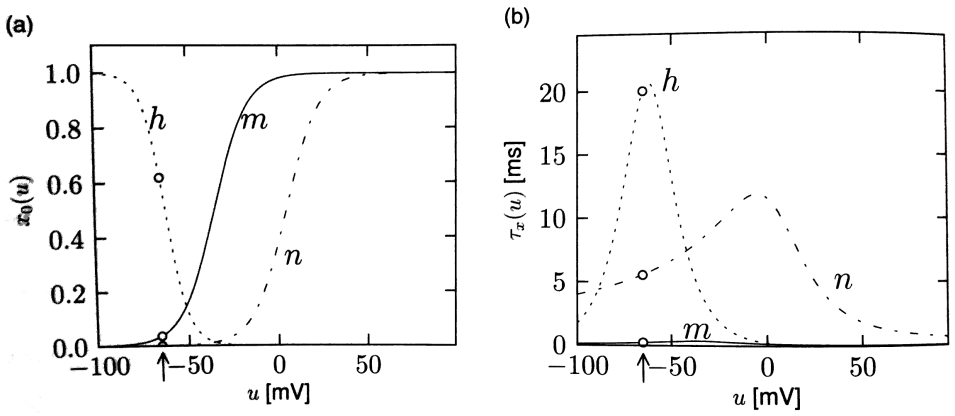

FIGURE 3. Target values and time constants for the gating variables of the Hodgkin-Huxley model. Taken from [GKNP14, p. 32].

Hodgkin and Huxley deduced the form of the functions x_0 and τ_x as well as the reversal potentials and the maximum conductances of the different channels from empirical measurements. Figure 3 features a plot of the functions x_0 and τ_x.

Note that there are two gating variables for sodium channels. This is because sodium channels can not only be open or closed but also attain a refractory state where they are blocked and do not open even if the membrane becomes depolarized. The opening of sodium channels is controlled by the gating variable m whereas h describes the blocking (i.e. transition to a refractory state) of sodium channels.

The behavior of potassium channels is simpler. Here, we only have one gating variable n which describes the opening of the channels.

Remember that the resting membrane potential is around $-70mV$, so sodium and potassium channels are both closed at rest.

Remark: The Hodgkin-Huxley model can easily be extended to incorporate other ion species/channels. See [GKNP14, section 2.3] for example.

The Hodgkin-Huxley model is quite powerful as it captures a great deal of the dynamics of the local membrane potential. For example, it can explain the generation of action potentials. We will now see what an action potential is and why action potentials are important for neural signal processing.

1.3.2. *The action potential.* Assume that a strong short current is injected into the axon of a neuron. If the membrane is depolarized above a certain threshold, voltage-gated sodium channels open. Now (positively charged) sodium ions start flowing into the cell, causing the membrane potential to become even more positive. However, soon two other effects can be observed:

First, if some other threshold is passed, voltage-gated potassium channels open. Potassium ions leave the cell, depolarizing the membrane again.

Secondly, sodium channels close after a short while and enter a refractory state. It then takes a little while until they become receptive again.

These two effects together cause the membrane potential to drop below its resting value and make it almost impossible for the membrane to become excited immediately after an action potential has been triggered. Hence, action potentials are separated from one another and the firing frequency of a neuron is practically limited.

Note how these effects are captured by the variable conductances (involving the gating variables m, h and n) in the Hodgkin-Huxley model.

Since the described process does not depend on the precise form of the injected current (it mainly matters whether the sodium channel threshold is exceeded or not), the time course of the membrane potential after such a current injection has a characteristic shape that is pretty much the same for all sufficiently strong inputs. We call this special response of the membrane (or also the time course of the membrane potential during such an event) *action potential*.

Also note that the action potential does not change shape when propagated along the axon, i.e. the amplitude does not decrease as in dendritic signal transmission. This is important for signaling since it means that axons transmit (sort of) binary signals. Hence, frequency and timing are used to encode information instead of different amplitudes or other shape related information.

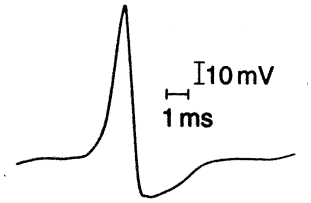

FIGURE 4. Example of an action potential. Taken from [GKNP14, p. 5].

We have so far covered the major aspects of local membrane behavior. The next step is to analyze signal propagation.

1.4. **Signal propagation.** If a current is injected at some point, some of it flows through the membrane, but some of it also spreads inside the neuron. These observations lead to the general cable equation, which actually is a 1D diffusion equation describing how the membrane potential propagates.

Again we also have an electrical circuit schematically representing the model which is depicted in figure 5.

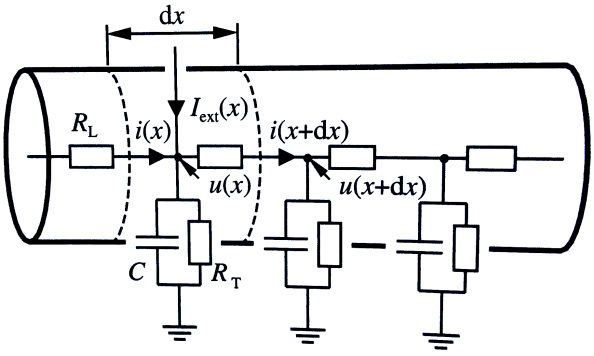

FIGURE 5. Schematic diagram of the general cable equation. Note that the compartments are simplified: In the general form the circuits at the membrane are of the same type as the circuit for the Hodgkin-Huxley model. (See figure 2.) Picture taken from [GKNP14, p. 66].

The cable equation assumes some regularity of the conducting structure that is at most given locally in neurons. To account for irregularity, the conductor can be divided into small approximately regular compartments and treat each of them as

a circuit as depicted in figure 5). This approach leads to large systems of ordinary differential equations called *compartment models*.

The dynamics for the individual compartments are similar to Hodgkin-Huxley but usually simpler channel dynamics are assumed to keep things tractable. Note that compartments models are rather flexible and can be applied to dendrites as well as the cell body and the axon. Some of the parameters have to be adjusted as the densities of channels in the membrane are different for dendrites and axons.

Remark: Roughly speaking, there are only very few voltage-gated channels in the dendrite membrane, making it unlikely for an action potential to be generated there. That explains why it is often assumed that dendrites only passively conduct signals.

So, the cable equation and compartment models explain signal propagation in neurons: The propagation of signals is based on the fact that changes of the membrane potential at one place affects the potential across the neighboring membrane. The details depend largely on the local ion channel composition.

In particular, we can now explain how action potentials are propagated:

(1) Assume that at some place an action potential is generated.
(2) Now the potential of the nearby membrane changes as well. If this change is big enough (which depends on the densities and sorts of present ion channels) an action potential is created there too.
(3) Again, neighboring membrane potentials are changed.
(4) In the part of the membrane where an action potential has just been generated no new action potential will be triggered since the voltage-gated sodium channels are still in refractory state.
(5) The part of the membrane that has not been excited yet will respond by action potential generation if the change across its membrane is sufficiently large.

Let us now talk about synaptic transmission in more detail.

1.5. **Synaptic transmission.** The basic structure of a chemical synapse looks as follows:

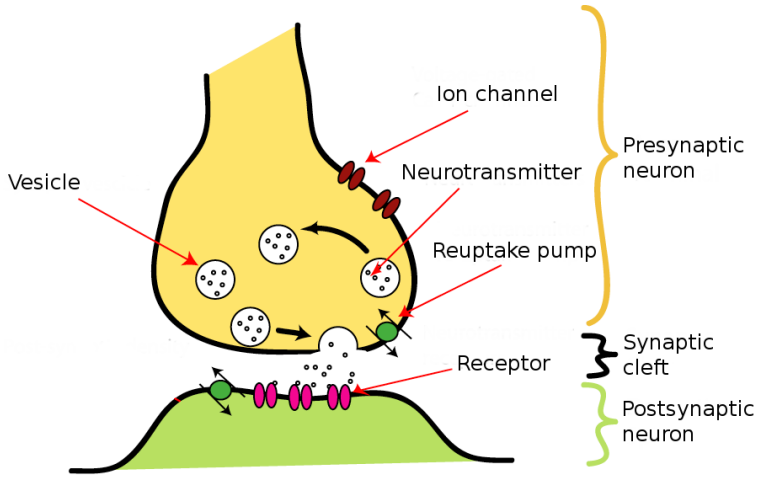

FIGURE 6. Basic structure of a chemical synapse. (Modified public domain picture from http://commons.wikimedia.org.)

- Ion channels and transporters are contained in the membranes of the pre- and postsynaptic neurons.
- *Synaptic vesicles* are a kind of containers in the presynaptic terminal that fill with neurotransmitters. It is commonly distinguished between vesicles in the *reserve pool* and vesicles in the *release ready* or *readily releasable pool*.
- The *synaptic cleft* is a small ($\approx 20nm$) gap between the pre- and postsynaptic neurons.
- *Postsynaptic receptors* are proteins in the postsynaptic membrane. This is where neurotransmitter from the synaptic cleft bind to.

Remark: There are roughly 10^9 synapses in every cubic millimeter of cerebral cortex. In particular, synapses are very small structures, making it quite a challenging task to analyze them.

The basic steps of synaptic transmission:

(1) An action potential arrives at the presynaptic terminal.
(2) Calcium channels of the presynaptic terminal open.
(3) Calcium ions flow into the cell.
(4) Calcium ions bind to receptors, causing release-ready vesicles to fuse with the membrane. This process is called *exocytosis*.
(5) NTs from fused vesicles flow into the synaptic cleft.
(6) NTs move around in the synaptic cleft by means of diffusion.
(7) The transmitters now either dock to receptors of the postsynaptic cell where they stay for a while[10] and cause some sort of response or are removed from the synaptic cleft by one of three mechanisms: Diffusion, enzymatic degradation (which is only used in cholinergic synapses) or reuptake.[11]
(8) If neurotransmitters bind to receptors in the postsynaptic membrane, ion channels in the postsynaptic membrane are opened (either directly or indirectly). This causes a flux of ions which implies a postsynaptic current. The postsynaptic current finally changes the postsynaptic potential.

Remark (Spontaneous release)**:** Sometimes vesicles might also spontaneously fuse with the membrane without an action potential triggering the release.

There are some other related ongoing processes in neurons we haven't talked about yet:

- Neurotransmitters are synthesized in the synaptic terminal or soma (and transported to the terminal).
- Vesicles are built in the soma and then transported to the synaptic terminal via fast axonal transport.

1.6. **The vesicle cycle.** As we have already seen, vesicles play a vital role in synaptic transmission. Our model also includes a variable for the vesicles but we will not explicitly describe processes like vesicle endocytosis.

Still, knowing more about these processes helps to get a complete picture of synaptic transmission. So we handle the vesicle cycle explicitly in a little more detail. The basic steps are:[12]

[10] Bound transmitters then become inactivated or just undock again, depending on the synapse.

[11] If NTs diffuse away from the synaptic cleft, they might be absorbed by glial cells and delivered back to the presynaptic neuron.

[12] Note that the last steps are different for the so-called "kiss-and-run" endocytosis. For reference, see [KSJ+13, p. 277]. (The fusion with endosomes has not been mentioned because it might be outdated. Cf. [SDC12, p. 4–5].)

(1) Vesicles from the reserve pool dock to the membrane at the *active zones* and are primed. They are then readily releasable.
(2) Release-ready vesicles are connected to calcium sensors which make them fuse with the membrane if enough calcium ions bind.
(3) If a release-ready vesicle fuses with the membrane, its contents are expelled into the synaptic cleft.
(4) The fusion of vesicles with the membrane causes the membrane to grow.
(5) Excessive membrane is invaginated. This process is called *endocytosis*.
(6) The invaginated membrane is turned into new vesicles which move to the reserve pool.

At all times, vesicles are filled with neurotransmitters by active transport mechanisms.

Remark (Different forms of endocytosis)**:** In real neurons, different forms of endocytosis coexist:[13]

- In the so-called "kiss-and-run" endocytosis the docked vesicle does not completely fuse with the membrane. Instead, a kind of pore is opened at the junction between membrane and vesicle for about one second, allowing the contents of the vesicle to flow out into the synaptic cleft. After that time, the pore is closed again and the vesicle is again readily releasable.
- In clathrin-mediated endocytosis excessive membrane is invaginated and coated with the protein clathrin. So first, clathrin-coated vesicles are formed. The clathrin is then disassembled from the new vesicles before they move to the vesicle cluster and are filled with transmitters.
- In bulk endocytosis large amounts of excessive membrane are invaginated lateral to the active zone. These invaginations (of about 4 times the size of a vesicle) then form vacuoles (similar to endosomes) which eventually convert into synaptic vesicles.

However, lots of details about endocytosis are still under investigation. For more information, see e.g. [SDC12] for a rather recent overview. Also see [WRCP$^+$13] for further details.

Remark (Rate of endocytosis)**:** As clathrin-mediated endocytosis and bulk endocytosis are mostly compensatory to keep the amount of synaptic membrane roughly constant, it is clear that generally higher rates of exocytosis result in higher rates of endocytosis. This dependency, however, is not linear: Excessive membrane can make the cell kind of disorganized (cf. [KvG09]). Keep this effect in mind when working with high frequency stimulation.

Also note that the different forms of endocytosis happen at different speeds.

1.7. **Calcium and the presynaptic terminal.** We have already seen that the (local) calcium concentration is very important for synaptic transmission because it is calcium that makes release-ready vesicles fuse with the membrane.[14] However, the effects of calcium in synaptic transmission are more diverse than that.

First keep in mind that the extracellular calcium concentration is generally much higher than the calcium concentration inside neurons because calcium ions are constantly transported out of the cell by ion pumps. (Cf. table 1.) So, if the presynaptic membrane becomes depolarized — e.g. because of an arriving action potential — and exceeds a certain threshold, voltage gated calcium channels open and calcium ions flow into the presynaptic cell.

[13] Cf. [SDC12].

[14] In fact, we will later model the local calcium concentration in order to determine the rate of exocytosis.

What happens now is: The local calcium concentration inside the cell near the channels increases dramatically. Calcium channels are located near release-ready vesicles, so the incoming ions bind to nearby receptors, causing the primed vesicles to fuse with the membrane. If we have a high stimulation frequency calcium ions might also spread in the presynaptic terminal and have other effects. For instance, primed vesicles that are a bit further away from the open calcium channels may fuse with the membrane, too, leading to a sort of facilitation effect for successive action potentials. Additionally, a rise in global calcium concentration speeds up the recruitment of release-ready vesicles.[15]

Yet another interesting fact is that calcium can accelerate vesicle endocytosis.[16]

See for instance [NS08] for more information on the different roles of calcium.

Remark (Modeling local calcium concentration)**:** The Hodgkin-Huxley model can be extended to account for calcium channels. This way, the behavior of the local calcium concentration in response to changes in the membrane potential can be modeled. (See [GKNP14, p. 48–51] for details.)

[15] Cf. [NS08].

[16] Cf. [AMF+13]. Also see [WRCP+13, p. 4].

2. The basic model

In this work several different models will be proposed and analyzed. We start with the basic PDE model. It is basic in the sense that most of the other models we will introduce later are closely related to it.

Four state variables are used:

- $N_{in}(t)$ denotes the amount of neurotransmitters present in the presynaptic terminal at time t and not contained in vesicles.
- $v(t,s)$ describes how many vesicles of "size"[17] s are there in the presynaptic terminal at time t.
- $N_{out}(t)$ equals the amount of free neurotransmitters in the synaptic cleft at time t.
- $R(t)$ describes the amount of free receptors in the postsynaptic membrane at time t.

The behavior of the different state variables is described as follows:

- N_{in}:
  - $\beta(w - N_{in})^+$ describes the supply of "new" neurotransmitters. The rate of supply attains its maximum βw if N_{in} is zero and decreases linearly as N_{in} increases, until it reaches zero. So no transmitters are produced if N_{in} exceeds w. This way, saturation effects are taken into account.
  - αN_{out} describes the movement of neurotransmitters from the synaptic cleft back into the presynaptic terminal. So we assume that this happens with the fixed rate α.
  - $-N_{in}\int_{s_0}^{s_1}\tau(s)v(t,s)ds$ accounts for the filling of vesicles with transmitters. This term is basically a product of the amount of neurotransmitters and the number of vesicles where an extra factor $\tau(s)$ has been added to the integral to describe the filling speed of vesicles of size s, again making it possible to take saturation effects into account.
- v:
  - v is modeled by a linear transport equation where vesicle growth corresponds to transport and is given by the term $N_{in}(t)\frac{\partial(\tau(s)v(t,s))}{\partial s}$.
  - Vesicles fuse with the membrane with some rate $\mu(t)$ (where $\mu(t)$ depends on the membrane potential at time t). So, $-\mu(t)v(t,s)$ accounts for the fusion of vesicles of size s with the membrane at time t.
- N_{out}:
  - As vesicles fuse with the membrane, all neurotransmitters that are stored in these vesicles are released into the synaptic cleft. This fact is described by the term $\mu(t)\int_{s_0}^{s_1}\nu(s)v(t,s)ds$, where $\nu(s)$ can be interpreted as average amount of transmitters stored in a vesicle of size s.
  - Neurotransmitters bind to receptors with some rate k. If they do that they are not free anymore. The term $-kR(t)N_{out}$ is used to describe that process.
  - Neurotransmitters may just move away from the synaptic cleft or are transported back into the presynapse. This happens with rates δ and α respectively, so the term $-(\alpha+\delta)N_{out}$ is introduced.
  - There is another source term $\gamma(R_{ges}-R)$ because transmitters that are bound to receptors eventually unbind with some rate γ and are again freely moving in the synaptic cleft. (Note that we assume that the total number of receptors R_{ges} is constant so the number of occupied receptors is given by $R_{ges} - R$.)

[17] Actually s describes the filling state and not the physical size.

- R:
  - Free receptors become occupied as neurotransmitters bind to them. Hence the term $-kRN_{out}$.
  - As for N_{out}, there is another source term $\gamma(R_{ges}-R)$ for R, the reason being exactly the same.

Putting things together, the behavior of the system (for all $s \in (s_0, s_1)$ and $t \in (0, T)$) is described by the following set of equations:

$$\frac{dN_{in}}{dt} = \underbrace{\beta(w - N_{in})^+}_{\text{“production”}} + \underbrace{\alpha N_{out}(t)}_{\text{re-uptake}} \underbrace{- N_{in} \int_{s_0}^{s_1} \tau(s) v(t,s) ds}_{\text{transport into vesicles}} \tag{1}$$

$$\underbrace{\frac{\partial v}{\partial t} + N_{in}(t) \frac{\partial(\tau(s) v(t,s))}{\partial s}}_{\text{growth}} = \underbrace{-\mu(t) v(t,s)}_{\text{fusion}} \tag{2}$$

$$\frac{dN_{out}}{dt} = \underbrace{\mu(t) \int_{s_0}^{s_1} \nu(s) v(t,s) ds}_{\text{exocytosis}} \underbrace{- kR(t) N_{out}}_{\text{binding}} \underbrace{- \alpha N_{out}}_{\text{re-uptake}} \underbrace{- \delta N_{out}}_{\text{diffusion}} + \underbrace{\gamma(R_{ges} - R)}_{\text{unbinding}} \tag{3}$$

$$\frac{dR}{dt} = \underbrace{-kN_{out}(t)R}_{\text{binding}} + \underbrace{\gamma(R_{ges} - R)}_{\text{unbinding}} \tag{4}$$

We use the boundary conditions

$$v(t, s_0) =: h(t) \geq 0, \quad 0 < t \leq T \tag{5}$$

$$v(0, s) =: v_0(s) \geq 0, \quad s_0 \leq s < s_1 \tag{6}$$

$$N_{in}(0) =: N_{in}^0 > 0 \tag{7}$$

$$N_{out}(0) =: N_{out}^0 \geq 0 \tag{8}$$

$$R(0) =: R_0 \geq 0 \tag{9}$$

where $s_0, s_1, T, w, k, \alpha, \beta, \gamma, \delta, R_{ges} \in \mathbb{R}_{\geq 0}$, $s_0 < s_1$, $\tau, \nu : [s_0, s_1] \to \mathbb{R}_{\geq 0}$ and $\mu : [0, T] \to \mathbb{R}_{\geq 0}$ are *model parameters* and $N_{in}^0, N_{out}^0, R_0 \in \mathbb{R}_{\geq 0}$, $v_0 : [s_0, s_1] \to \mathbb{R}_{\geq 0}$, $h : [0, T] \to \mathbb{R}_{\geq 0}$ are referred to as *given data*.

Below we will talk about some model parameters in a little more detail and see which choices are reasonable from a modeling point of view. After that we will also formulate the precise requirements which ensure well-posedness of the system.

Before we do that, let us stress out some implicit assumptions the model makes:

2.1. **Assumptions and simplifications.** The above system implies the following assumptions and simplifications:

- Kiss-and-run exocytosis is ignored. ($\mu(t)$ only scales down v. To model kiss-and-run exocytosis, another, negative and time dependent growth term would be necessary.) However, kiss-and-run exocytosis is generally believed to play a minor role in synaptic transmission.
- We do not distinguish between different types of neurotransmitters.
- The total number of receptors (free + occupied) is assumed to be constant. This is motivated by the fact that changes in membrane structure are relatively slow and our model operates on a rather small time scale. Without this assumption, another state variable would be necessary. (Note that changing the numbers of receptors might be essential for long-term effects like learning.)
- We do not model the vesicle cycle directly. Different types of vesicle synthesis and recycling are not distinguished and only indirectly modeled by h.

- All variables of the model are continuous, hence we describe a kind of average case. In particular, we do not really have individual vesicles but rather a vesicle density. And in case of action potential arrival, some fraction μ of all vesicles gets lost by means of exocytosis.
- Stochastic properties are neglected. So care has to be taken in the case where only very few vesicles are modeled. (Also see [RST11].)

There are actually two different possible interpretations of the model:

(1) v describes all vesicles in the synaptic terminal and N_{in} the global neurotransmitter concentration. Note that in this case, the amplitude of μ in response to action potentials should decrease for (fast) successive stimulation to account for the fact that the release ready pool has to be filled again. (The details are far from trivial.)
(2) v stands for primed vesicles only and N_{in} describes the local neurotransmitter concentration near vesicles of the release ready pool. Here, μ can be of a simpler form. However, the function h describes the movement from the reserve pool to the release ready pool. If varying numbers of vesicles in the reserve pool are to be accounted for, things are getting complicated.

Thus it is important to decide which interpretation to use before picking suitable functions μ and h. For the rest of this work, the second interpretation is used.

2.2. **Modeling $\mu(t)$.** The function μ determines the rate of vesicle fusion. In neurons, this rate mainly depends on the calcium concentration near readily releasable vesicles. (Vesicles of the reserve pool have to dock to the membrane and be primed before they can fuse with the membrane.)

We simplify this dependency in our model and will assume that $\mu(t)$ is proportional to the calcium concentration in the presynaptic cell at time t. Also we do not distinguish between different local concentrations.

Assumption 2.1
$\mu(t) = \mu \cdot [Ca](t)$ for some $\mu > 0$ and all $t \in [0, T]$ where we write $[Ca](t)$ for the calcium concentration inside the presynaptic terminal at time t.[18]

So we have to estimate the behaviour of the calcium concentration in order to determine μ. As mentioned in section 1.7, the calcium concentration can be modeled by extending the Hodgkin-Huxley model appropriately. In that case one gets a jump in concentration followed by exponential decay as response to a single action potential. (Cf. [GKNP14, Fig. 2.15].)

However, some of the parameters for the extended Hodgkin-Huxley model are hard to determine. (Especially since we are only interested in the local concentration near the active zones and usually, the parameters you find are for modeling the concentration over a larger domain.) We therefore choose a simpler model that outputs a calcium curve of the same shape given the same (pulselike) input:

Assumption 2.2 ($[Ca]$ behavior)
We assume that the time course of the calcium concentration is given by

$$[Ca](t) = [Ca]_0 + b\left(\sum_i \mathbb{1}_{[t_i+\delta_{Ca},\infty)}(t)\exp(-a(t-(\delta_{Ca}+t_i)))\right),$$

where $t_0, t_1, \ldots$ are arrival times of action potentials and $a, b, \delta_{Ca}, [Ca]_0 \geq 0$ are model parameters.

[18] To be precise, we mean the local concentration near the membrane at the release sites inside the presynaptic terminal. This is in contrast to the global calcium concentration which is relevant e.g. for vesicle recruitment.

See figure 7 for an exemplary plot of the calcium concentration time course under assumption 2.2.

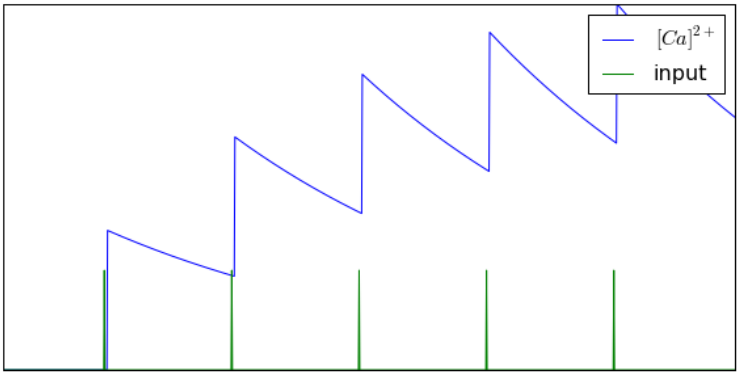

FIGURE 7. Exemplary plot of the calcium concentration that is evolving according to assumption 2.2 in response to a train of action potentials.

Remark: Note that under assumptions 2.1 and 2.2, $\mu(t)$ is *not* continuous as it makes a jump every time an action potential arrives at the presynaptic terminal. However, since μ can be approximated arbitrarily well by a smooth function and such a smooth approximation is also more realistic, we will later assume μ to be continuously differentiable.

2.3. **Modeling $h(t)$.** The time-dependent parameter h is highly related to the refilling of the readily releasable pool. But finding a suitable h is quite tricky. In particular because of the following issues:

Remark (Difficulties in choosing h):

- $h(t)$ does not directly describe how many vesicles move to the readily releasable pool and is rather difficult to interpret: For the same h, the behavior of the vesicle number $\int_{s_0}^{s_1} v(t,s)ds$ might be very different for different time courses of N_{in}! This is somewhat undesired since it makes it difficult to come up with a suitable function for h.
- h is part of the boundary conditions and hence, should not depend on any state variables. However, in reality vesicles can not dock to the membrane if the release-ready pool is already full. The number of vesicles in that pool is described by the state variable v, though. So we need to find a direct relation between the input signal and h but it is not completely clear how this should be done. (Especially when keeping in mind the previous point.)
- The number of vesicles in the reserve pool clearly affects the refilling speed of the release-ready pool. And this number can vary (particularly for longer time scales) and depends on the past events and also on endocytosis.

Still, it makes sense to pick a function h with the following general properties:

- Some time after each stimulus, $h(t)$ should increase. This is because stimulation generally triggers fusion of vesicles which in turn leads to refilling of the readily releasable pool.
- If no further stimulation occurs, $h(t)$ should drop again because saturation effects will take over as the empty spots at the active zones become occupied.

- h should be "sufficiently" regular: We will later need some regularity to ensure well-posedness of the model. Moreover, as we are modeling the average behavior at synapses some smoothness seems reasonable.

It is, however, not so clear how to deal with the details. We will later try out the following function that has been suggested by Prof. Dr. Surulescu:

Example 2.3 (χ^2-based h)
h could be chosen to be a sum of χ^2-distributions: Let $\chi^2(x, f)$ denote the probability density function of the χ^2 distribution at x with f degrees of freedom. Set

$$h(t) := h_{amp} \cdot \left(\sum_i \chi^2\Big(\frac{h_{width}}{100}(t - (h_\delta + t_i)), 3 \Big) \right),$$

where $t_0, t_1, \ldots$ are arrival times of action potentials and h_{width}, h_{amp} and $h_\delta \geq 0$ are model parameters.

Figure 8 features an exemplary plot of h. Note that this function for h is continuous and smooth on $[0, T] \setminus \{h_\delta + t_i \mid i = 0, 1, \ldots\}$. As for μ, we will still assume h to be continuously differentiable on the whole domain $[0, T]$.

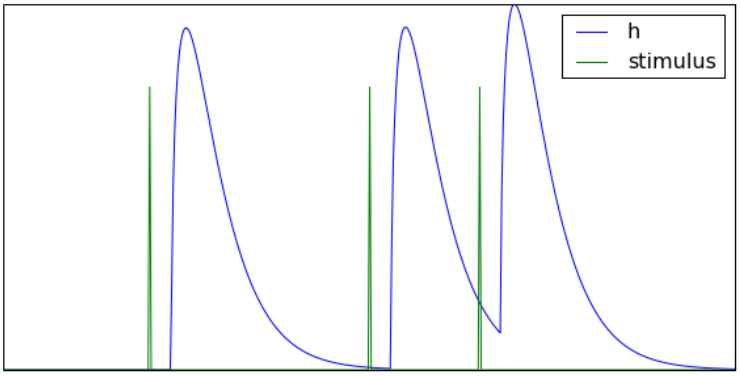

FIGURE 8. Exemplary plot of the time course of a χ^2-based h in response to a train of action potentials.

Because of the issues stated above we will later also use a constant function h to check how badly a seemingly poor choice for h effects the performance of the whole model.

2.4. **Choosing $\tau(s)$.** $\tau(s)$ describes the filling speed of vesicles of filling state s. It can be used to model saturation effects which are relevant in the process of vesicle filling: The concentration gradient changes as vesicles become more filled, so more energy is necessary to transport transmitters into already filled up vesicles.

If we denote the minimal vesicle filling by s_0 and the maximal filling by s_1, we want the following conditions to hold:

$$\tau(s_0) \approx \tau_0 \text{ for some } \tau_0 > 0$$

and

$$\tau(s_1) \approx 0.$$

Also, $\tau(s)$ should be monotonously decreasing.

Example 2.4
Possible choices for such functions τ that take saturation effects into account:

- A (mirrored and translated) sigmoid function:
$$\tau(s) = \frac{\tau_0}{1 + \exp(\frac{2k}{s_1 - s_0} \cdot s + k - \frac{2ks_0}{s_1 - s_0})},$$
where $k > 0$ is some constant that has to be chosen sufficiently large.
- Any polynomial that is monotonously decreasing on $[s_0, s_1]$ and reaches 0 at s_1. In the simplest case, τ could be a straight line from τ_0 to 0.

3. Well-posedness

The idea for showing existence and uniqueness of the solution for the original PDE system is to decouple the different state variables by defining a (strictly contractive) operator that has the solution of the PDE as fixed-point and then apply a fixed-point argument.

The statements will be formulated such that they can also be used to prove the continuous dependence on the given data. Note that in this section the model parameters are assumed to be given and fixed.

Notation 3.1
We denote the L^1 norm by $\|.\|_1$ and the L^∞ norm by $\|.\|_\infty$.

The following technical assumption together with the restriction on the space for the given data will ensure that our model is indeed well-posed:

Assumption 3.2
We assume that the following conditions are met:

- $\mu \in C^1([0,T])$, $\nu, \tau \in C^1([s_0, s_1])$ and
- $\tau(s) > 0$ for all $s \in [s_0, s_1)$.

Definition 3.3 (Data space)
We define the space of the given data as

$$\begin{aligned}\Theta := \big\{(v_0, h, N_{in}^0, N_{out}^0, R_0) \mid v_0 \in C^1([s_0,s_1]) \text{ with } \int_{s_0}^{s_1} \frac{v_0(s)}{\tau(s)} ds < \infty,\\ N_{in}^0 > 0,\ N_{out}^0 \geq 0,\ R_0 \geq 0,\\ h \in C^1([0,T]) \text{ with } h(0) = v_0(s_0) \text{ and}\\ N_{in}^0 \cdot (\tau'(s_0)v_0(s_0) + \tau(s_0)v_0'(s_0)) + h(0)\mu(0) + h'(0) = 0\big\}\end{aligned}$$

For $\theta = (v_0, h, N_{in}^0, N_{out}^0, R_0) \in \Theta$ we write

$$\|\theta\|_\Theta := \|v_0\|_\infty + \|h\|_\infty + |N_{in}^0| + |N_{out}^0| + |R_0|.$$

Definition 3.4 (Bounds)
Let $\theta = (v_0, h, N_{in}^0, N_{out}^0, R_0) \in \Theta$. We define the following upper bounds:

$$\bar{\mu} := \max_{t\in[0,T]} \mu(t),\ \ \bar{\nu} := \max_{s\in[s_0,s_1]} \nu(s),\ \ \bar{h} := \max_{t\in[0,T]} h(t),\ \ \bar{\tau} := \max_{s\in[s_0,s_1]} \tau(s)$$

We also define the following functions that will serve as bounds for the solution variables:

$$C_1(\theta) := \frac{\bar{\nu}\bar{\mu}\|v_0\|_1 + \gamma R_{ges}}{\alpha + \delta}$$

$$C_2(\theta) := \frac{\bar{\nu}\bar{\mu}\tau(s_0)\bar{h}}{\alpha + \delta}$$

$$\overline{N_{in}} : [0,T] \times \Theta \to \mathbb{R},$$

$$\overline{N_{in}}(t,\theta) := \exp(\alpha C_2(\theta)\frac{t^2}{2}) \left(\int_0^t \exp(-\alpha C_2(\theta)\frac{\lambda^2}{2})(\alpha C_1(\theta) + \beta w) d\lambda + N_{in}^0 \right)$$

$$\bar{v} : [0,T] \times \Theta \to \mathbb{R},\ \ \bar{v}(t,\theta) := \tau(s_0)\bar{h} \cdot t \cdot \overline{N_{in}}(t) + \|v_0\|_1$$

$$\overline{N_{out}} : [0,T] \times \Theta \to \mathbb{R},\ \ \overline{N_{out}}(t,\theta) := C_1(\theta) + C_2(\theta)\overline{N_{in}}(t,\theta)$$

$$\underline{N_{in}} : [0,T] \times \Theta \to \mathbb{R},\ \ \underline{N_{in}}(t,\theta) := \frac{\beta w}{\beta + \bar{\tau}\bar{v}(t,\theta)}.$$

3.1. **Defining the solution operator.**

Lemma 3.5 (Parameter transform for s)
Let τ be as in assumption 3.2. Then there exists a number $\bar{s}_1 \in (0, \infty]$ and a function $s : [0, \bar{s}_1) \to [s_0, s_1)$ satisfying the following conditions:

(1) $\frac{ds(\bar{s})}{d\bar{s}} = \tau(s(\bar{s}))$ *for all* $\bar{s} \in (0, \bar{s}_1)$,
(2) $s(0) = s_0$ *and*
(3) $\lim_{\bar{s} \to \bar{s}_1} s(\bar{s}) = s_1$.

Proof. Define the function $\tilde{\tau} : \mathbb{R} \times \mathbb{R} \to [0, \bar{\tau}]$,

$$\tilde{\tau}(\bar{s}, s) := \begin{cases} \tau(s_0) & , s < s_0 \\ \tau(s) & , s \in [s_0, s_1] \\ \tau(s_1) & , s > s_1 \end{cases}$$

Now consider the following initial value problem:

$$\begin{aligned} \frac{d\tilde{s}(\bar{s})}{d\bar{s}} &= \tilde{\tau}(\bar{s}, \tilde{s}) \geq 0 \quad , (\bar{s}, \tilde{s}) \in \mathbb{R} \times \mathbb{R} \\ \tilde{s}(0) &= s_0 \end{aligned}$$

$\tilde{\tau}$ is continuous and Lipschitz w.r.t. s on $\mathbb{R} \times \mathbb{R}$, so we can apply the Picard-Lindelöf theorem to get that for all $C > 0$ there exists a unique solution $\tilde{s}[C] : [-C, C] \to \mathbb{R}$ to the above initial value problem. (Cf. theorem B.8.)

Note that for all $C > 0$, $\tilde{s}[C]$ is monotonously increasing and

$$\tilde{s}[C_1](\bar{s}) = \tilde{s}[C_2](\bar{s}) \quad \forall C_1, C_2 > 0, \bar{s} \in [0, \min\{C_1, C_2\}]. \tag{10}$$

We now set $\bar{s}_1 := \inf\{C > 0 \mid \tilde{s}[C](C) \geq s_1\} \in (0, \infty]$. We either have that $\bar{s}_1$ is finite or that it is infinite.

- If $\bar{s}_1 < \infty$, we set $s := \tilde{s}[\bar{s}_1]|_{[0, \bar{s}_1)}$. Conditions (1) and (2) are obviously satisfied. It is also clear by the definitions of s and $\bar{s}_1$ that s maps to $[s_0, s_1)$. To see that (3) is also fulfilled, consider

$$\begin{aligned} s_1 \geq \lim_{\bar{s} \to \bar{s}_1^-} \underbrace{\tilde{s}[\bar{s}](\bar{s})}_{\leq s_1} &\overset{(10)}{=} \lim_{\bar{s} \to \bar{s}_1^-} \tilde{s}[\bar{s}_1](\bar{s}) = \lim_{\bar{s} \to \bar{s}_1^-} s(\bar{s}) \\ &= \lim_{\bar{s} \to \bar{s}_1^-} \tilde{s}[\bar{s}_1](\bar{s}) = \tilde{s}[\bar{s}_1](\bar{s}_1) \geq s_1. \end{aligned}$$

- If $\bar{s}_1 = \infty$ we define

$$s : [0, \bar{s}_1) \to [s_0, s_1), \;\; s(\bar{s}) := \tilde{s}[\bar{s}](\bar{s}) \;\; , \bar{s} \in [0, \bar{s}_1).$$

  Then s satisfies condition (2) and s must map to $[s_0, s_1)$ since it is monotonous. Furthermore, for any $\bar{s} \in (0, \bar{s}_1), \hat{s} \in (0, \bar{s})$ we have by (10) that $s(\hat{s}) = \tilde{s}[\bar{s}](\hat{s})$ which gives us condition (1).

  By monotonicity and (10), we know that the limit

$$\lim_{C \to \infty} \tilde{s}[C](C) = \sup\{\tilde{s}[C](C) \mid C > 0\}$$

  exists. Now assume that $\lim_{C \to \infty} \tilde{s}[C](C) < s_1$. We define

$$\underline{\tau} := \min_{s \in [s_0, \hat{s}]} \tau(s).$$

  Then $\underline{\tau} > 0$ by assumption 3.2. So for $C := (s_1 - s_0)/\underline{\tau}$ it holds that

$$\tilde{s}[C](C) \geq s_0 + C \cdot \underline{\tau} = s_0 + s_1 - s_0 = s_1 > \sup\{\tilde{s}[\bar{C}](\bar{C}) \mid \bar{C} > 0\}$$

  which is a contradiction. Hence, condition (3) must also be satisfied.

□

Notation 3.6
From now on, $\bar{s}_1$ and s denote the number and function from the previous lemma.

Example 3.7
We compute the transform for the simplest function τ that is consistent with the requirements we formulated in section 2.4. Consider

$$\tau : [s_0, s_1] \to \mathbb{R}, \;\; \tau(s) := \tau_0 \cdot \left(\frac{s_1 - s}{s_1 - s_0} \right).$$

We try to find $\bar{s}_1$ and $s : [0, \bar{s}_1) \to [s_0, s_1)$ such that

$$\begin{aligned} \frac{ds(\bar{s})}{d\bar{s}} = \tau(s(\bar{s})) &= \frac{\tau_0 s_1}{s_1 - s_0} - \frac{\tau_0}{s_1 - s_0} s(\bar{s}), \\ s(0) &= s_0, \\ \lim_{\bar{s} \to \bar{s}_1} s(\bar{s}) &= s_1. \end{aligned}$$

By lemma B.1 we know that

$$\begin{aligned} s(\bar{s}) &= \exp\left(-\int_0^{\bar{s}} \frac{\tau_0}{s_1 - s_0} d\lambda \right) \left(\int_0^{\bar{s}} \exp\left(\int_0^{\lambda} \frac{\tau_0}{s_1 - s_0} d\varrho \right) \frac{\tau_0 s_1}{s_1 - s_0} d\lambda + s_0 \right) \\ &= \exp\left(-\frac{\tau_0}{s_1 - s_0} \bar{s} \right) \left(s_1 \int_0^{\bar{s}} \exp\left(\frac{\tau_0}{s_1 - s_0} \lambda \right) \frac{\tau_0}{s_1 - s_0} d\lambda + s_0 \right) \\ &= \exp\left(-\frac{\tau_0}{s_1 - s_0} \bar{s} \right) \left(s_1 \exp\left(\frac{\tau_0}{s_1 - s_0} \bar{s} \right) - s_1 + s_0 \right) \\ &= s_1 - (s_1 - s_0) \exp\left(-\frac{\tau_0}{s_1 - s_0} \bar{s} \right). \end{aligned}$$

We see that $\bar{s}_1$ must be set to ∞.

Let now $T' \in (0, T]$. It will be used to restrict our problem to a smaller time interval in order to ensure that the solution operator is contractive.

Definition 3.8 (Spaces of variables)
Define

$$U_{T'} := L^1([0, T'] \times [s_0, s_1)) \times L^1([0, T']) \times L^1([0, T']) \times L^1([0, T']).$$

For $\theta \in \Theta$ we define the following associated function spaces:

$$\begin{aligned} X_{T'}^{\theta,1} := \Big\{ & x_1 \in L^1([0, T'] \times [s_0, s_1)) \mid \int_{s_0}^{s_1} x_1(t, s) ds \le \bar{v}(t, \theta) \text{ for almost all} \\ & t \in [0, T'] \text{ and } x_1(t, s) \ge 0 \text{ for almost all } t \in [0, T'], s \in [s_0, s_1) \Big\} \\ X_{T'}^{\theta,2} := \big\{ & x_2 \in L^1([0, T']) \mid \underline{N_{in}}(t, \theta) \le x_2(t) \le \overline{N_{in}}(t, \theta) \text{ for almost all } t \in [0, T'] \big\} \\ X_{T'}^{\theta,3} := \big\{ & x_3 \in L^1([0, T']) \mid 0 \le x_3(t) \le \overline{N_{out}}(t, \theta) \text{ for almost all } t \in [0, T'] \big\} \\ X_{T'}^{\theta,4} := \big\{ & x_4 \in L^1([0, T']) \mid 0 \le x_4(t) \le R_{ges} \text{ for almost all } t \in [0, T'] \big\} \\ X_{T'}^{\theta} := & X_{T'}^{\theta,1} \times X_{T'}^{\theta,2} \times X_{T'}^{\theta,3} \times X_{T'}^{\theta,4} \subset U_{T'} \end{aligned}$$

For $u = (u_1, u_2, u_3, u_4) \in U_{T'}$ and $t \in [0, T']$ we set

$$\|u\|_t := \int_{s_0}^{s_1} |u_1(t, s)| ds + |u_2(t)| + |u_3(t)| + |u_4(t)|$$

and

$$\|u\|_U := \int_0^{T'} \|u\|_t dt.$$

We introduce two operators that will be used to make formulas more readable:

Definition 3.9
For a function (or L^1 equivalence class of functions) $f : [0,T] \to \mathbb{R}$ we denote by

$$I[f] : [0,T] \to \mathbb{R}, \;\; I[f](t) := \int_0^t f(\lambda)d\lambda \quad , t \in [0,T]$$

the primitive of f.

Furthermore, $t \in [0,T]$, $\theta \in \Theta$, $x_2 \in X_{T'}^{\theta,2}$ and $\bar{s} \in [0, I[x_2](t)]$ we write

$$C[x_2](t,\bar{s}) := I[x_2]^{-1}\left(I[x_2](t) - \bar{s}\right)$$

where arguments are sometimes omitted if they are clear by the context.

Remark: To see why it is possible to define C that way, remember that any $x_2 \in X_{T'}^{\theta,2}$ is bounded from below almost everywhere by $\underline{N_{in}} > 0$. So its antiderivative $I[x_2]$ is strictly monotonically increasing (and continuous).

Definition 3.10
For $\theta \in \Theta$ we define the operators

$$\begin{aligned}
&v^\theta : X_{T'}^\theta \to L^1([0,T']) \times [s_0, s_1),\\
&N_{in}^\theta : X_{T'}^\theta \to L^1([0,T']),\\
&N_{out}^\theta : X_{T'}^\theta \to L^1([0,T']) \text{ and}\\
&R^\theta : X_{T'}^\theta \to L^1([0,T'])
\end{aligned}$$

such that

$$\begin{aligned}
v^\theta[x](t, s(\bar{s})) &:= \frac{1}{\tau(s(\bar{s}))}\\
&\cdot \begin{cases} \exp\left(-\int_0^t \mu(\lambda)d\lambda\right)\tau(s(\bar{s} - I[x_2](t)))v_0(s(\bar{s} - I[x_2](t))), & \bar{s} \geq I[x_2](t)\\ \exp\left(-\int_{C[x_2]}^t \mu(\lambda)d\lambda\right)\tau(s_0)h\left(C[x_2]\right), & \bar{s} < I[x_2](t) \end{cases}\\
N_{in}^\theta[x](t) &:= \exp\left(-\int_0^t \int_{s_0}^{s_1} \tau(s)x_1(\lambda, s)dsd\lambda\right)\\
&\cdot \left(\int_0^t \exp\left(\int_0^\lambda \int_{s_0}^{s_1} \tau(s)x_1(\varrho, s)dsd\varrho\right)\left(\beta(w - x_2(\lambda))^+ + \alpha x_3(\lambda)\right)d\lambda + N_{in}^0\right)\\
N_{out}^\theta[x](t) &:= \exp\left(-\int_0^t kx_4(\lambda) + \alpha + \delta d\lambda\right)\\
&\cdot \left(\int_0^t \exp\left(\int_0^\lambda kx_4(\varrho) + \alpha + \delta d\varrho\right)\int_{s_0}^{s_1} \nu(s)\mu(\lambda)x_1(\lambda, s)ds + \gamma(R_{ges} - x_4(\lambda))d\lambda\right.\\
&\quad \left. + N_{out}^0\right)\\
R^\theta[x](t) &:= \exp\left(-\int_0^t kx_3(\lambda) + \gamma d\lambda\right)\\
&\cdot \left(\int_0^t \exp\left(\int_0^\lambda kx_3(\varrho) + \gamma d\varrho\right)\gamma R_{ges}d\lambda + R_0\right)
\end{aligned}$$

for all $x = (x_1, x_2, x_3, x_4) \in X_{T'}^\theta$ and *almost all* $t \in [0,T']$ and $\bar{s} \in [0, \bar{s}_1)$.

Furthermore, we define

$$\begin{aligned}
S^\theta : X_{T'}^\theta &\to L^1([0,T'] \times [s_0, s_1)) \times L^1([0,T']) \times L^1([0,T']) \times L^1([0,T']),\\
S^\theta[x] &:= (v^\theta[x], N_{in}^\theta[x], N_{out}^\theta[x], R^\theta[x]).
\end{aligned}$$

The relation between the operators we just defined and the basic PDE system we want to analyze might not be that obvious. We will now show that the operator S^θ actually defines a solution to the following decoupled version of the PDE system:

For given functions $\bar{x}_1 \in C^0([0,T]\times[s_0,s_1))$, $\bar{x}_2, \bar{x}_3, \bar{x}_4 \in C^0([0,T])$ with $\bar{x}_2(0) = N_{in}(0)$ and $\theta = (v_0, h, N^0_{in}, N^0_{out}, R_0) \in \Theta$, find v, N_{in}, N_{out} and R with

(11)
$$\frac{\partial v}{\partial t} + \bar{x}_2(t)\frac{\partial(\tau(s)v)}{\partial s} + \mu(t)v = 0$$

(12)
$$\frac{dN_{in}}{dt} = \beta(w - \bar{x}_2(t))^+ + \alpha\bar{x}_3(t) - N_{in}\int_{s_0}^{s_1}\tau(s)\bar{x}_1(t,s)ds$$

(13)
$$\frac{dN_{out}}{dt} = \mu(t)\int_{s_0}^{s_1}\nu(s)\bar{x}_1(t,s)ds - k\bar{x}_4(t)N_{out} - (\alpha+\delta)N_{out} + \gamma(R_{ges} - \bar{x}_4(t))$$

(14)
$$\frac{dR}{dt} = -k\bar{x}_3(t)R + \gamma R_{ges} - \gamma R$$

for *all* $t \in (0,T')$ and $s \in (s_0, s_1)$ and

(15) $$v(t,s_0) = h(t), \;\; 0 < t \le T',$$

(16) $$v(0,s) = v_0(s), \;\; s_0 \le s \le s_1,$$

(17) $$N_{in}(0) = N^0_{in},$$

(18) $$N_{out}(0) = N^0_{out},$$

(19) $$R(0) = R_0.$$

Remark: We need to take care because the operator S^θ operates on $X^\theta_{T'}$, a space where each component is from a subspace of L^1, and for every differentiable function f there exists an equivalent (w.r.t. the L^1 norm) function that is *nowhere* differentiable.[19]

Hence, it will not be possible to argue that all representatives of S^θ solve such a PDE system. Instead, we will focus on one particular representative of S^θ — namely the unique continuous representative.

Similarly, as S^θ is actually applied to equivalence classes of functions, we will have to argue why we are allowed to "choose" the continuous ones in order to do our computations. The key here will be the first part of the fundamental theorem of analysis which is only applicable to integrals over continuous functions. So when we will use the theorem in the calculations of the derivatives, the continuous representative will be chosen implicitly.

3.2. **Relation to the PDE system.** Throughout this section, we write $\theta = (v_0, h, N^0_{in}, N^0_{out}, R_0)$ to denote some fixed element of Θ.

Lemma 3.11
Let $x = (x_1, x_2, x_3, x_4) \in X_{T'}$ such that there exists a continuous representative $\bar{x} = (\bar{x}_1, \bar{x}_2, \bar{x}_3, \bar{x}_4)$ of x with $\bar{x}_2(0) = N^0_{in}$. Then the unique continuous representatives of $v^\theta[x]$, $N^\theta_{in}[x]$, $N^\theta_{out}[x]$ and $R^\theta[x]$ solve the decoupled PDE system (11)-(19).

Proof. First note that the unique continuous representatives of the operator values are precisely the functions on the right hand side in the definition of the operators.

[19] One can for instance change the values of f at each rational point without leaving the equivalence class of f.

The claim for $N^\theta_{in}[x], N^\theta_{out}[x]$ and $R^\theta[x]$ follows from basic ODE theory (cf. lemma B.1). It is left to prove that the continuous representative of $v^\theta[x]$ satisfies (11), (15) and (16).

The boundary conditions (15) and (16) are obviously satisfied. It is left to show that (11) is fulfilled. So let $t \in (0,T)$ and $\bar{s} \in (0, \bar{s}_1)$. We denote the continuous representative of $v^\theta[x]$ by v and introduce the notation $\tilde{v}(t, s(\bar{s})) := \tau(s(\bar{s}))v(t, s(\bar{s}))$.

- Considering $\frac{\partial}{\partial \bar{s}}$: If $\bar{s} \geq I[x_2](t)$ by using the definition of v^θ we have that

$$\begin{aligned}
&\frac{\partial(\tau(s(\bar{s}))v(t,s(\bar{s})))}{\partial \bar{s}} = \frac{\partial \tilde{v}(t,s(\bar{s}))}{\partial \bar{s}} \\
&= \exp\left(-\int_0^t \mu(\lambda)d\lambda\right) \cdot \Big(\tau'(s(\bar{s}-I[x_2](t)))\tau(s(\bar{s}-I[x_2](t)))v_0(s(\bar{s}-I[x_2](t))) \\
&\quad + \tau^2(s(\bar{s}-I[x_2](t)))v_0'(s(\bar{s}-I[x_2](t)))\Big) \\
&= \tau'(s(\bar{s}-I[x_2](t)))\tilde{v}(t,s(\bar{s})) \\
&\quad + \tau^2(s(\bar{s}-I[x_2](t)))v_0'(s(\bar{s}-I[x_2](t)))\exp\left(-\int_0^t \mu(\lambda)d\lambda\right)
\end{aligned}$$

and thus

$$\begin{aligned}
&\lim_{\bar{s}\to I[x_2](t)^+} \frac{\partial \tilde{v}(t,s(\bar{s}))}{\partial \bar{s}} \\
&= \lim_{\bar{s}\to I[x_2](t)^+} \exp\left(-\int_0^t \mu(\lambda)d\lambda\right) \\
&\quad \cdot \Big(\tau'(s(\bar{s}-I[x_2](t)))\tau(s(\bar{s}-I[x_2](t)))v_0(s(\bar{s}-I[x_2](t))) \\
&\quad + \tau^2(s(\bar{s}-I[x_2](t)))v_0'(s(\bar{s}-I[x_2](t)))\Big) \\
&= \exp\left(-\int_0^t \mu(\lambda)d\lambda\right) \cdot \Big(\tau'(s_0)\tau(s_0)v_0(s_0) + \tau^2(s_0)v_0'(s_0)\Big).
\end{aligned}$$

For the case $\bar{s} < I[x_2](t)$ first consider

$$\begin{aligned}
\frac{\partial}{\partial \bar{s}} \exp\left(-\int_{C[x_2]}^t \mu(\lambda)d\lambda\right) &= \frac{\partial}{\partial \bar{s}} \exp\left(\int_0^{C[x_2]} \mu(\lambda)d\lambda - \int_0^t \mu(\lambda)d\lambda\right) \\
&= \exp\left(-\int_{C[x_2]}^t \mu(\lambda)d\lambda\right) \cdot \frac{\partial}{\partial \bar{s}} \int_0^{C[x_2]} \mu(\lambda)d\lambda \\
&= \exp\left(-\int_{C[x_2]}^t \mu(\lambda)d\lambda\right) \cdot \mu(C[x_2]) \frac{\partial C[x_2]}{\partial \bar{s}}.
\end{aligned}$$

So we have that

$$\begin{aligned}
&\frac{\partial(\tau(s(\bar{s}))v(t,s(\bar{s})))}{\partial \bar{s}} = \frac{\partial \tilde{v}(t,s(\bar{s}))}{\partial \bar{s}} \\
&= \exp\left(-\int_{C[x_2]}^t \mu(\lambda)d\lambda\right) \cdot \left(\tau(s_0)h'(C[x_2])\frac{\partial C}{\partial \bar{s}} + \tau(s_0)h(C[x_2])\mu(C[x_2])\frac{\partial C}{\partial \bar{s}}\right) \\
&= \exp\left(-\int_{C[x_2]}^t \mu(\lambda)d\lambda\right) \tau(s_0)h'(C[x_2])\frac{\partial C}{\partial \bar{s}} + \tilde{v}(t,s(\bar{s}))\mu(C[x_2])\frac{\partial C}{\partial \bar{s}}
\end{aligned}$$

where

$$\frac{\partial C}{\partial \bar{s}} = \frac{\partial\big(I[x_2]^{-1}\big(I[x_2](t) - \bar{s}\big)\big)}{\partial \bar{s}} = \frac{-1}{\bar{x}_2(I[x_2]^{-1}(I[x_2](t) - \bar{s}))}$$

and thus

$$\begin{aligned}
&\lim_{\bar{s}\to I[x_2](t)^-} \frac{\partial \tilde{v}(t, s(\bar{s}))}{\partial \bar{s}} \\
&= \lim_{\bar{s}\to I[x_2](t)^-} \exp\left(-\int_{C[x_2]}^{t} \mu(\lambda) d\lambda\right) \\
&\quad \cdot \left(\tau(s_0) h'(C[x_2]) \frac{\partial C}{\partial \bar{s}} + \tau(s_0) h(C[x_2]) \mu(C[x_2]) \frac{\partial C}{\partial \bar{s}}\right) \\
&= \exp\left(-\int_0^t \mu(\lambda) d\lambda\right) \cdot \left(\tau(s_0) h'(0) \frac{-1}{\bar{x}_2(0)} + \tau(s_0) h(0) \mu(0) \frac{-1}{\bar{x}_2(0)}\right).
\end{aligned}$$

Hence it holds that

$$\begin{aligned}
&\lim_{\bar{s}\to I[x_2](t)^-} \frac{\partial \tilde{v}(t, s(\bar{s}))}{\partial \bar{s}} = \lim_{\bar{s}\to I[x_2](t)^+} \frac{\partial \tilde{v}(t, s(\bar{s}))}{\partial \bar{s}} \\
\Leftrightarrow \quad & \tau'(s_0)\tau(s_0) v_0(s_0) + \tau^2(s_0) v_0'(s_0) = \tau(s_0) h'(0) \frac{-1}{\bar{x}_2(0)} + \tau(s_0) h(0) \mu(0) \frac{-1}{\bar{x}_2(0)} \\
\Leftrightarrow \quad & \bar{x}_2(0) \cdot (\tau'(s_0) v_0(s_0) + \tau(s_0) v_0'(s_0)) + h'(0) + h(0)\mu(0) = 0 \\
\Leftrightarrow \quad & N_{in}^0 \cdot (\tau'(s_0) v_0(s_0) + \tau(s_0) v_0'(s_0)) + h'(0) + h(0)\mu(0) = 0
\end{aligned}$$

where the last equation is true by definition 3.3.

We can now calculate the differential quotient at $(t, s(I[x_2](t)))$. First note that by the mean value theorem we can assign some

$$\xi_h \in (I[x_2](t), I[x_2](t) + h) \quad (\text{or } \xi_h \in (I[x_2](t) + h, I[x_2](t)))$$

to each $h > 0$ (or $h < 0$) such that

$$\frac{\tilde{v}(t, s(I[x_2](t) + h)) - \tilde{v}(t, s(I[x_2](t)))}{h} = \frac{\partial \tilde{v}}{\partial \bar{s}}(t, s(\xi_h)).$$

So we get that

$$\begin{aligned}
\frac{\partial \tilde{v}(t, s(I[x_2](t)))}{\partial \bar{s}} &= \lim_{h\to 0} \frac{\tilde{v}(t, s(I[x_2](t) + h)) - \tilde{v}(t, s(I[x_2](t)))}{h} \\
&= \lim_{h\to 0} \frac{\partial \tilde{v}}{\partial \bar{s}}(t, s(\xi_h)) \\
&= \lim_{\bar{s}\to I[x_2](t)} \frac{\partial \tilde{v}(t, s(\bar{s}))}{\partial \bar{s}} \\
&= \exp\left(-\int_0^t \mu(\lambda) d\lambda\right) \cdot \left(\tau'(s_0)\tau(s_0) v_0(s_0) + \tau^2(s_0) v_0'(s_0)\right)
\end{aligned}$$

exists and that the partial derivative is continuous in the direction $\bar{s}$.

- Considering $\frac{\partial}{\partial t}$: If $\bar{s} \geq I[x_2](t)$ we have that

$$\begin{aligned}
&\frac{\partial(\tau(s(\bar{s}))v(t,s(\bar{s})))}{\partial t} = \frac{\partial \tilde{v}(t,s(\bar{s}))}{\partial t} \\
&= \exp\left(-\int_0^t \mu(\lambda)d\lambda\right)\cdot\Big(-\mu(t)\tau(s(\bar{s}-I[x_2](t)))v_0(s(\bar{s}-I[x_2](t))) \\
&\quad + \tau'(s(\bar{s}-I[x_2](t)))\tau(s(\bar{s}-I[x_2](t)))(-\bar{x}_2(t))v_0(s(\bar{s}-I[x_2](t))) \\
&\quad + \tau(s(\bar{s}-I[x_2](t)))v_0'(s(\bar{s}-I[x_2](t)))\tau(s(\bar{s}-I[x_2](t)))(-\bar{x}_2(t))\Big) \\
&= -\mu(t)\tilde{v}(t,s(\bar{s})) - \bar{x}_2(t)\tau'(s(\bar{s}-I[x_2](t)))\tilde{v}(t,s(\bar{s})) \\
&\quad - \bar{x}_2(t)\tau^2(s(\bar{s}-I[x_2](t)))v_0'(s(\bar{s}-I[x_2](t)))\exp\left(-\int_0^t \mu(\lambda)d\lambda\right) \\
&= -\mu(t)\tilde{v}(t,s(\bar{s})) - \bar{x}_2(t)\frac{\partial \tilde{v}(t,s(\bar{s}))}{\partial \bar{s}}.
\end{aligned}$$

  Otherwise, it holds that

$$\begin{aligned}
&\frac{\partial(\tau(s(\bar{s}))v(t,s(\bar{s})))}{\partial t} = \frac{\partial \tilde{v}(t,s(\bar{s}))}{\partial t} \\
&= \exp\left(-\int_{C[x_2]}^t \mu(\lambda)d\lambda\right) \\
&\quad\cdot\left(\tau(s_0)h'(C[x_2])\frac{\partial C}{\partial t} + \tau(s_0)h(C[x_2])\big(\mu(C[x_2])\frac{\partial C}{\partial t} - \mu(t)\big)\right) \\
&= \exp\left(-\int_{C[x_2]}^t \mu(\lambda)d\lambda\right)\tau(s_0)h'(C[x_2])\frac{\partial C}{\partial t} + \tilde{v}(t,s(\bar{s}))\big(\mu(C[x_2])\frac{\partial C}{\partial t} - \mu(t)\big).
\end{aligned}$$

  With

$$\frac{\partial C}{\partial t} = \frac{\partial\big(I[x_2]^{-1}\big(I[x_2](t)-\bar{s}\big)\big)}{\partial t} = -\bar{x}_2(t)\frac{\partial C}{\partial \bar{s}}$$

  we also get in this case that

$$\frac{\partial(\tau(s(\bar{s}))v(t,s(\bar{s})))}{\partial t} \quad = -\mu(t)\tilde{v}(t,s(\bar{s})) - \bar{x}_2(t)\frac{\partial \tilde{v}(t,s(\bar{s}))}{\partial \bar{s}}.$$

  We now get the claim by continuity of $\tilde{v}$ and $\frac{\partial \tilde{v}}{\partial \bar{s}}$.

□

Remark: Not every equivalence class in $L^1([0,T'])$ contains a continuous representative. Consider, for example, the set of functions that are almost everywhere equal to the indicator function of the set $[0, \frac{T'}{2}]$.

However, for all $x \in X^\theta_{T'}$ the classes $v^\theta[x]$, $N^\theta_{in}[x]$, $N^\theta_{out}[x]$ and $R^\theta[x]$ each contain a continuous representative. (Cf. proof of lemma 3.11.) So in particular, for each fixed-point of S^θ there exists a continuous representative.

Lemma 3.12
Let $x = (x_1, x_2, x_3, x_4) \in X^\theta_{T'}$ with continuous representative $(\bar{x}_1, \bar{x}_2, \bar{x}_3, \bar{x}_4)$ where $\bar{x}_2(0) = N^0_{in}$. Then there exists a unique solution to the system (11)-(19).

Proof. The existence of a solution was already shown in lemma 3.11. The uniqueness of functions N_{in}, N_{out} and R follows from basic ODE theory. (Cf. lemma B.1.) It is left to show that v is unique.

For that purpose we will derive an explicit formula for v. This includes several steps. So let v be a solution of (11), (15) and (16). We will first transform the PDE and then use the method of characteristics to obtain an explicit solution.

(1) For $t \in [0, T']$ and $s \in [s_0, s_1)$ we write $\tilde{v}(t,s) := \tau(s)v(t,s)$. Then for all $t \in (0, T')$ and $s \in (s_0, s_1)$ we have that[20]

$$\begin{aligned}(11) \quad &\Leftrightarrow \quad \frac{\partial}{\partial t}\left(\frac{\tilde{v}(t,s)}{\tau(s)}\right) + \bar{x}_2(t)\frac{\partial \tilde{v}(t,s)}{\partial s} + \mu(t)\left(\frac{\tilde{v}(t,s)}{\tau(s)}\right) = 0 \\ &\Leftrightarrow \quad \frac{\partial \tilde{v}(t,s)}{\partial t} + \bar{x}_2(t)\tau(s)\frac{\partial \tilde{v}(t,s)}{\partial s} + \mu(t)\tilde{v}(t,s) = 0\end{aligned}$$

(2) The idea now is to get rid of the size dependent growth factor $\tau(s)$ by transforming the size variable. I.e. we want to interpret the variable s as function $s(\bar{s})$ and then use $\bar{s}$ as "new" size variable.

Using the function $s(\bar{s})$ defined above, it holds that

$$\frac{\partial \tilde{v}(t, s(\bar{s}))}{\partial \bar{s}} = \frac{ds}{d\bar{s}}\frac{\partial \tilde{v}(t,s)}{\partial s} \overset{\text{lemma 3.5}}{=} \tau(s(\bar{s}))\frac{\partial \tilde{v}(t,s)}{\partial s}$$

and hence

$$\begin{aligned}(11) \quad &\Leftrightarrow \quad \frac{\partial \tilde{v}(t, s(\bar{s}))}{\partial t} + \bar{x}_2(t)\tau(s(\bar{s}))\frac{\partial \tilde{v}(t, s(\bar{s}))}{\partial s} + \mu(t)\tilde{v}(t, s(\bar{s})) = 0 \\ &\Leftrightarrow \quad \frac{\partial \tilde{v}(t, s(\bar{s}))}{\partial t} + \bar{x}_2(t)\frac{\partial \tilde{v}(t, s(\bar{s}))}{\partial \bar{s}} + \mu(t)\tilde{v}(t, s(\bar{s})) = 0\end{aligned}$$

for all $t \in (0, T')$ and $\bar{s} \in (0, \bar{s}_1)$.

(3) We now use the method of characteristics in order to find an explicit formula for $\tilde{v}(t, s(\bar{s}))$. We introduce

$$\begin{aligned}\phi_1(y) &:= y + c_1, \\ \phi_2(y) &:= I[x_2](y + c_1) + c_2 \\ \text{and} \quad z(y) &:= \tilde{v}(\phi_1(y), s(\phi_2(y))),\end{aligned}$$

where $c_1, c_2 \in \mathbb{R}$ are constants.

It holds that

$$\begin{aligned}\frac{dz(y)}{dy} &= \frac{d\tilde{v}(\phi_1(y), s(\phi_2(y)))}{dy} \\ &= \frac{\partial \tilde{v}(\phi_1(y), s(\phi_2(y)))}{\partial \phi_1} \cdot \frac{d\phi_1(y)}{dy} \\ &\quad + \frac{\partial \tilde{v}(\phi_1(y), s(\phi_2(y)))}{\partial s} \cdot \frac{ds(\phi_2(y))}{d\phi_2} \cdot \frac{d\phi_2(y)}{dy} \\ &= \frac{\partial \tilde{v}(\phi_1(y), s(\phi_2(y)))}{\partial \phi_1} \cdot 1 + \frac{\partial \tilde{v}(\phi_1(y), s(\phi_2(y)))}{\partial s} \cdot \bar{x}_2(\phi_1(y)) \\ &= -\mu(\phi_1(y))\tilde{v}(\phi_1(y), s(\phi_2(y))) \\ &= -\mu(\phi_1(y))z(y).\end{aligned}$$

Hence, $\tilde{v}$ can be described by this ODE along the curve $(\phi_1(y), s(\phi_2(y)))$:

$$\begin{aligned}\tilde{v}(y + c_1, s(I[x_2](y + c_1) + c_2)) = \tilde{v}(\phi_1(y), s(\phi_2(y))) &= z(y) \\ &= \exp\left(-\int_0^y \mu(\phi_1(\lambda))d\lambda\right) z(0) \\ &= \exp\left(-\int_0^y \mu(\lambda + c_1)d\lambda\right) \tilde{v}(c_1, s(I[x_2](c_1) + c_2))\end{aligned}$$

(4) Define the set $\Gamma := \{\{0\} \times [s_0, s_1)\} \cup \{[0, T'] \times \{s_0\}\}$. Now, if a curve $(\phi_1(y), s(\phi_2(y)))$ starts in Γ then one of the boundary conditions (15) and (16) can be applied in order to determine $\tilde{v}(c_1, s(I[x_2](c_1) + c_2))$.

[20] Recall that $\tau(s) > 0$ for all $s \in [s_0, s_1)$.

Let us analyze how c_1 and c_2 have to be chosen to get the curve starting in Γ: If we want $(c_1, s(I[x_2](c_1) + c_2))$ to be in Γ then it must hold that $c_1 = 0$ or $s(I[x_2](c_1) + c_2)) = s_0$ ($\Leftrightarrow I[x_2](c_1) + c_2 = 0$). This leads to two different cases:

(a) $c_1 = 0$, $c_2 \in [0, \bar{s}_1)$ arbitrary:
For all $y \in [0, T']$ with $I[x_2](y) \leq \bar{s}_1 - c_2$ we have that

$$\tilde{v}(y, s(I[x_2](y) + c_2)) = \exp\left(-\int_0^y \mu(\lambda)d\lambda\right)\tau(s(c_2))v_0(s(c_2)).$$

We can now use the solution along those characteristics in order to get a solution in $\{(t, s(\bar{s})) \mid t \in [0, T'], \bar{s} \in [I[x_2](t), \bar{s}_1)\}$ that takes the parameters t and $\bar{s}$:

$$\begin{aligned}
&t \stackrel{!}{=} \phi_1(y) = y + c_1 = y,\\
&\bar{s} \stackrel{!}{=} \phi_2(y) = I[x_2](y + c_1) + c_2 = I[x_2](y) + c_2\\
\Rightarrow &y = t,\ c_2 = \bar{s} - I[x_2](y) = \bar{s} - I[x_2](t)\\
\Rightarrow &\tilde{v}(t, s(\bar{s})) = \tilde{v}(y, s(I[x_2](y) + c_2))\\
&\qquad = \exp\left(-\int_0^t \mu(\lambda)d\lambda\right)\tau(s(\bar{s} - I[x_2](t)))v_0(s(\bar{s} - I[x_2](t)))
\end{aligned}$$

This proves the equation for $\tau(s(\bar{s}))v(t, s(\bar{s}))$ in the case that $\bar{s} \geq I[x_2](t)$.

(b) $c_1 \in [0, T']$ arbitrary, $c_2 = -I[x_2](c_1)$:
Here we have

$$\begin{aligned}
&\tilde{v}(y + c_1, s(I[x_2](y + c_1) - I[x_2](c_1)))\\
&\qquad = \exp\left(-\int_0^y \mu(\lambda + c_1)d\lambda\right)\tau(s_0)h(c_1).
\end{aligned}$$

It holds that

$$\begin{aligned}
&\bar{s} \stackrel{!}{=} \phi_2(y) = I[x_2](y + c_1) - I[x_2](c_1)\\
\Rightarrow\quad &I[x_2](c_1) = I[x_2](t) - \bar{s}\\
\Rightarrow\quad &c_1 = I[x_2]^{-1}\left(I[x_2](t) - \bar{s}\right) = C[x_2](t, \bar{s}).
\end{aligned}$$

Hence

$$\begin{aligned}
&t \stackrel{!}{=} \phi_1(y) = y + c_1 = y + C[x_2](t, \bar{s})\\
\Rightarrow\quad &y = t - C[x_2](t, \bar{s}) = t - I[x_2]^{-1}\left(I[x_2](t) - \bar{s}\right)
\end{aligned}$$

and we get

$$\begin{aligned}
\tilde{v}(t, s(\bar{s})) &= \tilde{v}(y + c_1, s(I[x_2](y + c_1) - I[x_2](c_1)))\\
&= \exp\left(-\int_0^{t - C[x_2]} \mu(\lambda + C[x_2])d\lambda\right)\tau(s_0)h\left(C[x_2]\right)\\
&= \exp\left(-\int_{C[x_2]}^{t} \mu(\lambda)d\lambda\right)\tau(s_0)h\left(C[x_2]\right)
\end{aligned}$$

as solution in

$$\{(t, s(\bar{s})) \mid t \in [0, T'], \bar{s} \in [0, \min(\bar{s}_1, I[x_2](t)))\}.$$

This proves the equation for $\tau(s(\bar{s}))v(t, s(\bar{s}))$ in the case that $\bar{s} < I[x_2](t)$.

□

Theorem 3.13
Let $x = (x_1, x_2, x_3, x_4) \in X^\theta_{T'}$. Then x is a fixed-point of S^θ if and only if its continuous representative solves the basic PDE on $[0, T']$.

Proof. "$\Rightarrow$" follows by lemma 3.11. On the other hand, if the continuous representative $\bar{x}$ of x solves the basic PDE on $[0, T']$, then it also solves the system (11)-(19). But since the solution to this system is unique by lemma 3.12 and equal to the continuous representative of

$$S^\theta[x] = (v^\theta[x], N^\theta_{in}[x], N^\theta_{out}[x], R^\theta[x])$$

by lemma 3.11, we get that x must coincide $S^\theta[x]$ almost everywhere, i.e. x must be a fixed-point of S^θ. □

3.3. **Bounds.** As in the previous section, $\theta = (v_0, h, N^0_{in}, N^0_{out}, R_0)$ denotes some fixed element of Θ throughout this section.

Proposition 3.14 (Solution bounds)
For all $x = (x_1, x_2, x_3, x_4) \in X^\theta_{T'}$ that have a continuous representative it holds that

$$\begin{aligned}
&\int_{s_0}^{s_1} v^\theta[x](t,s)ds \le \bar{v}(t,\theta),\\
&v^\theta[x](t,s) \ge 0,\\
&N^\theta_{in}[x](t) \in [\underline{N_{in}}(t,\theta), \overline{N_{in}}(t,\theta)],\\
&N^\theta_{out}[x](t) \in [0, \overline{N_{out}}(t,\theta)] \text{ and}\\
&R^\theta[x](t) \in [0, R_{ges}]
\end{aligned}$$

for almost all $t \in [0, T']$ and $s \in [s_0, s_1)$.

Proof. It can easily be seen that $v^\theta, N^\theta_{in}, N^\theta_{out}$ and R^θ are non-negative almost everywhere by checking the definition of the operators.

To prove the other bounds we let $\bar{x} = (\bar{x}_1, \bar{x}_2, \bar{x}_3, \bar{x}_4)$ denote the continuous representative of x and use v, N_{out}, N_{in} and R to refer to the continuous representatives of $v^\theta[x]$, $N^\theta_{in}[x]$, $N^\theta_{out}[x]$ and $R^\theta[x]$ respectively.

v : Let $t \in [0, T']$. We have that

$$\begin{aligned}
\int_{s_0}^{s_1} v(t,s)ds &= \int_0^{\bar{s}_1} \tau(s(\bar{s}))v(t, s(\bar{s}))d\bar{s}\\
&= \int_0^{I[x_2](t)} \tau(s(\bar{s}))v(t, s(\bar{s}))d\bar{s} + \int_{I[x_2](t)}^{\bar{s}_1} \tau(s(\bar{s}))v(t, s(\bar{s}))d\bar{s}\\
&\le \int_0^{I[x_2](t)} \tau(s_0)h(C[x_2])d\bar{s}\\
&\quad + \int_{I[x_2](t)}^{\bar{s}_1} \tau(s(\bar{s} - I[x_2](t)))v(t, s(\bar{s} - I[x_2](t)))d\bar{s}\\
&\le \tau(s_0)\bar{h}I[x_2](t) + \int_0^{\bar{s}_1} \tau(s(\bar{s}))v_0(s(\bar{s}))d\bar{s}\\
&\le \tau(s_0)\bar{h}t\overline{N_{in}}(t,\theta) + \int_{s_0}^{s_1} v_0(s)ds\\
&= \tau(s_0)\bar{h}t\overline{N_{in}}(t,\theta) + \|v_0\|_1.
\end{aligned}$$

N_{out} : By lemma 3.11 we have for all $t \in (0, T')$ that

$$\begin{aligned}\frac{d}{dt}N_{out}(t) &= \int_{s_0}^{s_1} \nu(s)\mu(t)\bar{x}_1(t,s)ds - k\bar{x}_4(t)N_{out}(t) \\ &\quad - (\alpha+\delta)N_{out}(t) + \gamma(R_{ges} - \bar{x}_4(t)) \\ &\leq \bar{\nu}\bar{\mu}\int_{s_0}^{s_1} \bar{x}_1(t,s)ds - (k\bar{x}_4(t) + \alpha + \delta)N_{out}(t) + \gamma(R_{ges} - \bar{x}_4(t)) \\ &\leq \bar{\nu}\bar{\mu}\bar{v}(t,\theta) - (\alpha+\delta)N_{out}(t) + \gamma R_{ges}.\end{aligned}$$

Hence

$$N_{out}(t) = \overline{N_{out}}(t,\theta) \quad \Rightarrow \quad \frac{d}{dt}N_{out}(t) \leq 0.$$

This implies that $N_{out}(t) \leq \overline{N_{out}}(t,\theta)$ for all $t \in [0, T']$ (by lemmata B.2 and B.3).

R : Here we have for all $t \in (0, T')$ that

$$\begin{aligned}\frac{d}{dt}R(t) &= -k\bar{x}_3(t)R + \gamma R_{ges} - \gamma R \\ &\leq \gamma(R_{ges} - R).\end{aligned}$$

We get that

$$R(t) = R_{ges} \quad \Rightarrow \quad \frac{d}{dt}R \leq 0$$

which proves that $R(t) \leq R_{ges}$ for all $t \in [0, T']$ if $R(0) = R_0 \leq R_{ges}$.

N_{in} : For all $t \in (0, T')$ it holds that

$$\begin{aligned}\frac{d}{dt}N_{in}(t) &= \beta(w - \bar{x}_2(t))^+ + \alpha\bar{x}_3(t) - \tau N_{in}\int_{s_0}^{s_1} \bar{x}_1(t,s)ds \\ &\leq \beta w + \alpha\bar{x}_3(t) \leq \beta w + \alpha\overline{N_{out}}(t,\theta) \\ &\leq \alpha C_1 + \beta w + \alpha C_2 t\overline{N_{in}}(t,\theta) = \frac{\partial\overline{N_{in}}(t,\theta)}{\partial t}.\end{aligned}$$

Together with

$$\overline{N_{in}}(0,\theta) = N_{in}^0 = N_{in}(0)$$

we get that $N_{in}(t) \leq \overline{N_{in}}(t,\theta)$.

For the lower bound let again $t \in (0, T')$. It holds that

$$\begin{aligned}\frac{d}{dt}N_{in}(t) &= \beta(w - \bar{x}_2(t))^+ + \alpha\bar{x}_3(t) - N_{in}\int_{s_0}^{s_1} \tau(s)\bar{x}_1(t,s)ds \\ &\geq \beta(w - \bar{x}_2(t)) - N_{in}\bar{\tau}\bar{v}(t,\theta).\end{aligned}$$

Hence

$$N_{in}(t) = \underline{N_{in}}(t,\theta) \quad \Rightarrow \quad \frac{d}{dt}N_{in}(t) \geq 0$$

which gives us the lower bound for N_{in}. (Cf. lemmata B.2 and B.3).

This finishes the proof since members of the same equivalence class in $U_{T'}$ must coincide almost everywhere. □

The proposition we just proved tells us that the operator S^θ maps all elements from $X^\theta_{T'}$ with continuous representative in $X^\theta_{T'}$. This will later be important since we intend to use an approach similar to the Banach's fixed-point theorem.

3.4. **Auxiliary results.** The final goal of this section is to prove a statement of the form

$$\|S^{\theta^a}[x^a] - S^{\theta^b}[x^b]\|_t \leq const(\theta^a, \eta) \left(\int_0^t \|x^a - x^b\|_\lambda d\lambda + \|\theta^a - \theta^b\|_\Theta \right)$$

for (almost all) $t \in [0, T']$, $\theta^a, \theta^b \in \Theta$ with $\|\theta^a - \theta^b\|_\Theta - \eta$ and $x^a \in X_{T'}^{\theta^a}$, $x^b \in X_{T'}^{\theta^b}$.

This statement is very similar to Lipschitz continuity and will then later be exploited in order to prove both that S^θ is contractive for T' sufficiently small and that the solution to the basic PDE system depends continuously on the given data θ.

In order to achieve that goal we now handle individual parts of the solution operator functions by the following lemma:

Lemma 3.15
Let $\theta^a = (v_0^a, h^a, N_{in}^{0,a}, N_{out}^{0,a}, R_0^a) \in \Theta$ and $\eta > 0$. Then for all

$$\theta^b = (v_0^b, h^b, N_{in}^{0,b}, N_{out}^{0,b}, R_0^b) \in \Theta$$

with $\|\theta^a - \theta^b\|_\Theta < \eta$ it holds that

$$h^i(t),\ v_0^i(s),\ \underline{N_{in}}(t, \theta^i),\ \overline{N_{in}}(t, \theta^i),\ \overline{N_{out}}(t, \theta^i),\ \bar{v}(t, \theta^i) \leq const(\theta^a, \eta)$$

for $i = a, b$ and all $t \in [0, T], s \in [s_0, s_1]$.

Proof. For $i = a$ the statement is trivial. Now let $t \in [0, T]$. It holds that

$$|h^a(t) - h^b(t)| \leq \|h^a - h^b\|_\infty \leq \|\theta^a - \theta^b\|_\Theta < \eta.$$

This implies that

$$h^b(t) \leq const(\theta^a, \eta)$$

and also

$$\bar{h}(t, \theta^b) \leq \bar{h}(t, \theta^a) + \eta \leq const(\theta^a, \eta).$$

The rest is clear by definitions 3.3 and 3.4. □

$N_{in}^\theta[x]$, $N_{out}^\theta[x]$ and $R^\theta[x]$ are all of the same form. So here, a general result for such functions will prove beneficial:

Proposition 3.16
Let $\theta^a \in \Theta$, $\eta > 0$, p and g both be non-negative functions defined on $[0, T'] \times U_{T'} \times \Theta$ and y_0 be a function defined on Θ. Furthermore, for $t \in [0, T']$, $u \in U_{T'}$ and $\theta \in \Theta$ define

$$y(t, u, \theta) := \exp\left(- \int_0^t p(\lambda, u, \theta) d\lambda \right) \cdot \left(\int_0^t \exp\left(\int_0^\lambda p(\varrho, u, \theta) d\varrho \right) g(\lambda, u, \theta) d\lambda + y_0(\theta) \right).$$

If it holds that

$$p(t, x^a, \theta^a),\ p(t, x^b, \theta^b),\ g(t, x^a, \theta^a),\ g(t, x^b, \theta^b) \leq const(\theta^a, \eta) \tag{20}$$

and

$$|p(t, x^a, \theta^a) - p(t, x^b, \theta^b)|,\ |g(t, x^a, \theta^a) - g(t, x^b, \theta^b)| \leq const(\theta^a, \eta) \cdot \|x^a - x^b\|_t \tag{21}$$

for all $\theta^b \in \Theta$ with $\|\theta^a - \theta^b\| < \eta$ and $x^a \in X_{T'}^{\theta^a}$, $x^b \in X_{T'}^{\theta^b}$, then we also have

$$|y(t, x^a, \theta^a) - y(t, x^b, \theta^b)| \leq const(\theta^a, \eta) \cdot \left(\int_0^t \|x^a - x^b\|_\lambda d\lambda + |y_0(\theta^a) - y_0(\theta^b)| \right)$$

for all $\theta^b \in \Theta$ with $\|\theta^a - \theta^b\| < \eta$ and $x^a \in X_{T'}^{\theta^a}$, $x^b \in X_{T'}^{\theta^b}$.

Proof. Let θ^a, θ^b, x^a, x^b, p, g and y_0 all be defined as described above and assume that equations (20) and (21) hold.

It holds that

$$
\begin{aligned}
(22)\qquad & \Big| \exp\left(-\int_0^t p(\lambda, x^a, \theta^a)d\lambda\right) - \exp\left(-\int_0^t p(\lambda, x^b, \theta^b)d\lambda\right) \Big| \\
& \overset{\text{lemma B.6}}{\leq} \Big| \int_0^t p(\lambda, x^a, \theta^a) - p(\lambda, x^b, \theta^b)d\lambda \Big| \\
& \leq \int_0^t |p(\lambda, x^a, \theta^a) - p(\lambda, x^b, \theta^b)|d\lambda \\
& \overset{(21)}{\leq} const(\theta^a, \eta) \cdot \int_0^t \|x^a - x^b\|_\lambda d\lambda.
\end{aligned}
$$

Analogously we get that

$$
\begin{aligned}
(23)\qquad & \Big| \exp\left(\int_0^t p(\lambda, x^a, \theta^a)d\lambda\right) - \exp\left(\int_0^t p(\lambda, x^b, \theta^b)d\lambda\right) \Big| \\
& \leq const(\theta^a, \eta) \cdot \int_0^t \|x^a - x^b\|_\lambda d\lambda.
\end{aligned}
$$

We also have that

$$
\begin{aligned}
(24)\qquad & \Big| \int_0^t \exp\left(\int_0^\lambda p(\varrho, x^a, \theta^a)d\varrho\right) g(\lambda, x^a, \theta^a)d\lambda \Big| \\
& \overset{(20)}{\leq} \int_0^t \exp\left(\int_0^\lambda const(\theta^a, \eta)d\varrho\right) const(\theta^a, \eta)d\lambda \\
& \leq const(\theta^a, \eta).
\end{aligned}
$$

So we get that

$$
\begin{aligned}
(25)\quad & \Big| \int_0^t \exp\left(\int_0^\lambda p(\varrho, x^a, \theta^a)d\varrho\right) g(\lambda, x^a, \theta^a)d\lambda \\
& \quad - \int_0^t \exp\left(\int_0^\lambda p(\varrho, x^b, \theta^b)d\varrho\right) g(\lambda, x^b, \theta^b)d\lambda \Big| \\
& \leq \int_0^t \Big| \exp\left(\int_0^\lambda p(\varrho, x^a, \theta^a)d\varrho\right) g(\lambda, x^a, \theta^a) \\
& \quad - \exp\left(\int_0^\lambda p(\varrho, x^b, \theta^b)d\varrho\right) g(\lambda, x^b, \theta^b) \Big| d\lambda \\
& \overset{\text{lemma B.4}}{\leq} \int_0^t \exp\left(\int_0^\lambda p(\varrho, x^a, \theta^a)d\varrho\right) \cdot |g(\lambda, x^a, \theta^a) - g(\lambda, x^b, \theta^b)| \\
& \quad + g(\lambda, x^b, \theta^b) \cdot \Big| \exp\left(\int_0^\lambda p(\varrho, x^a, \theta^a)d\varrho\right) - \exp\left(\int_0^\lambda p(\varrho, x^b, \theta^b)d\varrho\right) \Big| d\lambda \\
& \overset{(20),(21),(23)}{\leq} \int_0^t const(\theta^a, \eta) \cdot \|x^a - x^b\|_\lambda d\lambda \\
& \leq const(\theta^a, \eta) \cdot \int_0^t \|x^a - x^b\|_\lambda d\lambda.
\end{aligned}
$$

Putting things together, we get that

$$\begin{aligned}
&|y(t,x^a,\theta^a) - y(t,x^b,\theta^b)| \\
&\overset{\text{lemma B.4}}{\underset{(22)-(25)}{\leq}} const(\theta^a,\eta)\cdot\int_0^t \|x^a - x^b\|_\lambda d\lambda + |y_0(\theta^a) - y_0(\theta^b)| \\
&\qquad + (const(\theta^a,\eta) + y_0(\theta^a))\cdot const(\theta^a,\eta)\cdot\int_0^t \|x^a - x^b\|_\lambda \\
&\leq const(\theta^a,\eta)\cdot\Big(\int_0^t \|x^a - x^b\|_\lambda d\lambda + |y_0(\theta^a) - y_0(\theta^b)|\Big).
\end{aligned}$$

□

We now apply the previous lemma to $N^\theta_{in}[x]$, $N^\theta_{out}[x]$ and $R^\theta[x]$:

Proposition 3.17
Let $\theta^a \in \Theta$ and $\eta > 0$. There exist non-negative constants $C_{in}(\theta^a,\eta)$, $C_{out}(\theta^a,\eta)$ and $C_R(\theta^a,\eta)$ such that for all $\theta^b \in \Theta$ with $\|\theta^a - \theta^b\|_\Theta < \eta$ and $x^a \in X^{\theta^a}_{T'}$, $x^b \in X^{\theta^b}_{T'}$ it holds that

$$\begin{aligned}
\big|N^{\theta^a}_{in}[x^a](t) - N^{\theta^b}_{in}[x^b](t)\big| &\leq C_{in}(\theta^a,\eta)\left(\int_0^t \|x^a - x^b\|_\lambda d\lambda + \|\theta^a - \theta^b\|_\Theta\right), \\
\big|N^{\theta^a}_{out}[x^a](t) - N^{\theta^b}_{out}[x^b](t)\big| &\leq C_{out}(\theta^a,\eta)\left(\int_0^t \|x^a - x^b\|_\lambda d\lambda + \|\theta^a - \theta^b\|_\Theta\right), \\
\big|R^{\theta^a}[x^a](t) - R^{\theta^b}[x^b](t)\big| &\leq C_R(\theta^a,\eta)\left(\int_0^t \|x^a - x^b\|_\lambda d\lambda + \|\theta^a - \theta^b\|_\Theta\right)
\end{aligned}$$

for almost all $t \in [0,T']$.

Proof. We prove the statement for N^θ_{in}. Analogously, the statements for N^θ_{out} and R^θ can be proved.

For $t \in [0,T']$, $u = (u_1,u_2,u_3,u_4) \in U_{T'}$, $\theta \in \Theta$ define

$$\begin{aligned}
p(t,u,\theta) &:= \int_{s_0}^{s_1} \tau(s)u_1(t,s)ds, \\
g(t,u,\theta) &:= \beta(w - u_2(t))^+ + \alpha u_3(t).
\end{aligned}$$

Now let $\theta^a,\theta^b \in \Theta$ with $\|\theta^a - \theta^b\| < \eta$ and $x^a \in X^{\theta^a}_{T'}$, $x^b \in X^{\theta^b}_{T'}$. For $i \in a,b$ it holds that

$$\begin{aligned}
p(t,x^i,\theta^i) \leq \bar\tau\int_{s_0}^{s_1} x^i_1(t,s)ds \leq \bar\tau\bar v(t,\theta^i) &\overset{\text{lemma 3.15}}{\leq} const(\theta^a,\eta), \\
g(t,x^i,\theta^i) \leq \beta w + \alpha N_{out}(t,\theta^i) &\overset{\text{lemma 3.15}}{\leq} const(\theta^a,\eta)
\end{aligned}$$

and

$$\begin{aligned}
|p(t,x^a,\theta^a) - p(t,x^b,\theta^b)| &\leq \bar\tau\int_{s_0}^{s_1} |x^a_1(t,s) - x^b_1(t,s)|ds \\
&\leq const(\theta^a,\eta)\cdot\|x^a - x^b\|_t, \\
|g(t,x^a,\theta^a) - g(t,x^b,\theta^b)| &\leq \beta\cdot|x^a_2(t) - x^b_2(t)| + \alpha\cdot|x^a_3(t) - x^b_3(t)| \\
&\leq const(\theta^a,\eta)\cdot\|x^a - x^b\|_t.
\end{aligned}$$

Applying proposition 3.16 gives us the claim for N^θ_{in}. □

We will now derive the same kind of estimation for $v^\theta[x]$:

Proposition 3.18
Let $\theta^a \in \Theta$ and $\eta > 0$. There exists a non-negative constant $C_v(\theta^a, \eta)$ such that for all $\theta^b \in \Theta$ with $\|\theta^a - \theta^b\|_\Theta < \eta$ and $x^a \in X_{T'}^{\theta^a}$, $x^b \in X_{T'}^{\theta^b}$ it holds that

$$\int_{s_0}^{s_1} \left| v^{\theta^a}[x^a](t,s) - v^{\theta^b}[x^b](t,s) \right| ds \leq C_v(\theta^a, \eta) \left(\int_0^t \|x^a - x^b\|_\lambda d\lambda + \|\theta^a - \theta^b\|_\Theta \right)$$

for almost all $t \in [0, T']$.

Proof. Let $t \in [0, T']$, $\theta^a \in \Theta$, $\eta > 0$, $\theta^b \in \Theta$ with $\|\theta^a - \theta^b\|_\Theta < \eta$ and $x^a \in X_{T'}^{\theta^a}$, $x^b \in X_{T'}^{\theta^b}$. Throughout this proof, v^a and v^b denote the continuous representatives of the equivalence classes of $v^{\theta^a}[x^a]$ and $v^{\theta^b}[x^b]$ respectively.

Set

$$\bar{s}_{min} := \min\left\{ I[x_2^a](t), I[x_2^b](t), \bar{s}_1 \right\},$$
$$\bar{s}_{max} := \min\left\{ \max\{I[x_2^a](t), I[x_2^b](t)\}, \bar{s}_1 \right\}.$$

We will use these constants to split the integral over s into three parts where v^a and v^b are described by the same kind of formula on $[s_0, s(\bar{s}_{min}))$ and $(s(\bar{s}_{max}), s(\bar{s}_1))$.

As before, the general approach will then be to show that the individual parts of some product are bounded and satisfy the claim so we can invoke lemma B.4 to get the statement for the whole term.

We first handle the integral over the interval $(s(\bar{s}_{max}), s(\bar{s}_1))$. It holds that

$$\begin{aligned} (26) \qquad & \int_{\bar{s}_{max}}^{\bar{s}_1} \tau(s(\bar{s} - I[x_2^b](t))) \cdot \left| v_0^a(s(\bar{s} - I[x_2^b](t))) - v_0^b(s(\bar{s} - I[x_2^b](t))) \right| d\bar{s} \\ & \leq \int_{\bar{s}_{max} - I[x_2^b](t)}^{\bar{s}_1 - I[x_2^b](t)} \tau(s(\bar{s})) \cdot \left| v_0^a(s(\bar{s})) - v_0^b(s(\bar{s})) \right| d\bar{s} \\ & = \int_{s_0}^{s_1} \left| v_0^a(s) - v_0^b(s) \right| ds \\ & \leq \|\theta^a - \theta^b\|_\Theta. \end{aligned}$$

With $L_v := \sup_{s \in (s_0, s_1)} (v_0^a)'(s)$ we get that

$$\begin{aligned} (27) \qquad & \int_{\bar{s}_{max}}^{\bar{s}_1} \tau(s(\bar{s} - I[x_2^b](t))) \cdot \left| v_0^a(s(\bar{s} - I[x_2^a](t))) - v_0^a(s(\bar{s} - I[x_2^b](t))) \right| d\bar{s} \\ & \overset{\text{lemma B.5}}{\leq} L_v \bar{\tau} \cdot |I[x_2^a](t) - I[x_2^b](t)| \cdot \int_{\bar{s}_{max}}^{\bar{s}_1} \tau(s(\bar{s} - I[x_2^b](t))) d\bar{s} \\ & \leq L_v \bar{\tau} \cdot \int_0^t |x_2^a(\lambda) - x_2^b(\lambda)| d\lambda \cdot (s_1 - s_0) \\ & \leq const(\theta^a) \cdot \int_0^t \|x^a - x^b\|_\lambda d\lambda. \end{aligned}$$

Now define $L_\tau := \sup_{s \in (s_0, s_1)} \tau'(s)$. It holds that

$$\begin{aligned} (28) \qquad & \int_{\bar{s}_{max}}^{\bar{s}_1} v_0^a(s(\bar{s} - I[x_2^a](t))) \cdot \left| \tau(s(\bar{s} - I[x_2^a](t))) - \tau(s(\bar{s} - I[x_2^b](t))) \right| d\bar{s} \\ & \overset{\text{lemma B.5}}{\leq} L_\tau \bar{\tau} \cdot |I[x_2^a](t) - I[x_2^b](t)| \cdot \int_{\bar{s}_{max}}^{\bar{s}_1} v_0^a(s(\bar{s} - I[x_2^a](t))) d\bar{s} \\ & \leq L_\tau \bar{\tau} \cdot \int_0^t |x_2^a(\lambda) - x_2^b(\lambda)| d\lambda \cdot \int_{s_0}^{s_1} \frac{v_0^a(s)}{\tau(s)} ds \\ & \leq const(\theta^a) \cdot \int_0^t \|x^a - x^b\|_\lambda d\lambda. \end{aligned}$$

So we get the following estimation on the interval $(\bar{s}_{max}, \bar{s}_1)$:

$$
\begin{aligned}
(29)\quad \int_{s(\bar{s}_{max})}^{s_1} |v^a(t,s) - v^b(t,s)|ds &= \int_{\bar{s}_{max}}^{\bar{s}_1} \tau(s(\bar{s}))\cdot|v^a(t,s(\bar{s})) - v^b(t,s(\bar{s}))|d\bar{s} \\
&= \int_{\bar{s}_{max}}^{\bar{s}_1} \exp(-I[\mu](t))\cdot\big|\tau(s(\bar{s}-I[x_2^a](t)))v_0^a(s(\bar{s}-I[x_2^a](t))) \\
&\qquad - \tau(s(\bar{s}-I[x_2^b](t)))v_0^b(s(\bar{s}-I[x_2^b](t)))\big|d\bar{s} \\
&\overset{\text{lemma B.4}}{\leq} \int_{\bar{s}_{max}}^{\bar{s}_1} \tau(s(\bar{s}-I[x_2^b](t)))\cdot\big|v_0^a(s(\bar{s}-I[x_2^a](t))) - v_0^b(s(\bar{s}-I[x_2^b](t)))\big| \\
&\quad + v_0^a(s(\bar{s}-I[x_2^a](t)))\cdot\big|\tau(s(\bar{s}-I[x_2^a](t))) - \tau(s(\bar{s}-I[x_2^b](t)))\big|d\bar{s} \\
&\leq \int_{\bar{s}_{max}}^{\bar{s}_1} \tau(s(\bar{s}-I[x_2^b](t)))\cdot\big|v_0^a(s(\bar{s}-I[x_2^a](t))) - v_0^a(s(\bar{s}-I[x_2^b](t)))\big|d\bar{s} \\
&\quad + \int_{\bar{s}_{max}}^{\bar{s}_1} \tau(s(\bar{s}-I[x_2^b](t)))\cdot\big|v_0^a(s(\bar{s}-I[x_2^b](t))) - v_0^b(s(\bar{s}-I[x_2^b](t)))\big|d\bar{s} \\
&\quad + \int_{\bar{s}_{max}}^{\bar{s}_1} v_0^a(s(\bar{s}-I[x_2^a](t)))\cdot\big|\tau(s(\bar{s}-I[x_2^a](t))) - \tau(s(\bar{s}-I[x_2^b](t)))\big|d\bar{s} \\
&\overset{(27)-(28)}{\leq} const(\theta^a)\cdot\int_0^t \|x^a - x^b\|_\lambda d\lambda + \|\theta^a - \theta^b\|_\Theta.
\end{aligned}
$$

Considering the interval $(s(\bar{s}_{min}), s(\bar{s}_{max}))$, it holds that

$$
\begin{aligned}
(30)\qquad &\int_{s(\bar{s}_{min})}^{s(\bar{s}_{max})} |v^a(t,s) - v^b(t,s)|ds \\
&= \int_{\bar{s}_{min}}^{\bar{s}_{max}} \tau(s(\bar{s}))\cdot|v^a(t,s(\bar{s})) - v^b(t,s(\bar{s}))|d\bar{s} \\
&\leq \int_{\bar{s}_{min}}^{\bar{s}_{max}} \tau(s(\bar{s}))v^a(t,s(\bar{s})) + \tau(s(\bar{s}))v^b(t,s(\bar{s})))d\bar{s} \\
&\overset{\text{lemma 3.15}}{\leq} \int_{\bar{s}_{min}}^{\bar{s}_{max}} const(\theta^a,\eta)d\bar{s} \\
&\leq const(\theta^a,\eta)\cdot(\bar{s}_{max} - \bar{s}_{min}) \\
&= const(\theta^a,\eta)\cdot\Big|\int_0^t x_2^a(\lambda) - x_2^b(\lambda)d\lambda\Big| \\
&\leq const(\theta^a,\eta)\cdot\int_0^t \|x^a - x^b\|_\lambda d\lambda.
\end{aligned}
$$

This only leaves the integral over $[s_0, s(\bar{s}_{min}))$ to be handled. Here the formula is slightly more complicated since it includes the operator C which again includes the operator I^{-1}. However, the approach is basically the same as before.

We first deal with I^{-1}. Let $\bar{s} \leq \bar{s}_{min}$ be fixed. If $I[x_2^b]^{-1}(\bar{s}) \leq I[x_2^a]^{-1}(\bar{s})$, then it holds that

$$
\begin{aligned}
&I[x_2^a]\left(I[x_2^b]^{-1}(\bar{s}) + \frac{\bar{s} - I[x_2^a](I[x_2^b]^{-1}(\bar{s}))}{\underline{N_{in}}(T,\theta^a)}\right) \\
&\overset{\text{MVT}}{\geq} I[x_2^a](I[x_2^b]^{-1}(\bar{s})) + \bar{s} - I[x_2^a](I[x_2^b]^{-1}(\bar{s})) = \bar{s}
\end{aligned}
$$

and hence

$$
(31)\qquad I[x_2^a]^{-1}(\bar{s}) \leq I[x_2^b]^{-1}(\bar{s}) + \frac{\bar{s} - I[x_2^a](I[x_2^b]^{-1}(\bar{s}))}{\underline{N_{in}}(T,\theta^a)}.
$$

We also have that

$$
\begin{aligned}
(32) \qquad I[x_2^b](I[x_2^b]^{-1}(\bar{s})) - I[x_2^a](I[x_2^b]^{-1}(\bar{s})) &\leq \int_0^{I[x_2^b]^{-1}(\bar{s})} |x_2^a(\lambda) - x_2^b(\lambda)| d\lambda \\
&\leq \int_0^t |x_2^a(\lambda) - x_2^b(\lambda)| d\lambda \\
&\leq \int_0^t \|x^a - x^b\|_\lambda d\lambda
\end{aligned}
$$

which now gives us

$$
\begin{aligned}
I[x_2^a]^{-1}(\bar{s}) - I[x_2^b]^{-1}(\bar{s}) &\overset{(31)}{\leq} \frac{\bar{s} - I[x_2^a](I[x_2^b]^{-1}(\bar{s}))}{\underline{N_{in}}(T, \theta^a)} \\
&\overset{(32)}{\leq} \frac{\int_0^t \|x^a - x^b\|_\lambda d\lambda}{\underline{N_{in}}(T, \theta^a)}.
\end{aligned}
$$

By symmetry we get (also for the case $I[x_2^b]^{-1}(\bar{s}) \geq I[x_2^a]^{-1}(\bar{s})$) that

$$
\begin{aligned}
(33) \qquad |I[x_2^a]^{-1}(\bar{s}) - I[x_2^b]^{-1}(\bar{s})| &\leq \frac{\int_0^t \|x^a - x^b\|_\lambda d\lambda}{\max\{\underline{N_{in}}(T, \theta^a), \underline{N_{in}}(T, \theta^b)\}} \\
&\overset{\text{lemma 3.15}}{\leq} const(\theta^a, \eta) \cdot \int_0^t \|x^a - x^b\|_\lambda d\lambda.
\end{aligned}
$$

Now let $i := a$ if $I[x_2^a](t) \leq I[x_2^b](t)$ and $i := b$ else. Let $j \in \{a, b\} \setminus \{i\}$. We obtain for the integral

$$
\begin{aligned}
(34) \qquad &\int_0^{\bar{s}_{min}} \left| I[x_2^i]^{-1}(I[x_2^i](t) - \bar{s}) - I[x_2^j]^{-1}(I[x_2^i](t) - \bar{s}) \right| d\bar{s} \\
&\leq \int_0^{\bar{s}_{min}} \left| I[x_2^i]^{-1}(\bar{s}) - I[x_2^j]^{-1}(\bar{s}) \right| d\bar{s} \\
&\overset{(33)}{\leq} \bar{s}_{min} \cdot const(\theta^a, \eta) \cdot \int_0^t \|x^a - x^b\|_\lambda d\lambda \\
&\leq const(\theta^a, \eta) \cdot \int_0^t \|x^a - x^b\|_\lambda d\lambda.
\end{aligned}
$$

This can now be used to handle C:

$$
\begin{aligned}
(35) \qquad &\int_0^{\bar{s}_{min}} \left| C[x_2^a](t, \bar{s}) - C[x_2^b](t, \bar{s}) \right| d\bar{s} \\
&= \int_0^{\bar{s}_{min}} \left| I[x_2^j]^{-1}(I[x_2^j](t) - \bar{s}) - I[x_2^i]^{-1}(I[x_2^i](t) - \bar{s}) \right| d\bar{s} \\
&\leq \int_0^{\bar{s}_{min}} \left| I[x_2^j]^{-1}(I[x_2^j](t) - \bar{s}) - I[x_2^j]^{-1}(I[x_2^i](t) - \bar{s}) \right| \\
&\qquad + \left| I[x_2^j]^{-1}(I[x_2^i](t) - \bar{s}) - I[x_2^i]^{-1}(I[x_2^i](t) - \bar{s}) \right| d\bar{s} \\
&\overset{\text{lemma B.5}}{\leq} \frac{\bar{s}_{min}}{\underline{N_{in}}(T, \theta^j)} \cdot \left| I[x_2^i](t) - I[x_2^j](t) \right| \\
&\qquad + \int_0^{\bar{s}_{min}} \left| I[x_2^j]^{-1}(I[x_2^i](t) - \bar{s}) - I[x_2^i]^{-1}(I[x_2^i](t) - \bar{s}) \right| d\bar{s} \\
&\overset{(34)}{\leq} const(\theta^a, \eta) \cdot \int_0^t \|x^a - x^b\|_\lambda d\lambda.
\end{aligned}
$$

We plan to invoke lemma B.4, so we need bounds for the absolute values and differences of the $h(\ldots)$ and $\exp(-\ldots)$ terms. Bounds for the absolute values are

given by $\bar{h}$ and 1 respectively. It remains to find suitable bounds for the differences. Here we will also apply the above equation for C.

We start with $h(\dots)$. We prove one intermediate result to keep things clear:

$$
\begin{aligned}
(36)\qquad & \int_0^{\bar{s}_{min}} |h^a(I[x_2^b]^{-1}(I[x_2^b](t)-\bar{s})) - h^b(I[x_2^b]^{-1}(I[x_2^b](t)-\bar{s}))| d\bar{s} \\
&\leq \int_0^{I[x_2^b](t)} |h^a(I[x_2^b]^{-1}(I[x_2^b](t)-\bar{s})) - h^b(I[x_2^b]^{-1}(I[x_2^b](t)-\bar{s}))| d\bar{s} \\
&= \int_0^{I[x_2^b](t)} |h^a(I[x_2^b]^{-1}(\bar{s})) - h^b(I[x_2^b]^{-1}(\bar{s}))| d\bar{s} \\
&= \int_0^t |h^a(I[x_2^b]^{-1}(I[x_2^b](\lambda))) - h^b(I[x_2^b]^{-1}(I[x_2^b](\lambda)))| \cdot x_2^b(\lambda) d\lambda \\
&\leq \overline{N_{in}}(T,\theta^b) \cdot \int_0^t |h^a(\lambda) - h^b(\lambda)| d\lambda \\
&\overset{\text{lemma 3.15}}{\leq} const(\theta^a,\eta) \cdot \|\theta^a - \theta^b\|_\Theta
\end{aligned}
$$

Now let $L_h := \sup_{s\in(s_0,s_1)} (h^a)'(s)$. We get that

$$
\begin{aligned}
(37)\quad & \int_0^{\bar{s}_{min}} |h^a(C[x_2^a](t,\bar{s})) - h^b(C[x_2^b](t,\bar{s}))| d\bar{s} \\
&= \int_0^{\bar{s}_{min}} |h^a(C[x_2^a](t,\bar{s})) - h^a(C[x_2^b](t,\bar{s}))| + |h^a(C[x_2^b](t,\bar{s})) - h^b(C[x_2^b](t,\bar{s}))| d\bar{s} \\
&= L_h \int_0^{\bar{s}_{min}} |C[x_2^a](t,\bar{s}) - C[x_2^b](t,\bar{s})| d\bar{s} \\
&\quad + \int_0^{\bar{s}_{min}} |h^a(I[x_2^b]^{-1}(I[x_2^b](t)-\bar{s})) - h^b(I[x_2^b]^{-1}(I[x_2^b](t)-\bar{s}))| d\bar{s} \\
&\overset{(35),(36)}{\leq} const(\theta^a,\eta) \cdot \Big(\int_0^t \|x^a - x^b\|_\lambda d\lambda + \|\theta^a - \theta^b\|_\Theta \Big).
\end{aligned}
$$

Considering the exp$(\dots)$ term:

$$
\begin{aligned}
(38)\qquad & \int_0^{\bar{s}_{min}} \Big| \exp\Big(- \int_{C[x_2^a](t,\bar{s})}^t \mu(\lambda) d\lambda \Big) - \exp\Big(- \int_{C[x_2^b](t,\bar{s})}^t \mu(\lambda) d\lambda \Big) \Big| d\bar{s} \\
&\overset{\text{lemma B.6}}{\leq} \int_0^{\bar{s}_{min}} \Big| \int_{C[x_2^a](t,\bar{s})}^t \mu(\lambda) d\lambda - \int_{C[x_2^b](t,\bar{s})}^t \mu(\lambda) d\lambda \Big| d\bar{s} \\
&= \int_0^{\bar{s}_{min}} \Big| \int_{C[x_2^a](t,\bar{s})}^{C[x_2^b](t,\bar{s})} \mu(\lambda) d\lambda \Big| d\bar{s} \\
&\leq \bar{\mu} \cdot \int_0^{\bar{s}_{min}} |C[x_2^a](t,\bar{s}) - C[x_2^b](t,\bar{s})| d\bar{s} \\
&\overset{(35)}{\leq} const(\theta^a,\eta) \cdot \int_0^t \|x^a - x^b\|_\lambda d\lambda.
\end{aligned}
$$

So we finally get for the integral over $[s_0, s(\bar{s}_{min}))$ that

$$
\begin{aligned}
(39) \qquad & \int_{s_0}^{s(\bar{s}_{min})} |v^a(t,s) - v^b(t,s)| ds \\
& = \int_0^{\bar{s}_{min}} \tau(s(\bar{s})) \cdot |v^a(t, s(\bar{s})) - v^b(t, s(\bar{s}))| d\bar{s} \\
& \underset{(37),(38)}{\overset{\text{lemma B.4}}{\leq}} const(\theta^a, \eta) \cdot \Big(\int_0^t \|x^a - x^b\|_\lambda d\lambda + \|\theta^a - \theta^b\|_\Theta \Big).
\end{aligned}
$$

Putting together the results for the different parts, we obtain that

$$
\begin{aligned}
& \int_{s_0}^{s_1} |v^a(t,s) - v^b(t,s)| ds \\
& = \int_{s_0}^{s(\bar{s}_{min})} |v^a(t,s) - v^b(t,s)| ds \\
& \quad + \int_{s(\bar{s}_{min})}^{s(\bar{s}_{max})} |v^a(t,s) - v^b(t,s)| ds \\
& \quad + \int_{s(\bar{s}_{max})}^{s_1} |v^a(t,s) - v^b(t,s)| ds \\
& \overset{(29),(30),(39)}{\leq} const(\theta^a, \eta) \cdot \Big(\int_0^t \|x^a - x^b\|_\lambda d\lambda + \|\theta^a - \theta^b\|_\Theta \Big).
\end{aligned}
$$

□

We are now ready to formulate and prove the main statement of this section:

Theorem 3.19
Let $\theta^a \in \Theta$ and $\eta > 0$. There exists a non-negative constant $C_S(\theta^a, \eta)$ such that for all $\theta^b \in \Theta$ with $\|\theta^a - \theta^b\|_\Theta < \eta$ and $x^a \in X_{T'}^{\theta^a}$, $x^b \in X_{T'}^{\theta^b}$ it holds that

$$
\|S^{\theta^a}[x^a] - S^{\theta^b}[x^b]\|_t \leq C_S(\theta^a, \eta) \left(\int_0^t \|x^a - x^b\|_\lambda d\lambda + \|\theta^a - \theta^b\|_\Theta \right)
$$

for almost all $t \in [0, T']$.

Proof. Immediate consequence of propositions 3.17 and 3.18 and definition 3.8. □

3.5. **Existence and uniqueness of a solution.** Let $\theta \in \Theta$ be fixed and $\eta > 0$ be arbitrary. We now choose $T' \in (0, T]$ such that $T' \cdot C_S(\theta, \eta) \leq q < 1$ and $\frac{T}{T'} \in \mathbb{N}$. We will show by induction the existence of a unique solution to the basic PDE system in $X_{nT'}^\theta$ for all $n = 1, 2, \ldots, \frac{T}{T'}$:

(1) Let first $n = 1$. For all $x^a, x^b \in X_{T'}^\theta$ with continuous representatives it holds that

$$
\begin{aligned}
\|S^\theta[x^a] - S^\theta[x^b]\|_U &= \int_0^{T'} \|S^\theta[x^a] - S^\theta[x^b]\|_t dt \\
&\overset{\text{theorem 3.19}}{\leq} T' \cdot C_S(\theta, \eta) \cdot \left(\int_0^t \|x^a - x^b\|_\lambda d\lambda + \|\theta - \theta\|_\Theta \right) \\
&\leq q \cdot \|x^a - x^b\|_U.
\end{aligned}
$$

Hence, S^θ is a contraction on the space

$$
\tilde{X}_{T'}^\theta := \left\{ f \in X_{T'}^\theta \mid \exists \text{ cont. repr. of } f \right\}.
$$

Analogous to the standard proof of the Banach fixed-point theorem, we see that applying S^θ iteratively gives a Cauchy sequence in $X^\theta_{T'}$:[21]

For any $x^{(0)} \in X^\theta_{T'}$ define the sequence $(x^{(i)})_{i\in\mathbb{N}}$ by setting $x^{(i+1)} := S^\theta[x^{(i)}] \in X^\theta_{T'}$ for $i = 0, 1, \ldots$. Then for all $i = 1, 2, \ldots$ we have that

$$\begin{aligned}\|S^\theta[x^{(i+1)}] - S^\theta[x^{(i)}]\|_U &\leq q \cdot \|x^{(i+1)} - x^{(i)}\|_U \\ &= q \cdot \|S^\theta[x^{(i)}] - S^\theta[x^{(i-1)}]\|_U\end{aligned}$$

and hence for all $j \geq i$

$$\begin{aligned}\|x^{(j)} - x^{(i)}\|_U &= \|S^\theta[x^{(j-1)}] - S^\theta[x^{(i-1)}]\|_U \\ &\leq \sum_{k=i-1}^{j-2} \|S^\theta[x^{(k+1)}] - S^\theta[x^{(k)}]\|_U \\ &\leq \|S^\theta[x^{(0)}] - x^{(0)}\|_U \sum_{k=i-1}^{j-2} q^k.\end{aligned}$$

Since $X^\theta_{T'}$ is a complete metric space and $\tilde{X}^\theta_{T'} \subset X^\theta_{T'}$, the limit of this Cauchy sequence exists in $X^\theta_{T'}$. However, we know that every fixed-point of S^θ must have a continuous representative. Hence, the sequence converges to a fixed-point in $\tilde{X}^\theta_{T'}$, which is unique because of the contraction property of S^θ.

By theorem 3.13 we now get the existence of a unique solution to the basic PDE system in $X^\theta_{T'}$.

(2) Let now $1 < n \leq \frac{T}{T'}$. By induction hypothesis, we know that there exists a unique solution $x^* = (x_1^*, x_2^*, x_3^*, x_4^*)$ in $X^\theta_{(n-1)T'}$.

We define the restricted space

$$\begin{aligned}\tilde{X}^\theta_{nT'} := \Big\{(x_1, x_2, x_3, x_4) \in X^\theta_{nT'} \;|x_1(t,.) \overset{a.e.}{\equiv} x_1^*(t,.), x_2(t) = x_2^*(t), \\ x_3(t) = x_3^*(t), x_4(t) = x_4^*(t) \\ \text{for almost all } t \in [0, (n-1)T']\Big\}.\end{aligned}$$

$\tilde{X}^\theta_{nT'}$ is a closed subset of $X^\theta_{nT'}$ and therefore again a complete metric space. Furthermore, when applied to any $x \in \tilde{X}^\theta_{nT'}$ with continuous representative, the operator S^θ (defined on $X^\theta_{nT'}$) returns again an element of $\tilde{X}^\theta_{nT'}$ with continuous representative, since x^* is a fixed-point of S^θ acting on $X^\theta_{(n-1)T'}$.

[21] Cf. [Eva10, p.534]. Note, however, that $\tilde{X}^\theta_{T'}$ is *not* closed. So the Banach fixed-point theorem can not be applied directly.

Hence, we get for all $x^a, x^b \in \tilde{X}^\theta_{T'}$ with continuous representative that

$$\begin{aligned}
\|S[x^a] - S[x^b]\|_U &= \int_0^{nT'} \|S[x^a] - S[x^b]\|_t dt \\
&= \int_{(n-1)T'}^{nT'} \|S[x^a] - S[x^b]\|_t dt \\
&\overset{\text{theorem 3.19}}{\leq} \int_{(n-1)T'}^{nT'} C_S(\theta,\eta) \int_0^t \|x^a - x^b\|_\lambda d\lambda dt \\
&\leq C_S(\theta,\eta) \int_{(n-1)T'}^{nT'} \int_0^{nT'} \|x^a - x^b\|_\lambda d\lambda dt \\
&= (nT' - (n-1)T') \cdot C_S(\theta,\eta) \cdot \|x^a - x^b\|_U \\
&\leq q \cdot \|x^a - x^b\|_U.
\end{aligned}$$

By the same argument as in the induction start we get the existence of a unique fixed-point in $\tilde{X}^\theta_{nT'}$. This implies the existence and uniqueness of a solution in $X^\theta_{nT'}$: Existence is clear by theorem 3.13. For uniqueness, let $x \in X^\theta_{nT'}$ be any solution to the basic PDE system. By induction hypothesis, x restricted to the time interval $[0,(n-1)T']$ must be equal to x^*. Hence, $x \in \tilde{X}^\theta_{nT'}$ is the unique fixed-point in $\tilde{X}^\theta_{nT'}$.

Since $nT' = T$ we have just proved the existence and uniqueness of a solution to our basic PDE system (within the bounds from definition 3.4).

3.6. **Continuous dependence on the given data.** For this section we choose $T' = T$. For $i \in \{a, b\}$ let

$$\theta^i = (v_0^i, h^i, N_{in}^{0,i}, N_{out}^{0,i}, R_0^i) \in \Theta$$

and $x^i = (v^i, N_{in}^i, N_{out}^i, R^i)$ be the unique solution of (1)-(4) with

$$\begin{aligned}
&v^i(t, s_0) =: h^i(t), \;\; 0 < t \leq T, \\
&v^i(0, s) =: v_0^i(s), \;\; s_0 \leq s \leq s_1, \\
&N_{in}^i(0) =: N_{in}^{0,i}, \\
&N_{out}^i(0) =: N_{out}^{0,i}, \\
&R^i(0) =: R_0^i.
\end{aligned}$$

Then x^a and x^b are fixed-points of S^{θ^a} and S^{θ^b} respectively by 3.13. By theorem 3.19 it holds that

$$\begin{aligned}
\|x^a - x^b\|_t &= \|S^{\theta^a}[x^a] - S^{\theta^a}[x^b]\|_t \\
&\leq C_S(\theta^a,\eta) \left(\int_0^t \|x^a - x^b\|_\lambda d\lambda + \|\theta^a - \theta^b\|_\Theta \right)
\end{aligned}$$

for almost all $t \in [0,T]$.

Hence, we get by Gronwall's inequality[22] that

$$\begin{aligned}
\|x^a - x^b\|_t &\leq C_S(\theta^a,\eta) \cdot \|\theta^a - \theta^b\|_\Theta \cdot \left(1 + C_S(\theta^a,\eta) t e^{C_S(\theta^a,\eta)t}\right) \\
&\leq C_S(\theta^a,\eta) \cdot \left(1 + C_S(\theta^a,\eta) T e^{C_S(\theta^a,\eta)T}\right) \cdot \|\theta^a - \theta^b\|_\Theta \\
&= const(\theta^a,\eta) \cdot \|\theta^a - \theta^b\|_\Theta
\end{aligned}$$

for almost all $t \in [0,T]$.

[22] This is lemma B.7 in the appendix.

This implies that

$$\|x^a - x^b\|_U \leq const(\theta^a, \eta) \cdot \|\theta^a - \theta^b\|_\Theta$$

which means that the solution to the basic PDE system continuously depends on the given data.

3.7. **Summary.** The following theorem summarizes the main results concerning the well-posedness of the basic PDE system:

Theorem 3.20
Let assumption 3.2 be valid and

$$\theta = (v_0, h, N_{in}^0, N_{out}^0, R_0) \in \Theta.$$

Then the PDE system (1)-(9) *has exactly one continuous solution* (v, N_{in}, N_{out}, R) *that satisfies*

$$\begin{aligned}
&\int_{s_0}^{s_1} v(t,s)ds \leq \bar{v}(t,\theta),\\
&v(t,s) \geq 0,\\
&\underline{N_{in}}(t,\theta) \leq N_{in}(t) \leq \overline{N_{in}}(t,\theta),\\
&0 \leq N_{out}(t) \leq \overline{N_{out}}(t,\theta) \text{ and}\\
&0 \leq R(t) \leq R_{ges}
\end{aligned}$$

for all $t \in [0,T]$ *and* $s \in [s_0, s_1)$.

For the solution (v, N_{in}, N_{out}, R) *it holds that*

$$\begin{aligned}
v(t, s(\bar{s})) &:= \frac{1}{\tau(s(\bar{s}))}\\
&\cdot \begin{cases} \exp\left(-\int_0^t \mu(\lambda)d\lambda\right)\tau(s(\bar{s} - I[N_{in}](t)))v_0(s(\bar{s} - I[N_{in}](t))), & \bar{s} \geq I[N_{in}](t)\\ \exp\left(-\int_{C[N_{in}]}^t \mu(\lambda)d\lambda\right)\tau(s_0)h\left(C[N_{in}]\right), & \bar{s} < I[N_{in}](t) \end{cases}\\
N_{in}(t) &:= \exp\left(-\int_0^t \int_{s_0}^{s_1} \tau(s)v(\lambda,s)dsd\lambda\right)\\
&\cdot \left(\int_0^t \exp\left(\int_0^\lambda \int_{s_0}^{s_1} \tau(s)v(\varrho,s)dsd\varrho\right)\left(\beta(w - N_{in}(\lambda))^+ + \alpha N_{out}(\lambda)\right)d\lambda + N_{in}^0\right)\\
N_{out}(t) &:= \exp\left(-\int_0^t kR(\lambda) + \alpha + \delta d\lambda\right)\\
&\cdot \left(\int_0^t \exp\left(\int_0^\lambda kR(\varrho) + \alpha + \delta d\varrho\right)\int_{s_0}^{s_1} \nu(s)\mu(\lambda)v(\lambda,s)ds + \gamma(R_{ges} - R(\lambda))d\lambda\right.\\
&\qquad \left. + N_{out}^0\right)\\
R(t) &:= \exp\left(-\int_0^t kN_{out}(\lambda) + \gamma d\lambda\right)\\
&\cdot \left(\int_0^t \exp\left(\int_0^\lambda kN_{out}(\varrho) + \gamma d\varrho\right)\gamma R_{ges}d\lambda + R_0\right)
\end{aligned}$$

for all $t \in [0,T]$ *and* $\bar{s} \in [0, \bar{s}_1)$.

Furthermore, the solution continuously depends on θ and it holds that

$$v \in C^1((0,T) \times (s_0, s_1)),$$
$$N_{in}, N_{out}, R \in C^1([0,T]).$$

Proof. Existence, uniqueness and continuous dependence on the given data θ were all shown above.

The validity of the formulas follows by theorem 3.13 and definition 3.10.

The differentiability of N_{in}, N_{out} and R is clear since these functions satisfy (1), (3) and (4). Boundedness of their derivatives follows by (1), (3), (4) and the bounds for $\int_{s_0}^{s_1} v ds$, N_{in}, N_{out} and R.

For the regularity of v, consider the proof of lemma 3.11: By the computations in the proof and theorem 3.13 we see that the partial derivatives

$$\frac{\partial \tau(s(\bar{s}))v(t,s(\bar{s}))}{\partial t} \text{ and } \frac{\partial \tau(s(\bar{s}))v(t,s(\bar{s}))}{\partial \bar{s}}$$

exist and are continuous on $(0,T) \times (0, \bar{s}_1)$. Since

$$\begin{aligned}\frac{\partial \tau(s(\bar{s}))v(t,s(\bar{s}))}{\partial \bar{s}} &= \tau'(s(\bar{s}))s'(\bar{s})v(t,s(\bar{s})) + \tau^2(s(\bar{s}))\frac{\partial v(t,s(\bar{s}))}{\partial s} \\ &= \tau'(s)\tau(s)v(t,s) + \tau^2(s)\frac{\partial v(t,s)}{\partial s}\end{aligned}$$

we also get that $\partial \tau(s)v(t,s)/\partial t$ and $\partial \tau(s)v(t,s)/\partial s$ exist and are continuous on $(0,T) \times (s_0, s_1)$. This implies that $v \in C^1((0,T) \times (s_0, s_1))$.[23] □

[23] This is a basic result from analysis. See [Sau14, p. 197-206] for example

4. Related models

4.1. **Size independent growth.** Assume that $\tau \in C^1([s_0, s_1])$.

We may use the parameter transform described in lemma 3.5 in order to get an equivalent system with constant growth rate:

(40)
$$\frac{dN_{in}}{dt} = \underbrace{\beta(w - N_{in})^+}_{\text{“production”}} + \underbrace{\alpha N_{out}(t)}_{\text{re-uptake}} \underbrace{- N_{in} \int_0^{\bar{s}_1} \tilde{v}(t, s(\bar{s}))\tau(s(\bar{s}))d\bar{s}}_{\text{transport into vesicles}}$$

(41)
$$\frac{\partial \tilde{v}(t, s(\bar{s}))}{\partial t} + \underbrace{N_{in}(t)\frac{\partial \tilde{v}(t, s(\bar{s}))}{\partial \bar{s}}}_{\text{growth}} = \underbrace{-\mu(t)\tilde{v}(t, s(\bar{s}))}_{\text{fusion}}$$

(42)
$$\frac{dN_{out}}{dt} = \underbrace{\mu(t) \int_0^{\bar{s}_1} \tilde{v}(t, s(\bar{s}))\nu(s(\bar{s}))d\bar{s}}_{\text{exocytosis}} \underbrace{- kR(t)N_{out}}_{\text{binding}} \underbrace{- \alpha N_{out}}_{\text{re-uptake}} \underbrace{- \delta N_{out}}_{\text{diffusion}} + \underbrace{\gamma(R_{ges} - R)}_{\text{unbinding}}$$

(43)
$$\frac{dR}{dt} = \underbrace{-kN_{out}(t)R}_{\text{binding}} + \underbrace{\gamma(R_{ges} - R)}_{\text{unbinding}}$$

using the boundary conditions

$$\tilde{v}(t, s(0)) = \tau(s(0))h(t) \geq 0, \;\; 0 < t \leq T \tag{44}$$

$$\tilde{v}(0, s(\bar{s})) = \tau(s(\bar{s}))v_0(s(\bar{s})) \geq 0, \;\; 0 \leq \bar{s} < \bar{s}_1 \tag{45}$$

$$N_{in}(0) = N_{in}^0 > 0 \tag{46}$$

$$N_{out}(0) = N_{out}^0 \geq 0 \tag{47}$$

$$R(0) = R_0 \geq 0 \tag{48}$$

where the same sets of model parameters and given data as in the basic PDE model are used and s and $\bar{s}_1$ are characterized by lemma 3.5.

The equivalence to the basic PDE system is clear by the proof of lemma 3.12. By these same computations we also see that $\tilde{v}(t, s(\bar{s}))$ corresponds to $\tau(s(\bar{s}))v(t, s(\bar{s}))$ where v is part of the solution to the basic PDE system. This relation is important to keep in mind because it tells how the statements for v can be applied to $\tilde{v}$.

Note, however, that the integrals in (40) and (42) are in general more complex than in the basic PDE system. Also remember that $\bar{s}_1$ might be infinite. This has to be taken into account when deciding which formulation of the PDE system to use.

4.2. **The ODE system.** We will now use the transformed PDE system (40)-(48) to derive an ODE model.

Throughout this section we assume that assumption 3.2 is satisfied and that $(v_0, h, N_{in}^0, N_{out}^0, R_0) \in \Theta$.

Additionally, we need to make the following assumption:

Assumption 4.1 (Supplementary regularity)
We assume that $\tau, v_0 \in C^2([s_0, s_1])$ and $h \in C^2([0, T])$. (Where C^2 over closed intervals is defined analogously to C^1.)

Notation 4.2
In the proofs of the following lemmata we will use the notation

$$\overline{N_{in}} := \sup_{t\in[0,T]} N_{in}(t)$$

to denote the maximum of N_{in}.

Lemma 4.3
Let $(a_n)_{n\in\mathbb{N}}$ be a sequence of numbers in $(0,\bar{s}_1)$ which tends to $\bar{s}_1$ as n goes to infinity. Then

$$\sup_{t\in[0,T]} |\tilde{v}(t,s(a_n)) - \lim_{m\to\infty} \tilde{v}(t,s(a_m))| \to 0 \quad \text{as } n\to\infty.$$

Proof. Let $n\in\mathbb{N}$. If $\bar{s}_1=\infty$, then $\bar{s}_1 > I[N_{in}](t)$, so we may w.l.o.g. assume that $a_n > I[N_{in}](t)$. We have that

$$\begin{aligned}
&\sup_{t\in[0,T]} |\tilde{v}(t,s(a_n)) - \lim_{m\to\infty} \tilde{v}(t,s(a_m))| \\
&= \sup_{t\in[0,T]} \exp\left(-\int_0^t \mu(\lambda)d\lambda\right) \\
&\quad \cdot |\tau(s(a_n - I[N_{in}](t)))v_0(s(a_n - I[N_{in}](t))) - \tau(s_1)v_0(s_1)| \\
&\leq \sup_{\bar{s}\geq a_n - I[N_{in}](T)} |\tau(s(\bar{s}))v_0(s(\bar{s})) - \tau(s_1)v_0(s_1)| \to 0 \quad \text{as } n\to\infty.
\end{aligned}$$

So let now $\bar{s}_1<\infty$. First let $t\in[0,T]$ such that $I[N_{in}](t) < \bar{s}_1$. Define

$$g:[0,\bar{s}_1]\to\mathbb{R}, \quad g(\bar{s}) := \tau(s(\bar{s}))v_0(s(\bar{s})).$$

It holds that

$$\begin{aligned}
&|\tilde{v}(t,s(a_n)) - \lim_{m\to\infty} \tilde{v}(t,s(a_m))| \\
&\quad = \exp\left(-\int_0^t \mu(\lambda)d\lambda\right) \cdot \Big|\tau(s(a_n - I[N_{in}](t)))v_0(s(a_n - I[N_{in}](t))) \\
&\qquad - \lim_{m\to\infty} \tau(s(a_m - I[N_{in}](t)))v_0(s(a_m - I[N_{in}](t)))\Big| \\
&\quad \leq \Big|g(a_n - I[N_{in}](t)) - \lim_{m\to\infty} g(a_m - I[N_{in}](t))\Big| \\
&\quad \leq |g(a_n - I[N_{in}](t)) - g(\bar{s}_1 - I[N_{in}](t))| \\
&\quad = |g'(\xi_n)| \cdot |\bar{s}_1 - a_n| \\
&\quad \leq \sup_{\bar{s}\in(0,\bar{s}_1)} |g'(\bar{s})| \cdot |\bar{s}_1 - a_n|
\end{aligned}$$

where $\xi_n \in (a_n - I[N_{in}](t), \bar{s}_1 - I[N_{in}](t))$ exists by the mean value theorem and $\sup_{\bar{s}\in(0,\bar{s}_1)} |g'(\bar{s})| < \infty$ by assumption 3.2 and lemma 3.5.

Now let $t\in[0,T]$ such that $I[N_{in}](t) \geq \bar{s}_1$. Define

$$\begin{aligned}
&f:[0,\bar{s}_1]\to\mathbb{R}, \\
&f(\bar{s}) := \exp\left(-\int_{C[N_{in}](t,\bar{s})}^t \mu(\lambda)d\lambda\right) \cdot h(C[N_{in}](t,\bar{s})).
\end{aligned}$$

We have that

$$\begin{aligned}|\tilde{v}(t,s(a_n)) - \lim_{m\to\infty}\tilde{v}(t,s(a_m))| &= \tau(s_0)\cdot\Big|f(a_n) - \lim_{m\to\infty} f(a_m)\Big| \\ &= \tau(s_0)\cdot\Big|f(a_n) - f(\bar{s}_1)\Big| \\ &= |f'(\xi_n)|\cdot|\bar{s}_1 - a_n| \\ &\leq \sup_{\bar{s}\in(0,\bar{s}_1)}|f'(\bar{s})|\cdot|\bar{s}_1 - a_n|\end{aligned}$$

where $\xi_n \in (a_n, \bar{s}_1)$ again exists by the mean value theorem.

It holds that $\sup_{\bar{s}\in(0,\bar{s}_1)}|f'(\bar{s})| < \infty$. To see that, let $\bar{s}\in(0,\bar{s}_1)$. First note that

$$\Big|\frac{\partial C[N_{in}](t,\bar{s})}{\partial\bar{s}}\Big| = \Big|\frac{-1}{N_{in}(C[N_{in}](t,\bar{s}))}\Big| \leq \frac{1}{\underline{N_{in}}(T)}. \tag{49}$$

So we have that

$$\begin{aligned}\frac{\partial}{\partial\bar{s}}h(C[N_{in}](t,\bar{s})) &= h'(C[N_{in}](t,\bar{s}))\cdot\frac{\partial C[N_{in}](t,\bar{s})}{\partial\bar{s}} \\ &\overset{(49)}{\leq} \sup_{t\in(0,T)} h'(t)\cdot\frac{1}{\underline{N_{in}}(T)},\end{aligned}$$

where $\sup_{t\in(0,T)}h'(t) < \infty$ since $h\in C^1([0,T])$. Analogous to the calculation in the proof of lemma 3.11, we obtain that

$$\begin{aligned}&\frac{\partial}{\partial\bar{s}}\exp\left(-\int_{C[N_{in}](t,\bar{s})}^{t}\mu(\lambda)d\lambda\right) \\ &\quad= \exp\left(-\int_{C[N_{in}](t,\bar{s})}^{t}\mu(\lambda)d\lambda\right)\cdot\mu(C[N_{in}](t,\bar{s}))\cdot\frac{\partial C[N_{in}](t,\bar{s})}{\partial\bar{s}} \\ &\quad\overset{(49)}{\leq} \bar{\mu}\cdot\frac{1}{\underline{N_{in}}(T)}.\end{aligned}$$

h is also bounded, so we see by the product rule that the absolute value of $f'(\bar{s})$ must be bounded (by a number not depending on $\bar{s}$).

Hence, we got that

$$\begin{aligned}&\sup_{t\in[0,T]}|\tilde{v}(t,s(a_n)) - \lim_{m\to\infty}\tilde{v}(t,s(a_m))| \\ &\quad\leq \max\Big\{\sup_{\bar{s}\in(0,\bar{s}_1)}|f'(\bar{s})|, \sup_{\bar{s}\in(0,\bar{s}_1)}|g'(\bar{s})|\Big\}\cdot|\bar{s}_1 - a_n| \to 0 \quad \text{as } n\to\infty.\end{aligned}$$

□

The previous lemma can now be used to prove the following statement:

Theorem 4.4
Let $f\in C^1([0,\bar{s}_1))$. If $|f|$ is bounded and has a bounded derivative f', then equation (41) *of the transformed PDE system implies that:*

$$\begin{aligned}&\frac{d}{dt}\Big(\int_0^{\bar{s}_1} f(\bar{s})\tilde{v}(t,s(\bar{s}))d\bar{s}\Big) \\ &\quad= N_{in}(t)\left(\int_0^{\bar{s}_1} f'(\bar{s})\tilde{v}(t,s(\bar{s}))d\bar{s} + f(0)\tau(s_0)h(t) - \lim_{\bar{s}\to\bar{s}_1} f(\bar{s})\tilde{v}(t,s(\bar{s}))\right) \\ &\qquad - \mu(t)\int_0^{\bar{s}_1} f(\bar{s})\tilde{v}(t,s(\bar{s}))d\bar{s}\end{aligned}$$

Proof. Let $f \in C^1([0, \bar{s}_1))$ such that $|f|$ is bounded by $\bar{f}$ and f' bounded by L_f. Furthermore, let $(a_n)_{n\in\mathbb{N}}$ be a sequence of numbers in $(0, \bar{s}_1)$ which tends to $\bar{s}_1$ as n goes to infinity. We will first prove that for each $n \in \mathbb{N}$ it holds that:

$$\begin{aligned}(50)\qquad &\frac{d}{dt}\Big(\int_0^{a_n} f(\bar{s})\tilde{v}(t, s(\bar{s}))d\bar{s}\Big) \\ &\quad = N_{in}(t)\left(\int_0^{a_n} f'(\bar{s})\tilde{v}(t, s(\bar{s}))d\bar{s} + f(0)\tau(s_0)h(t) - f(a_n)\tilde{v}(t, s(a_n))\right) \\ &\qquad - \mu(t)\int_0^{a_n} f(\bar{s})\tilde{v}(t, s(\bar{s}))d\bar{s}\end{aligned}$$

So let $n \in \mathbb{N}$ and $t \in (0, T)$. Now multiply (41) by $f(s)$ and integrate over $\bar{s}$ (from 0 to a_n) to obtain that

$$(51)\qquad \underbrace{\int_0^{a_n} f(\bar{s})\frac{\partial \tilde{v}}{\partial t}d\bar{s}}_{A} + N_{in}(t)\underbrace{\int_0^{a_n} f(\bar{s})\frac{\partial \tilde{v}(t, s(\bar{s}))}{\partial \bar{s}}d\bar{s}}_{B} = -\mu(t)\int_0^{a_n} f(\bar{s})\tilde{v}(t, s(\bar{s}))d\bar{s}.$$

Since $f, \tilde{v} \in C^1([0, T] \times [0, a_n])$ we have (by lemma B.9) that

$$(52)\qquad \frac{d}{dt}\Big(\int_0^{a_n} f(\bar{s})\tilde{v}(t, s(\bar{s}))d\bar{s}\Big) = \int_0^{a_n} \frac{\partial f(\bar{s})\tilde{v}(t, s(\bar{s}))}{\partial t}d\bar{s} = \int_0^{a_n} f(\bar{s})\frac{\partial \tilde{v}(t, s(\bar{s}))}{\partial t}d\bar{s} = A.$$

Considering the term B, it holds that:

$$\begin{aligned}B &\overset{\text{part. int.}}{=} [f(\bar{s})\tilde{v}(t, s(\bar{s}))]_0^{a_n} - \int_0^{a_n} f'(\bar{s})\tilde{v}(t, s(\bar{s}))d\bar{s} \\ &= f(a_n)\tilde{v}(t, s(a_n)) - f(0)\tilde{v}(t, s_0) - \int_0^{a_n} f'(\bar{s})\tilde{v}(t, s(\bar{s}))d\bar{s} \qquad (53) \\ &= f(a_n)\tilde{v}(t, s(a_n)) - f(0)\tau(s_0)h(t) - \int_0^{a_n} f'(\bar{s})\tilde{v}(t, s(\bar{s}))d\bar{s}\end{aligned}$$

Putting (51), (52) and (53) together yields equation (50).

The final step is to show that

$$(54)\qquad \lim_{n\to\infty}\frac{d}{dt}\left(\int_0^{a_n} f(\bar{s})\tilde{v}(t, s(\bar{s}))d\bar{s}\right) = \frac{d}{dt}\left(\lim_{n\to\infty}\int_0^{a_n} f(\bar{s})\tilde{v}(t, s(\bar{s}))d\bar{s}\right).$$

Together with equation (50) this then completes the proof.

We want to show (54) by applying lemma B.10. So it is only left to verify that all requirements of lemma B.10 are met:

- For every $t \in [0, T]$, the limit

  $$\lim_{n\to\infty}\int_0^{a_n} f(\bar{s})\tilde{v}(t, s(\bar{s}))d\bar{s}$$

  exists since f is bounded on $[0, \bar{s}_1]$ and $v(t, .)$ is Riemann-integrable for all $t \in [0, T]$.
- The integral

  $$\int_0^{a_n} f(\bar{s})\tilde{v}(t, s(\bar{s}))d\bar{s}$$

  is differentiable w.r.t. t for all $t \in [0, T]$ by equation (50).

- And finally, $\frac{d}{dt}\left(\int_0^{a_n} f(\bar{s})\tilde{v}(t,s(\bar{s}))d\bar{s}\right)$ converges uniformly on $[0,T]$ as n tends to infinity:

$$
\begin{aligned}
&\sup_{t\in[0,T]}\left|\frac{d}{dt}\left(\int_0^{a_n} f(\bar{s})\tilde{v}(t,s(\bar{s}))d\bar{s}\right)-\lim_{m\to\infty}\frac{d}{dt}\left(\int_0^{a_m} f(\bar{s})\tilde{v}(t,s(\bar{s}))d\bar{s}\right)\right| \\
&\overset{(50)}{=}\sup_{t\in[0,T]}\Big|f(a_n)\tilde{v}(t,s(a_n))-\lim_{m\to\infty} f(a_m)\tilde{v}(t,s(a_m)) \\
&\quad+N_{in}(t)\cdot\left(\int_0^{a_n} f'(\bar{s})\tilde{v}(t,s(\bar{s}))d\bar{s}-\lim_{m\to\infty}\int_0^{a_m} f'(\bar{s})\tilde{v}(t,s(\bar{s}))d\bar{s}\right) \\
&\quad-\mu(t)\cdot\left(\int_0^{a_n} f(\bar{s})\tilde{v}(t,s(\bar{s}))d\bar{s}-\lim_{m\to\infty}\int_0^{a_m} f(\bar{s})\tilde{v}(t,s(\bar{s}))d\bar{s}\right)\Big| \\
&\leq\sup_{t\in[0,T]}|f(a_n)|\cdot|\tilde{v}(t,s(a_n))-\lim_{m\to\infty}\tilde{v}(t,s(a_m))| \\
&\quad+\sup_{t\in[0,T]}N_{in}(t)\cdot\left|\int_0^{a_n} f'(\bar{s})\tilde{v}(t,s(\bar{s}))d\bar{s}-\lim_{m\to\infty}\int_0^{a_m} f'(\bar{s})\tilde{v}(t,s(\bar{s}))d\bar{s}\right| \\
&\quad+\sup_{t\in[0,T]}\mu(t)\cdot\left|\int_0^{a_n} f(\bar{s})\tilde{v}(t,s(\bar{s}))d\bar{s}-\lim_{m\to\infty}\int_0^{a_m} f(\bar{s})\tilde{v}(t,s(\bar{s}))d\bar{s}\right| \\
&\leq\bar{f}\sup_{t\in[0,T]}|\tilde{v}(t,s(a_n))-\lim_{m\to\infty}\tilde{v}(t,s(a_m))| \\
&\quad+\overline{N_{in}}\cdot\sup_{t\in[0,T]}\left|\lim_{m\to\infty}\int_{a_n}^{a_m} f'(\bar{s})\tilde{v}(t,s(\bar{s}))d\bar{s}\right| \\
&\quad+\bar{\mu}\cdot\sup_{t\in[0,T]}\left|\lim_{m\to\infty}\int_{a_n}^{a_m} f(\bar{s})\tilde{v}(t,s(\bar{s}))d\bar{s}\right| \\
&\leq\bar{f}\sup_{t\in[0,T]}|\tilde{v}(t,s(a_n))-\lim_{m\to\infty}\tilde{v}(t,s(a_m))| \\
&\quad+\overline{N_{in}}L_f\bar{\tau}\max\{\bar{v_0},\bar{h}\}\cdot|\bar{s}_1-a_n| \\
&\quad+\bar{\mu}\bar{f}\bar{\tau}\max\{\bar{v_0},\bar{h}\}\cdot|\bar{s}_1-a_n| \\
&\to 0\quad\text{as } n\to\infty
\end{aligned}
$$

  where the bound for $\tilde{v}$ holds by theorem 3.20 and lemma 4.3 is applied to get the final convergence.

□

A few useful special cases of theorem 4.4 are presented in the following corollary:

Corollary 4.5
Under assumption 3.2, equation (41) *implies that*

$$
\begin{aligned}
\frac{d}{dt}\Big(\int_0^{\bar{s}_1}\tilde{v}(t,s(\bar{s}))d\bar{s}\Big)=&N_{in}(t)\left(\tau(s_0)h(t)-\lim_{\bar{s}\to\bar{s}_1}\tilde{v}(t,s(\bar{s}))\right) \\
&-\mu(t)\int_0^{\bar{s}_1}\tilde{v}(t,s(\bar{s}))d\bar{s}
\end{aligned}
$$

and that

$$
\begin{aligned}
&\frac{d}{dt}\Big(\int_0^{\bar{s}_1}\nu(s(\bar{s}))\tilde{v}(t,s(\bar{s}))d\bar{s}\Big) \\
&\quad=N_{in}(t)\Big(\int_0^{\bar{s}_1}\nu'(s(\bar{s}))\tau(s(\bar{s}))\tilde{v}(t,s(\bar{s}))d\bar{s}+\nu(s_0)\tau(s_0)h(t) \\
&\qquad-\lim_{\bar{s}\to\bar{s}_1}\nu(s(\bar{s}))\tilde{v}(t,s(\bar{s}))\Big)-\mu(t)\int_0^{\bar{s}_1}\nu(s(\bar{s}))\tilde{v}(t,s(\bar{s}))d\bar{s}
\end{aligned}
$$

Proof. Apply theorem 4.4 with $f \equiv 1$ and $f(\bar{s}) := \nu(s(\bar{s}))$, respectively. Also note that by lemma 3.5, $s'(\bar{s}) = \tau(s(\bar{s}))$. □

Notation 4.6
For $t \in [0,T]$ we write $N_v(t) := \int_{s_0}^{s_1} \nu(s)v(t,s)ds = \int_0^{\bar{s}_1} \nu(s(\bar{s}))\tilde{v}(t,s(\bar{s}))d\bar{s}$ and $V(t) := \int_{s_0}^{s_1} v(t,s)ds = \int_0^{\bar{s}_1} \tilde{v}(t,s(\bar{s}))d\bar{s}$.

Using the new notations we get the following equations from the transformed PDE model:

$$\frac{dN_{in}}{dt} = \beta(w - N_{in})^+ + \alpha N_{out}(t) - N_{in}\int_0^{\bar{s}_1} \tau(s(\bar{s}))\tilde{v}(t,s(\bar{s}))d\bar{s} \tag{55}$$

$$\frac{dV}{dt} = N_{in}(t)\big(\tau(s_0)h(t) - \lim_{\bar{s}\to\bar{s}_1} \tilde{v}(t,s(\bar{s}))\big) - \mu(t)V \tag{56}$$

$$\frac{dN_v}{dt} = N_{in}(t)\left(\nu(s_0)\tau(s_0)h(t) + \int_0^{\bar{s}_1} \nu'(s(\bar{s}))\tau(s(\bar{s}))\tilde{v}(t,s(\bar{s}))d\bar{s}\right) - \mu(t)N_v \tag{57}$$

$$\frac{dN_{out}}{dt} = \mu(t)N_v - kN_{out}R - (\alpha+\delta)N_{out} + \gamma(R_{ges} - R) \tag{58}$$

$$\frac{dR}{dt} = -kRN_{out} + \gamma(R_{ges} - R) \tag{59}$$

where (56) and (57) follow from corollary 4.5.

To obtain a complete ODE system, three parts still need to be handled:

- The integral $\int_0^{\bar{s}_1} \tau(s(\bar{s}))\tilde{v}(t,s(\bar{s}))d\bar{s}$ in equation (55).
- The term $\lim_{\bar{s}\to\bar{s}_1} \tilde{v}(t,s(\bar{s}))$ in equation (56).
- The integral $\int_0^{\bar{s}_1} \nu'(s(\bar{s}))\tau(s(\bar{s}))v(t,s(\bar{s}))d\bar{s}$ in equation (57).

We handle the limit term by making an extra assumption:

Assumption 4.7
We assume that $\lim_{\bar{s}\to\bar{s}_1} \tilde{v}(t,s(\bar{s})) = 0$, i.e. that there are no vesicles of maximal filling state.

Under assumption 4.7, equation (56) rewrites as follows:

$$\frac{dV}{dt} = N_{in}(t)\tau(s_0)h(t) - \mu(t)V$$

Note that this assumption is fulfilled whenever $\tau(s_1) = 0$ and $\bar{s}_1 = \infty$ for example.

To handle the integrals, one could of course just introduce new state variables and invoke theorem 4.4 to derive formulas for their behavior. Handling some integral

$$\int_0^{\bar{s}_1} f(s(\bar{s}))\tilde{v}(t,s(\bar{s}))d\bar{s}$$

this way, however, introduces a new integral

$$\int_0^{\bar{s}_1} f'(s(\bar{s}))\tau(s(\bar{s}))\tilde{v}(t,s(\bar{s}))d\bar{s}$$

which again requires some proper handling. Hence, applying theorem 4.4 repeatedly to handle all such integrals might fail to lead to an ODE system with finitely many variables.

We need to greatly restrict the functions τ and ν in order to make this approach work. The following assumption is restrictive enough and still leaves enough freedom to account for saturation effects:

Assumption 4.8 (Affine τ and ν)
We consider the case where $\nu(s) = c \cdot (s - s_0) + \nu_0$ and $\tau(s) = d \cdot (s - s_0) + \tau_0$ for some $c, \tau_0 > 0$, $\nu_0 \geq 0$, $d < 0$.

Note that this implies that

$$\tau(s) = d\cdot(s-s_0)+\tau_0 = \frac{d}{c}\big(c\cdot(s-s_0)+\nu_0\big) - \frac{d}{c}\nu_0 + \tau_0 = \frac{d}{c}(\nu(s)-\nu_0)+\tau_0. \tag{60}$$

Equation (57) now rewrites as follows:

$$\begin{aligned}
\frac{dN_v}{dt} &= N_{in}(t)\left(\nu(s_0)\tau(s_0)h(t) + \int_0^{\bar{s}_1} \nu'(s(\bar{s}))\tau(s(\bar{s}))\tilde{v}(t,s(\bar{s}))d\bar{s}\right) - \mu(t)N_v \\
&\overset{(60)}{=} N_{in}(t)\left(\nu_0\tau_0 h(t) + \int_0^{\bar{s}_1} c\big(\frac{d}{c}(\nu(s)-\nu_0)+\tau_0\big)\tilde{v}(t,s(\bar{s}))d\bar{s}\right) - \mu(t)N_v \\
&= N_{in}(t)\left(\nu_0\tau_0 h(t) + \int_0^{\bar{s}_1} \big(d\nu(s) - d\nu_0 + c\tau_0\big)\tilde{v}(t,s(\bar{s}))d\bar{s}\right) - \mu(t)N_v \\
&= N_{in}(t)\left(\nu_0\tau_0 h(t) + dN_v + (c\tau_0 - d\nu_0)V(t)\right) - \mu(t)N_v
\end{aligned}$$

Equation (55) becomes

$$\begin{aligned}
\frac{dN_{in}}{dt} &= \beta(w-N_{in})^+ + \alpha N_{out}(t) - N_{in}\int_0^{\bar{s}_1}\tau(s(\bar{s}))\tilde{v}(t,s(\bar{s}))d\bar{s} \\
&\overset{(60)}{=} \beta(w-N_{in})^+ + \alpha N_{out}(t) - N_{in}\int_0^{\bar{s}_1}\big(\frac{d}{c}(\nu(s)-\nu_0)+\tau_0\big)\tilde{v}(t,s(\bar{s}))d\bar{s} \\
&= \beta(w-N_{in})^+ + \alpha N_{out}(t) - N_{in}\left(\frac{d}{c}N_v(t) + \big(\tau_0 - \frac{d}{c}\nu_0\big)V(t)\right).
\end{aligned}$$

So the ODE system is described by:

$$\begin{aligned}
\frac{dN_{in}}{dt} &= \beta(w-N_{in})^+ + \alpha N_{out}(t) - N_{in}\left(\frac{d}{c}N_v(t) + \big(\tau_0 - \frac{d}{c}\nu_0\big)V(t)\right) \\
\frac{dV}{dt} &= N_{in}(t)\tau_0 h(t) - \mu(t)V \\
\frac{dN_v}{dt} &= N_{in}(t)\left(\nu_0\tau_0 h(t) + dN_v + (c\tau_0 - d\nu_0)V(t)\right) - \mu(t)N_v \\
\frac{dN_{out}}{dt} &= \mu(t)N_v - kN_{out}R - (\alpha+\delta)N_{out} + \gamma(R_{ges}-R) \\
\frac{dR}{dt} &= -kRN_{out} + \gamma(R_{ges}-R)
\end{aligned}$$

with boundary conditions

$$\begin{aligned}
N_{in}(0) &=: N_{in}^0 > 0 \\
V(0) &=: V_0 \geq 0 \\
N_v(0) &=: N_v^0 \geq 0 \\
N_{out}(0) &=: N_{out}^0 \geq 0 \\
R(0) &=: R_0 \geq 0
\end{aligned}$$

where the model parameters are given by $c, d, k, \alpha, \beta, \gamma, \delta, R_{ges}, \tau_0, \nu_0 \in \mathbb{R}_{\geq 0}$ and $\mu, h : [0,T] \to \mathbb{R}_{\geq 0}$ and we have N_{in}^0, V_0, N_v^0, N_{out}^0 and R_0 as given data.

Example 4.9
Let

$$\begin{aligned}
\tau &: [s_0, s_1] \to \mathbb{R}, \tau(s) := \tau_0 \cdot \left(\frac{s_1 - s}{s_1 - s_0}\right), \\
\nu &: [s_0, s_1] \to \mathbb{R}, \nu(s) := s.
\end{aligned}$$

Then

$$\nu_0 = s_0, c = 1, d = -\frac{\tau_0}{s_1 - s_0}$$

and the ODE system is governed by:

$$\begin{aligned}
\frac{dN_{in}}{dt} &= \beta(w - N_{in})^+ + \alpha N_{out}(t) - N_{in}\frac{\tau_0}{s_1 - s_0}\left(s_1 V(t) - N_v(t)\right) \\
\frac{dV}{dt} &= N_{in}(t)\tau_0 h(t) - \mu(t)V \\
\frac{dN_v}{dt} &= N_{in}(t)\frac{\tau_0}{s_1 - s_0}\left(s_1 V(t) - N_v\right) - \mu(t)N_v \\
\frac{dN_{out}}{dt} &= \mu(t)N_v - kN_{out}R - (\alpha + \delta)N_{out} + \gamma(R_{ges} - R) \\
\frac{dR}{dt} &= -kRN_{out} + \gamma(R_{ges} - R)
\end{aligned}$$

Unfortunately, the difficulties in finding a suitable h (or μ if the other interpretation of the system is chosen) carry over from the PDE system. We now write down an alternative model that does not face these problems:

4.3. **The DDE model.** The crucial points here are that we have two different vesicles pools and the building of new vesicles is described in the system equations — and not by the given data — and may therefore depend on the state variables:

- Building of new vesicles: The idea is to model the "superfluous" membrane by introducing a new state variable $m(t)$ that grows if vesicles fuse with the membrane and is turned into new vesicles. (A time delay δ_m is used since this process takes some time.)
- We model two different vesicle pools: The readily releasable (or primed) pool and the reserve pool. For each pool, we have a number of vesicles and an amount of neurotransmitters contained in the vesicles of that pool. Vesicles are primed with base rate χ and filled with base rate ϕ. But here, for both the priming and filling of vesicles saturation effects are taken into account by adding extra factors, assuming a maximal number p of primed vesicles and a maximum vesicle filling z.

Asides from that we keep the system unchanged for the most part.

This leads to a system with 8 state variables:

- n_p: number of primed vesicles
- n_r: number of readily releasable vesicles
- N_p: amount of neurotransmitters in all primed vesicles
- N_r: amount of neurotransmitters in all readily releasable vesicles
- N_{in}: amount of free neurotransmitters in the presynaptic terminal
- N_{out}: amount of free transmitters in the synaptic cleft
- R: number of free receptors in the postsynaptic membrane
- m: amount of superfluous membrane in the presynaptic terminal

The system is governed by the following set of equations:

$$\frac{dN_p}{dt} = \underbrace{\phi \cdot (zn_p - N_p)^+ \cdot n_p(t) N_{in}(t)}_{\text{filling of vesicles}} + \underbrace{\chi \cdot (p - n_p)^+ \cdot N_r(t)}_{\text{vesicle priming}} \underbrace{-\mu(t) N_p}_{\text{exocytosis}} \tag{61}$$

$$\frac{dN_r}{dt} = \underbrace{\phi \cdot (zn_r - N_r)^+ \cdot n_r(t) N_{in}(t)}_{\text{filling of vesicles}} \underbrace{-\chi \cdot (p - n_p)^+ \cdot N_r}_{\text{vesicle priming}} \tag{62}$$

$$\frac{dn_p}{dt} = \underbrace{\chi \cdot (p - n_p)^+ \cdot n_r(t)}_{\text{vesicle priming}} \underbrace{-\mu(t) n_p}_{\text{exocytosis}} \tag{63}$$

$$\frac{dn_r}{dt} = \underbrace{rm(t - \delta_m)}_{\text{endocytosis}} \underbrace{-\chi \cdot (p - n_p)^+ \cdot n_r}_{\text{vesicle priming}} \tag{64}$$

$$\frac{dN_{in}}{dt} = \underbrace{\beta(w - N_{in})^+}_{\text{“production”}} + \underbrace{\alpha N_{out}(t)}_{\text{re-uptake}} \underbrace{-\phi \cdot (zn_p - N_p)^+ \cdot n_p(t) N_{in}}_{\text{filling of primed vesicles}} \tag{65}$$

$$\underbrace{-\phi \cdot (zn_r - N_r)^+ \cdot n_r(t) N_{in}}_{\text{filling of other vesicles}} \tag{66}$$

$$\frac{dN_{out}}{dt} = \underbrace{\mu(t) N_p(t)}_{\text{exocytosis}} \underbrace{-kR(t) N_{out}}_{\text{binding}} \underbrace{-\alpha N_{out}}_{\text{re-uptake}} \underbrace{-\delta N_{out}}_{\text{diffusion}} + \underbrace{\gamma(R_{ges} - R)}_{\text{unbinding}} \tag{67}$$

$$\frac{dR}{dt} = \underbrace{-kN_{out}(t) R}_{\text{binding}} + \underbrace{\gamma(R_{ges} - R)}_{\text{unbinding}} \tag{68}$$

$$\frac{dm}{dt} = \underbrace{\mu(t) n_p(t)}_{\text{exocytosis}} \underbrace{-rm}_{\text{endocytosis}} \tag{69}$$

using the boundary conditions

$$N_p(0) =: N_p^0 \geq 0 \tag{70}$$

$$N_r(0) =: N_r^0 \geq 0 \tag{71}$$

$$n_p(0) =: n_p^0 \geq 0 \tag{72}$$

$$n_r(0) =: n_r^0 \geq 0 \tag{73}$$

$$N_{in}(0) =: N_{in}^0 > 0 \tag{74}$$

$$N_{out}(0) =: N_{out}^0 \geq 0 \tag{75}$$

$$R(0) =: R_0 \geq 0 \tag{76}$$

$$m(t) =: m_0(t) \geq 0, \quad -\delta_m \leq t \leq 0 \tag{77}$$

where we have as model parameters $k, \alpha, \beta, \gamma, \delta, \delta_m, R_{ges}, \phi, \chi, z, p, r, T \in \mathbb{R}_{\geq 0}$ and $\mu : [0, T] \to \mathbb{R}_{\geq 0}$ and the parameters N_p^0, N_r^0, n_p^0, n_r^0, N_{in}^0, N_{out}^0, R_0 and m_0 as given data.

Theorem 4.10
There exists a unique solution to the DDE system described by equations (61)-(77)*, given that* m_0 *is continuous.*

Proof. We do not give a detailed proof. The idea is to show by induction that there is a unique solution on the time interval $[0, n\delta_m]$ for $n = 1, 2, \ldots$:

(1) For the induction start show that there exists a unique solution on the time interval $[0, \delta_m]$. On this interval, $m(t - \delta_m) = m_0(t - \delta_m)$ is a given function,

so we only have to deal with an ODE system which can be done in the very same way as we handled the ODE part of the basic PDE system.

(2) As induction hypothesis we have that there exists a unique solution on the time interval $[0, (n-1)\delta_m]$.

(3) For the induction step consider the time interval $[0, n\delta_m]$. By induction hypothesis, we already know that the solution exists and is unique up to time point $t = (n-1)\delta_m$. But this implies that $m(t-\delta_m)$ can again be considered as a given function on $[(n-1)\delta_m, n\delta_m]$. So again, only a simple ODE system has to be handled.

□

Of course this modeling approach also implies some simplifications. For example the following facts are ignored:

- In reality, the vesicle priming rate is increased for high calcium concentrations in the presynaptic terminal. (Cf. [NS08]) To consider this, the parameter χ could be made time dependent and calculated by taking the calcium concentration into account but it is questionable whether the additional value of that change outweighs the extra modeling effort.
- Vesicles can also be built in the soma and then be transported to the synaptic terminal. However, to my knowledge this process only plays a minor role.
- The rate of filling depends on the local concentration of transmitters. This concentration is in general not equal for the different pools. In principle, the model can be modified in order to account for this fact: You could either indirectly model local concentrations by using different filling base rates for the pools or split N_{in} into two variables where each variable represents a local transmitter concentration.

Also, most of the simplifications we listed for the basic PDE are implied for the DDE model as well.

In addition, this model does not model vesicle sizes so some details are lost here too. Moreover, several new variables are involved which makes it more difficult to estimate. We now propose a new PDE model that includes the modeling of vesicle sizes and uses two vesicles pools:

4.4. **Two pool PDE model.** The model we are about to introduce is very similar to the basic PDE system but like the DDE model it has two different vesicle pools: v_r describes the vesicle distribution in the reserve pool whereas v_p is used for primed vesicles (in the readily releasable pool). Only primed vesicles are able to fuse with the membrane and do this with the rate $\mu(t)$ and vesicles of the reserve pool become primed with some rate $\chi(t)$.

The rest is basically the same as in the basic PDE system.

Remark: Here a time dependent priming rate χ is chosen instead of a product of base rate and saturation term with state variables as it was done for the DDE model. This way the proof for the well-posedness is essentially the same as for the basic PDE system.

So as state variables we are using:

- v_p: primed vesicles
- v_r: readily releasable vesicles
- N_{in}: amount of free neurotransmitters in the presynaptic terminal
- N_{out}: amount of free transmitters in the synaptic cleft
- R: number of free receptors in the postsynaptic membrane

The two pool PDE model is governed by the following equations:

$$\frac{\partial v_r}{\partial t} + \underbrace{N_{in}(t)\partial_s(\tau(s)v_r(t,s))}_{\text{growth}} = \underbrace{-\chi(t)v_r(t,s)}_{\text{priming}} \tag{78}$$

$$\frac{\partial v_p}{\partial t} + \underbrace{N_{in}(t)\partial_s(\tau(s)v_p(t,s))}_{\text{growth}} = \underbrace{\chi(t)v_r(t,s)}_{\text{priming}} \underbrace{-\mu(t)v_p(t,s)}_{\text{fusion}} \tag{79}$$

$$\frac{dN_{in}}{dt} = \underbrace{\beta(w-N_{in})^+}_{\text{“production”}} + \underbrace{\alpha N_{out}}_{\text{re-uptake}} \underbrace{- N_{in}\int_{s_0}^{s_1}\tau(s)(v_r(t,s)+v_p(t,s))ds}_{\text{filling of vesicles}} \tag{80}$$

$$\frac{dN_{out}}{dt} = \underbrace{\mu(t)\int_{s_0}^{s_1}\nu(s)v_p(t,s)ds}_{\text{exocytosis}} \underbrace{-kN_{out}R}_{\text{binding}} \underbrace{-\alpha N_{out}}_{\text{re-uptake}} \underbrace{-\delta N_{out}}_{\text{diffusion}} + \underbrace{\gamma(R_{ges}-R)}_{\text{unbinding}} \tag{81}$$

$$\frac{dR}{dt} = \underbrace{-kRN_{out}}_{\text{binding}} + \underbrace{\gamma(R_{ges}-R)}_{\text{unbinding}} \tag{82}$$

using the boundary conditions

$$v_r(t,s_0) =: h_r(t), \;\; 0 < t \leq T \tag{83}$$

$$v_p(t,s_0) =: h_p(t), \;\; 0 < t \leq T \tag{84}$$

$$v_r(0,s) =: v_0^r(s), \;\; s_0 \leq s < s_1 \tag{85}$$

$$v_p(0,s) =: v_0^p(s), \;\; s_0 \leq s < s_1 \tag{86}$$

$$N_{in}(0) =: N_{in}^0 > 0 \tag{87}$$

$$N_{out}(0) =: N_{out}^0 \geq 0 \tag{88}$$

$$R(0) =: R_0 \geq 0 \tag{89}$$

where $s_0, s_1, T, w, k, \alpha, \beta, \gamma, \delta, R_{ges} \in \mathbb{R}_{\geq 0}$, $s_0 < s_1$, $\tau, \nu : [s_0, s_1] \to \mathbb{R}_{\geq 0}$ and $\mu, \chi : [0,T] \to \mathbb{R}_{\geq 0}$ are the model parameters and the parameters $N_{in}^0, N_{out}^0, R_0 \in \mathbb{R}_{\geq 0}$, $v_0^r, v_0^p : [s_0, s_1] \to \mathbb{R}_{\geq 0}$, $h_r, h_p : [0,T] \to \mathbb{R}_{\geq 0}$ form the given data.

Remark: Under certain technical assumptions[24] the two pool PDE system is well-posed.

As remarked above, the proof works completely analogous to the well-posedness proof for the basic PDE system. In fact, only equation (79) is of a slightly new form. But even here, the characteristics for this PDE are still the same as for the PDE (2).

The major advantage of the two pool model over the basic PDE model is that here, h_r and h_p describe vesicle endocytosis and μ describes vesicle exocytosis. So the dilemma that troubled us as we chose an interpretation of the basic PDE model does not exist for this model.

Also, this model could possibly serve as a starting point for analyzing dynamics between different vesicle pools.

Remark (Related models)**:** As for the basic PDE system, other models can be derived from the two pool PDE model:

- Using the parameter transform from lemma 3.5 and redefining the state variables $v_r(t, s(\bar{s})) := \tau(s)v_r(t, s(\bar{s}))$ and $v_p(t, s(\bar{s})) := \tau(s)v_p(t, s(\bar{s}))$, an

[24] Including some regularity of the functional model parameters and the given data, plus a restriction of the data space similar to definition 3.3.

equivalent system with constant growth can be formulated. (Cf. section 4.1.)

- An ODE model can be derived. Note, however, that this might require stronger conditions than we need for the well-posedness of the system.

5. The data

All data we have come from experiments on one particular synapse. Hence, it makes sense to elaborate on the special properties of this synapse before analyzing the actual data:

5.1. **The MNTB-LSO synapse.** The synapse that is object to experiments is located in the auditory system and takes part in sound source localization. More precisely, the synapse we deal with forms the connection from the medial nucleus of the trapezoid body (MNTB) to the lateral superior olive (LSO).[25] Hence, it is also referred to as MNTB-LSO synapse.

The MNTB-LSO synapse is an inhibitory synapse, mainly using glycine as transmitter. The glycine cycle has some interesting characteristics:

- New glycine does *not* just come from the soma if glycine concentrations in the synaptic terminal are low: If glycine transporters (for re-uptake) are disabled by a poison, the glycine concentration in synaptic vesicles decreases over time. (Also see [AT13].) Hence, the production rate of glycine is probably very low or not even relevant.[26]
- The glycine cycle is very efficient (in the absence of poison):
  - Most glycine molecules are transported directly to the presynaptic terminal from the cleft.
  - Glycine that unbinds from receptors may bind again to receptors.
  - Glycine that diffuses away from the synaptic cleft is generally transported back to the soma (by glial cells for example).

It is also noteworthy that the glycine concentration is in general much higher near the transporters at the active zones (where the readily releasable vesicles are located) than around the reserve pool, hence vesicles in the reserve pool are filled slower with glycine than vesicles in the readily releasable pool because of lower local glycine concentration.

γ-Aminobutyric acid (GABA) also plays a role in the MNTB-LSO synapse but mediates only a rather small part of the postsynaptic response. (Cf. [Fis10] and [Bak13].)

Also, our model does not include different neurotransmitter species. Still, for developing more detailed models the following information could be relevant:

- GABA and glycine are transported into vesicles via the same transporters.
- GABA is synthesized directly at the vesicles in the reserve pool from glutamate and some other particles. The GABA production rate therefore depends on the local concentrations of these components.
- GABA constantly leaks out of vesicles.

Also recall that enzymatic degradation only happens for acetylcholine, so at the MNTB-LSO synapse, transmitters that bind to postsynaptic receptors go back into the synaptic cleft after unbinding.

5.2. **Experimental procedure.** The setting is displayed schematically in figure 9.

A slice of brain tissue from the auditory brainstem of a mouse is put into a dilution and placed under a microscope. Throughout the experiment, the preparation is held at physiological temperature. A micropipette is placed near the axon of the presynaptic neuron for stimulation and another micropipette is placed at the cell body of the postsynaptic neuron for recording of the response.

[25] This synapse comes directly after the well-studied calyx of held synapse in signal processing.

[26] Also note that glycine is harder to synthesize in comparison to other transmitters like GABA for example.

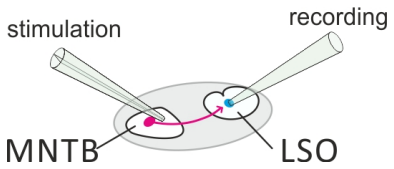

FIGURE 9. Illustration of the experimental layout.

The basic steps are now:

(1) Pulselike currents are injected through the stimulation electrode with a certain frequency over a certain time.
(2) Each time a current is injected, an electrical field is created, changing the membrane potentials of nearby axons.
(3) Consequently, an action potential is triggered in the axon leading to the MNTB-LSO synapse and propagated down to the synapse, causing neurotransmitters to be released into the synaptic cleft.[27]
(4) The released neurotransmitters bind to receptors of the postsynaptic cell, finally causing a current to flow through the postsynaptic membrane.
(5) The recording electrode maintains a constant postsynaptic potential (which is close to the resting potential) by injecting appropriate currents. So if synaptic transmission causes extra currents to flow through the postsynaptic membrane this electrode must respond by adjusting the amount of current injection to keep the membrane potential constant. The currents that flow through this electrode are recorded and form the output of the experiment. The recording takes place at 10000 Hz, i.e. 10000 samples are recorded each second.

So we actually have some sort of binary input: At a given time there either is a stimulus or there is none. However, the precise stimulation times are not recorded directly. Instead, the electrical field created by each current injection causes a pulselike artifact in the measurements of the recording electrode. Together with the information of the stimulation frequency, this can be used to determine the precise stimulation times.

There is another issue concerning the output of the experiment: The electrical field created by the current injection might cause several axons to fire. Hence, the measured response cannot really be assumed to be caused by the firing of a single axon. In fact, the response cannot even be assumed to be the result of the firing of a constant number of axons since single fibers occasionally fail to create any action potential. (The failure rate is highly dependent on the input frequency.)

5.3. **Recording protocol.** The recording protocol employed to obtain the data we used to test our model can be described by the following pseudo-code:[28]

(1) Set $f := [1, 2, 5, 10, 50, 100, 200]$.
(2) For $i = 0, \ldots, \text{size}(f) - 1$:
(3) Start measurements.
(4) No stimulation for 1s.
(5) 60s stimulation with frequency $f[i]$ Hz
(6) 60s stimulation with frequency 1 Hz
(7) No stimulation for 2s.
(8) End measurements.

[27]Shape and amplitude of the injected current were determined by trying out different variations and choosing a current that reliably triggers exactly one action potential.

[28]Cf. [Bak13, p. 10].

(9) No stimulation for 7s.

5.4. **The raw data.** The following figure shows the complete data for a certain frequency:

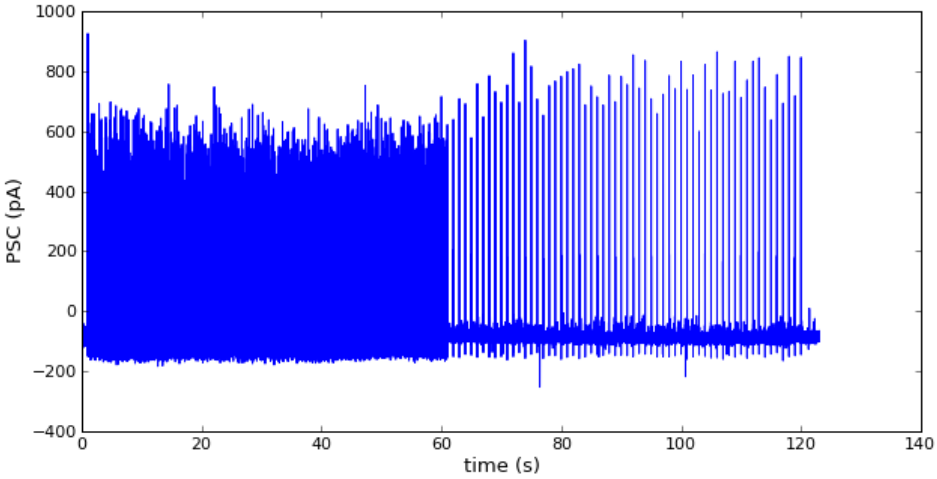

FIGURE 10. Raw data of the 10 Hz experiment.

If we zoom into the data around a single stimulus we get a picture as shown in figure 11. We see a typical response of the postsynaptic cell to a single stimulus. We also see that the measurements are noisy.

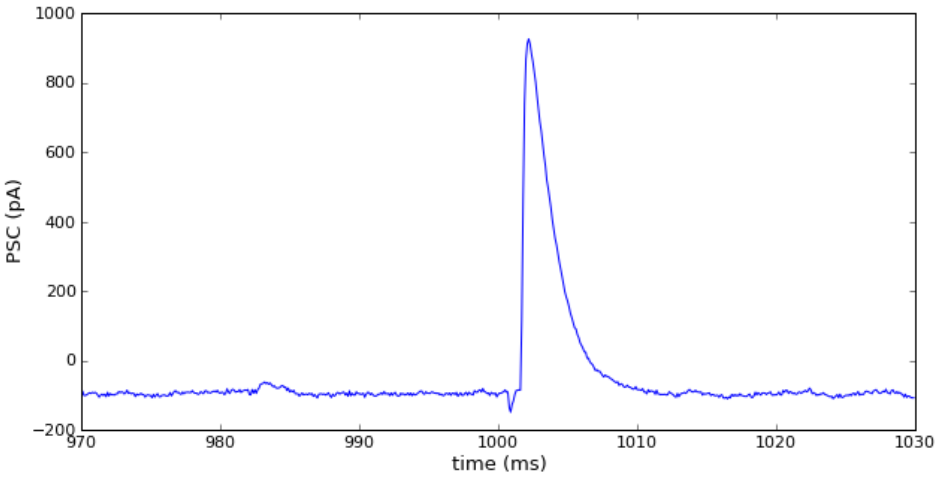

FIGURE 11. Raw data cutout showing the first postsynaptic response of the 10 Hz experiment. The stimulus occurs shortly after $t = 1000ms$ and is actually visible in the data as a small downward pointing spike. The response has an usual shape and is rather large in amplitude. Note that there is spontaneous release visible in the data in form of a small bump between $t = 980ms$ and $t = 990ms$.

Figure 12 shows an excerpt from the 100 Hz experiment. Here we can observe that the initial response is largest in amplitude. We also see that there is some supposedly random variation in the amplitudes of the successive responses.

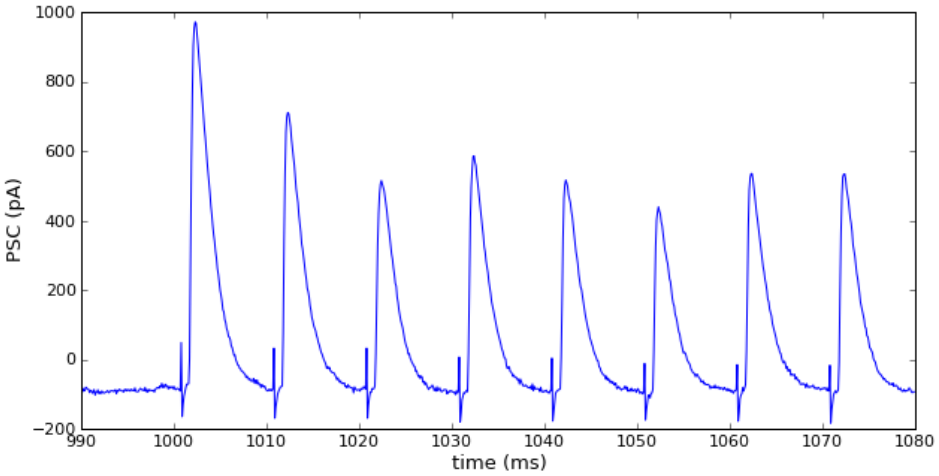

FIGURE 12. Sample output for stimulation with 100 Hz around the first stimuli. Note the initial drop and variation in response amplitude.

Asides from that, there are a few interesting effects that can be observed:

- There is in general a slight drift of stimulus (and responses) over time, i.e. we can not expect the stimuli of the 1 Hz experiment to occur precisely at times $t = 1s, 2s, 3s, \ldots$ but have to detect artifacts in order to determine the precise times of stimulation.
- The injected currents cause artifacts in the measurements of the PSC. These artifacts are of course not modeled in our system and thus, need to be removed.
- There is a baseline current which tends to drift into some direction during the experiment. The existence of this flux can be explained by the way the measurements are done: As the membrane is held at a constant potential which is in general not exactly equal to the resting potential, the recording electrode must constantly "work against the cell" in order to keep that potential. The precise cause of the variation in baseline current is not clear. Different reasons like for instance slight changes in temperature, measurement errors or some sort of fatigue of the cells are possible.

Additionally, the response amplitude decreases over time for frequencies of 10 Hz or more.[29]

For increasing frequencies, stochasticity becomes more and more relevant. See figure 13 for an example. Among other things, high frequency stimulus can indeed make the cell rather unorganized and in that way lead to a somehow extraordinary behavior. (Cf. [KvG09].) It has to be doubted whether our model is still applicable here so we chose not to use data of the 200 Hz experiment for our testing.

Remark ("Manic" filling state)**:** Synapses in biological preparations are in a somewhat unnatural state: In a working brain, neurons are permanently exposed to different kinds of inputs. These inputs are reduced close to zero in preparations over an extended period of time. This has some implications. For instance, the vesicles are fuller than usual.

[29]This might be in part due to single fiber failure. However, remember that we are modeling the average case.

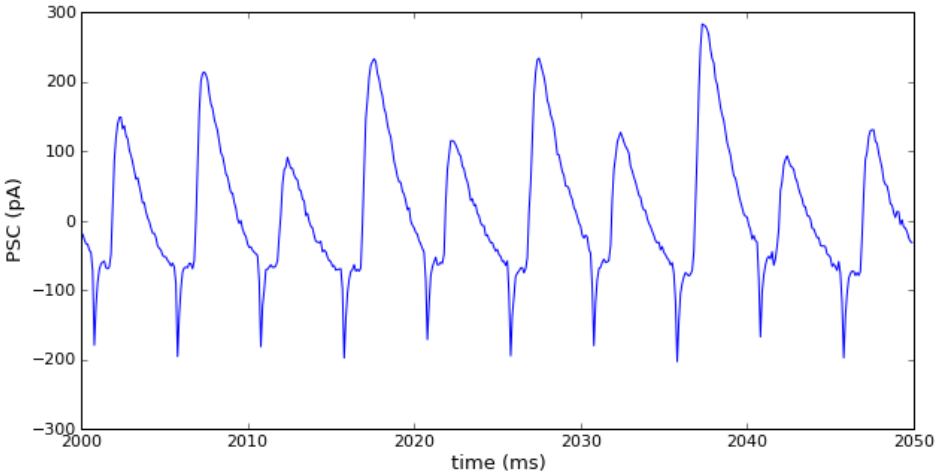

FIGURE 13. Sample output for stimulation with 200 Hz. Note that there are large variations in the response amplitude. Also, the baseline is hard to determine.

5.5. **Preprocessing.** As stated before, we need to remove artifacts. Also, as we need to know the precise stimulation times (which are not measured directly), preprocessing becomes necessary in order to extract this information from the data.

In addition, the baseline current should be removed, i.e. the data should be shifted so that there is zero flux in the resting case.

As our model is purely deterministic, we cannot expect to get a noisy output as it is observed in experiments. So some smoothing seems reasonable as well.

Remark (Difficulties):

- The shape of the artifacts differs because of limited temporal resolution of the measuring sensors.
- Only the approximate location of artifacts is known. There might be (and usually there is) a sort of drift over time.
- How to handle asynchronous and spontaneous release? Should this both be considered as noise and removed?
- It is not known how many fibers are stimulated in the experiments. (It is estimated that about 1-5 axons become active after stimulation.)

5.6. **Baseline correction.** We assume that for each run, the baseline current is constant and equal to the baseline current at the beginning of the experiment. We do this mainly for the following reasons:

- When using the data for testing our models, we will generally restrict ourselves to data of the first few seconds of the experiments. In that range, the baseline current remains more or less constant for low to mid frequency stimulus.
- A general shift in the baseline current during high frequency stimulus is part of the postsynaptic response and therefore, should not be removed.

Hence, we compute the average of the data at the beginning (prior to the first stimulus) and subtract that value from the entire data array.

5.7. **Determining stimulus times.** Most stimuli are visible in the data as artifacts. As mentioned above, the shape of the artifacts is variable. What most

artifacts have in common is the short duration and an especially high or low value of the flowing current. Asides from that, there is quite some variation as can be seen in the examples depicted in figure 14.

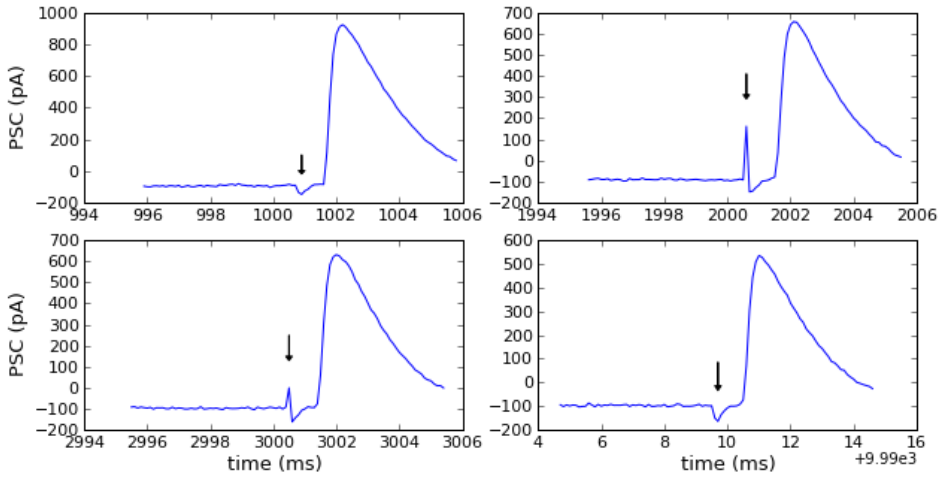

FIGURE 14. Different artifact shapes. The artifacts occur prior to the (large) postsynaptic response and are marked by arrows.

Remark: The amplitude of the artifacts oscillates for most frequencies. This is due to the limited temporal resolution of the sensors.

The precise times of stimulation are found in multiple steps:

(1) First release times are detected: It is assumed that releases can be characterized as points where the current is above some threshold for some duration. (Values for threshold and duration were determined empirically.)
(2) Next positions are located where the possibility of having an artifact is high: First a Laplacian filter is applied to the data. The artifact candidates are now the points where the absolute value of the Laplacian exceeds some fixed threshold, taking into account only points where no release has been detected and the current is either below some lower threshold or above some upper threshold.
(3) Now frequency information is taken into account and we move from one possible artifact position to the next: The first artifact must occur around time $t = 1s$. Since we know the frequency of the stimulation, we also know the approximate location of the next stimulus. So we choose among the artifact candidates the one that is closest to that approximate location. If there is no candidate within some given radius of the estimated location, it is assumed that the artifact has been overlooked by the artifact candidate detection and the approximated location is used as next artifact location. Then based on the computed location of the second artifact, the location of the next artifact is estimated and so on.

Note that the value of the Laplace threshold is particularly important for artifact detection: For a low threshold, there are too many candidates and for a high threshold, artifacts are often missed. We choose a rather low threshold and then use an estimation of the stimulus time (based on frequency information) to choose among the resulting candidates.

5.8. **Noise and artifact removal.** We want to remove artifacts and "randomness" while preserving features like the shapes of the responses for example.

Virtually any smoothing removes the tremor of the line to some point if used with suitable parameters. However, the shape of the responses is easily destroyed. In particular, the amplitude of the response is typically reduced to some extent. In our experiments, the best results were obtained for a median filter followed by a very light Gaussian smoothing. Most artifacts are removed completely by the median filter, the resulting lines look rather smooth and the overall shape is preserved pretty well as can be seen in figure 15.

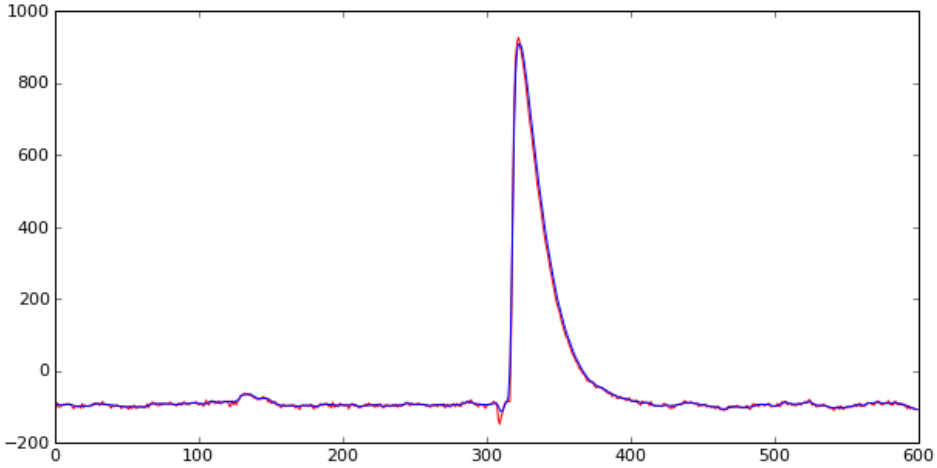

FIGURE 15. Noise removal. The red curve shows the original data and the blue curve the the smoothened data. It was smoothened by first applying a median filter and then using Gaussian smoothing.

Remark: There is also a theoretical justification for choosing a median filter over a Gaussian filter for our purposes: Gaussian smoothing works best for noise that is distributed according to some symmetric distribution with a mean value of zero. For optimization, that kind of noise does not do much harm asides from making the objective function value worse because the resulting errors kind of average out automatically. So it is far more important to remove artifacts and other unsymmetric noise. And for that task, a median filter is clearly the better choice.

5.9. **Summary.** Let us quickly recapitulate the most important points:

- The data we have consist of measurements of the postsynaptic current at the MNTB-LSO synapse.
- We obtain the input by determining points of stimuli which are visible in the measurements as artifacts and writing it into a binary array.
- To obtain the output, we first correct the baseline of the raw data and then remove the noise (including artifacts) by smoothing.

6. Optimization

We want to test if our models can be used to reproduce postsynaptic currents as measured in experiments, given only the stimulation times. As we have not determined any concrete values for the model parameters or the given data, this testing amounts to an optimization problem of the form

$$\min_{p\in\mathcal{P},\theta\in\Theta} \; dist\big(PSC(.,p,\theta), data(.)\big)dt \tag{90}$$

where $dist : L^1([0,T]) \times L^1([0,T]) \to \mathbb{R}_{\geq 0}$ denotes some function to measure the distance between two functions, $data(t)$ is the measured postsynaptic current at time $t \in [0,T]$, $\mathcal{P}$ defines the set of feasible model parameters, Θ is the set of feasible given data and $PSC(t,p,\theta)$ denotes the postsynaptic current that is output by the model at time $t \in [0,T]$, using parameter values $p \in \mathcal{P}$ and given data $\theta \in \Theta$, given the times of stimulation.

In this section, we will talk about this optimization problem in a rather abstract way. Here, we will not choose a specific model and stick to the general notations that have just been introduced. In the next section we will then see how this optimization works in specific cases for a few selected models.

Note that in the general form (90), our problem is nonlinear and of infinite dimension (since both $\mathcal{P}$ and Θ may include functions). Also, in general we have to solve a PDE/ODE system for each objective function evaluation. This makes it quite a hard task to find the optimal value to the problem.

We will later use some assumptions that will at least reduce the problem to finite dimensions. But before we do that, let us talk about the output of the model. So far, postsynaptic currents are not yet described by any of our models, so we first have to figure out the relation between the state variables and the PSC.

6.1. Modeling the PSC.

All of our models include the number R of free receptors of the postsynaptic cell as state variable. Since we generally assume a constant number of postsynaptic receptors, we have the number of occupied receptors given by $(R_{ges} - R)$.

The number of occupied receptors is related closely to the PSC: These two sizes are approximately proportional to each other. Since this linear relationship is only an approximation[30], we formulate it as an assumption:

Assumption 6.1
For any $p \in \mathcal{P}$ and $\theta \in \Theta$, we assume the PSC to be proportional to the number of occupied receptors:

$$PSC(t,p,\theta) = r(R_{ges} - R(t,p,\theta)),$$

where the factor $r > 0$ is a variable that is added to the model parameters (and has to be optimized as well) and $R(.,p,\theta)$ is part of the solution to the system using model parameters p and given data θ.

Under assumption 6.1 the problem (90) can be rewritten as follows:

$$\min_{p\in\mathcal{P},\theta\in\Theta} \; dist\big(r(R_{ges} - R(.,p,\theta)), data(.)\big)dt \tag{91}$$

6.2. Reduction to finite dimensions.

The basic idea here is to choose finite dimensional subsets of $\mathcal{P}$ and Θ. This can be done by making certain assumptions about the shape of the functional parameters. E.g. a function can be assumed to be a polynomial up to a fixed degree, which leaves a finite number of coefficients to be optimized. Of course, one should choose restrictions that also make sense from a modeling point of view and are biological plausible if possible.

[30] In real neurons the receptors' sensibility might change over time. They might become sensitized after repetitive input for example. Cf. [TZR93] for example.

We have in fact already seen such restrictions for the functions h (cf. example 2.3), μ (cf. assumptions 2.1 and 2.2), τ and ν (cf. assumption 4.8). For the testing we will actually only use the basic ODE model and the DDE model so these are all functions that need to be handled.

Remark (Infinite dimensional problems)**:** There are also some optimization problems related to our models where you might want to optimize over infinite dimensions.

For example, it would be interesting to determine biological plausible values for all of the variables except for one function which is then optimized as only variable and see how close the resulting function is to our proposed shape. This would be especially interesting for functions such as h where determining a reasonable shape is quite demanding.

6.3. **The distance function.** We haven't talked about reasonable distance functions yet. First note that the postsynaptic current measured in the experiments is discretized during the measurement process, i.e. the data we want to fit is an n-dimensional vector of currents where n denotes the number of measurements.

Therefore, we can use any metric on $\mathbb{R}^n$ to measure the distance. Since most nonlinear optimization algorithms assume differentiability of the objective function, we go for the squared Euclidean distance measure. (We square it to get rid of the root.)

With this choice we may again rewrite the optimization problem, so we now have:

$$\min_{p\in\mathcal{P},\theta\in\Theta} \sum_{i=0}^{n-1} \big(r(R_{ges} - R(t_i, p, \theta)) - data(t_i)\big)^2 dt, \tag{92}$$

denoting the measurement times by t_i, $i = 0, \ldots, n-1$.

6.4. **Summary.** Before we continue with the practical tests where such optimization problems are solved, we summarize the steps necessary to actually compute the objective function for given variables:

(1) The stimulation times are used to compute the time course of the local calcium concentration at the active zones. (Under assumption 2.2.)
(2) The release rate $\mu(t)$ is computed from the local calcium concentration. (Under assumption 2.1.)
(3) In one version of the ODE model, the vesicle source term h is now also computed from the local calcium concentration. (See example 2.3.)
(4) If necessary, other assumptions are applied in order to obtain a finite number of variables.
(5) Now the PDE/ODE system is solved.
(6) The postsynaptic current is calculated according to assumption 6.1.
(7) The distance of the computed current to the measurements is calculated as in 92.

7. Experiments

We implemented two versions of the ODE model (derived from the basic PDE system), one with a constant and one with a χ^2-based function h, plus the DDE model in Python and optimized all three versions on the preprocessed data from the MNTB-LSO synapse.[31]

7.1. **The models.** For all models we made assumptions as suggested in the previous section in order to reduce problem dimensionality while maintaining biological plausibility. We modify the earlier assumptions slightly and sum everything up here for the sake of clarity:

Assumption 7.1
Let $t_i \in [0,T]$ denote the times of stimulation. We assume that

$$\begin{aligned} PSC(t,p,\theta) &= 100 \cdot (R_{ges} - R(t,p,\theta)), \\ [Ca](t) &= b\left(\sum_i \mathbb{1}_{[t_i+\delta_{Ca},\infty)}(t)\exp(-a(t-(\delta_{Ca}+t_i)))\right), \\ \mu(t) &= \mu \cdot [Ca](t) \end{aligned}$$

for all $t \in [0,T]$, $s \in [s_0,s_1]$, model parameters p and given data θ where the constants $\mu, a, b, \delta_{Ca} \geq 0$ are added to the model parameters.

Additionally, we set R_0 to R_{ges} because we will always use data without any significant current flow at the very beginning.

Remark: Assumption 7.1 mainly consists of assumptions 6.1, 2.2 and 2.1 with the following modifications:

- r was set to 100 because scaling can also be achieved by changing other parameters.
- The calcium baseline $[Ca]_0$ was set to zero since the data was preprocessed to have a baseline current of zero.

7.1.1. *The ODE models.* There are still three functions included in the model parameters: $\nu(s)$, $\tau(s)$ and $h(t)$.

For both versions of the ODE model we choose the following functions ν and τ:

$$\begin{aligned} \nu(s) &:= s, \\ \tau(s) &:= \tau_0 \cdot \left(\frac{s_1 - s}{s_1 - s_0}\right) \end{aligned}$$

for all $s \in [s_0,s_1]$. Note that this is a special case of example 4.9.

The function $h(t)$ is the only part that differs for the two versions of the ODE system:

- In the first model we select the function that has been proposed in example 2.3:

$$h(t) := h_{amp} \cdot \left(\sum_i \chi^2\Big(\frac{h_{width}}{100}(t-(h_\delta+t_i)),3\Big)\right)$$

  for all $t \in [0,T]$, where $t_i \in [0,T]$ are the stimulation times and h_{width}, h_{amp} and $h_\delta \geq 0$ are added to the model parameters.
- For the second model we use a constant h, i.e. $h(t) := h$ for all $t \in [0,T]$ where $h \geq 0$ is used as model parameter.

[31] The preprocessing was done as outlined in section 5.

7.1.2. *The DDE model.* For the DDE model there only is one function that is yet unhandled: The function $m_0(t)$. We set this function to zero and justify this assumption with the fact that we will only use data from the beginning of the biological experiments where there has been a period of rest for at least 10 seconds[32] and that at the end of each run there was a longer period of stimulation with 1 Hz only. So it is reasonable to assume that there is no or at least very little excess membrane at the beginning.

Assumption 7.2
We assume that $m_0(t) = 0$ for all $t \in [-\delta_m, 0]$. Additionally, we assume that $\delta_m \geq T$.

The assumption that $\delta_m \geq T$ is reasonable because the data we will be using will in almost all cases be shorter than 1 second whereas endocytosis usually takes around 15 seconds (or $1 - 2$ seconds in some special cases). (Cf. [SDC12] for example.)

Assumption 7.2 changes our DDE system into an ODE system which, amongst others, makes it easier to compute the output of the model.

Remark: The particular data we are using might not be the best choice to test the DDE model since it disposes of a major part of its system dynamics as the state variable m becomes completely irrelevant for the output. (Cf. assumption 7.2.) Even so, we used this data and sticked to the assumption because of time- and performance-related reasons and think that the test results still give you a good idea of the system's ability to perform on biological data.

In future experiments, more specific experiments could be designed for the DDE model to see how good vesicle dynamics are captured.

7.2. **Optimization.** For all models and trials, we choose the square of the Euclidean distance measure as objective function. (Cf. section 6.3.)

The constraints depend on the chosen model of course but generally speaking, the only restriction we use is that we require all parameters to be non-negative.

There is only one exception to this: We require $s_1 \geq 1$ for the ODE models.[33] This extra constraint was added because we encountered some "divided by zero" errors without it.

Remark (Other possible constraints)**:** From a modeling point of view, two other constraints would actually be reasonable as well:

- The constraint $s_0 \leq s_1$: Clearly, the minimal size should not exceed the maximal size.
- The requirement that $s_0 > 0$: In our case, $s_0 = 0$ would be unrealistic because $\nu(s_0) = s_0$ and we chose the primed vesicle interpretation. (Cf. subsection 2.1.)

However, these assumptions were always fulfilled automatically (when the optimization was started with appropriate initial values) so they were not explicitly added to the constraints.

We can now formulate the specific optimization problems in detail:

7.2.1. *The specific problems.* For convenience we will use the following notation:

Notation 7.3
Here we denote the measurement times by t_i, $i = 0, \ldots, n-1$ and the stimulation times by $\bar{t}_j$, $j = 0, \ldots, z \leq n-1$.

---

[32] Check the recording protocol which has been described in section 5.3.

[33] The constraint would actually be reasonable as well.

Putting things together, the optimization problem for the ODE models that are used to perform the tests takes the following form:

$$
\begin{aligned}
\min \quad & \sum_{i=0}^{n-1} \big(100 \cdot (R_{ges} - R(t_i, p, \theta)) - data(t_i)\big)^2 dt \\
s.t. \quad & \frac{dR(t,p,\theta)}{dt} = -kRN_{out} + \gamma(R_{ges} - R), \\
& \frac{dN_{out}(t,p,\theta)}{dt} = \mu(t)N_v - kN_{out}R - (\alpha+\delta)N_{out} + \gamma(R_{ges} - R), \\
& \frac{dN_v(t,p,\theta)}{dt} = N_{in}\frac{\tau_0}{s_1 - s_0}(s_1 V - N_v) - \mu(t)N_v, \\
& \frac{dV(t,p,\theta)}{dt} = N_{in}\tau_0 h(t) - \mu(t)V, \\
& \frac{dN_{in}(t,p,\theta)}{dt} = \beta(w - N_{in})^+ + \alpha N_{out} - N_{in}\frac{\tau_0}{s_1 - s_0}(s_1 V - N_v), \\
& \mu(t) = \mu \cdot [Ca](t), \\
& [Ca](t) = b\left(\sum_j \mathbb{1}_{[\bar{t}_j + \delta_{Ca}, \infty)}(t) \exp(-a(t - (\delta_{Ca} + \bar{t}_j)))\right), \\
& R(0,p,\theta) = R_{ges}, \\
& (N_{out}(0,p,\theta), N_v(0,p,\theta), V(0,p,\theta), N_{in}(0,p,\theta)) \\
& \quad = (N_{out}^0, N_v^0, V_0, N_{in}^0) = \theta \in \mathbb{R}^4_{\geq 0}, \\
& \left.\begin{aligned}
& h(t) = h_{amp} \cdot \left(\sum_j \chi^2\Big(\frac{h_{width}}{100}(t - (h_\delta + \bar{t}_j)), 3\Big)\right), \\
& (a, b, k, w, \alpha, \beta, \gamma, \delta, \mu, R_{ges}, \tau_0, \delta_{Ca}, h_{amp}, h_\delta, h_{width}, s_0, s_1) \\
& \quad = p \in \mathbb{R}^{16}_{\geq 0} \times \mathbb{R}_{\geq 1},
\end{aligned}\right\} \text{ version 1} \\
& \left.\begin{aligned}
& h(t) = h, \\
& (a, b, h, k, w, \alpha, \beta, \gamma, \delta, \mu, R_{ges}, \tau_0, \delta_{Ca}, s_0, s_1) = p \in \mathbb{R}^{14}_{\geq 0} \times \mathbb{R}_{\geq 1},
\end{aligned}\right\} \text{ version 2} \\
& \text{for all } t \in [0, T],
\end{aligned}
$$

where the arguments of R, N_{out}, N_v, V and N_{in} on the right-hand side of the equations have been omitted for better readability.

For the DDE model we obtain the following optimization problem:

$$
\begin{aligned}
\min \quad & \sum_{i=0}^{n-1} \big(100 \cdot (R_{ges} - R(t_i, p, \theta)) - data(t_i)\big)^2 dt \\
s.t. \quad & \frac{dR(t,p,\theta)}{dt} = -kN_{out}R + \gamma(R_{ges} - R), \\
& \frac{dN_{out}(t,p,\theta)}{dt} = \mu(t)N_p - kRN_{out} - (\alpha+\delta)N_{out} + \gamma(R_{ges} - R), \\
& \frac{dN_p(t,p,\theta)}{dt} = \phi \cdot (zn_p - N_p)^+ \cdot n_p N_{in} + \chi \cdot (\tilde{p} - n_p)^+ \cdot N_r - \mu(t)N_p, \\
& \frac{dN_r(t,p,\theta)}{dt} = \phi \cdot (zn_r - N_r)^+ \cdot n_r N_{in} - \chi \cdot (\tilde{p} - n_p)^+ \cdot N_r, \\
& \frac{dn_p(t,p,\theta)}{dt} = \chi \cdot (\tilde{p} - n_p)^+ \cdot n_r - \mu(t)n_p, \\
& \frac{dn_r(t,p,\theta)}{dt} = -\chi \cdot (\tilde{p} - n_p)^+ \cdot n_r, \\
& \frac{dN_{in}(t,p,\theta)}{dt} = \beta(w - N_{in})^+ + \alpha N_{out} - \phi \cdot (zn_p - N_p)^+ \cdot n_p \\
& \qquad\qquad - \phi \cdot (zn_r - N_r)^+ \cdot n_r N_{in} \\
& \mu(t) = \mu \cdot [Ca](t), \\
& [Ca](t) = b \left(\sum_j \mathbb{1}_{[\bar{t}_j + \delta_{Ca}, \infty)}(t) \exp(-a(t - (\delta_{Ca} + \bar{t}_j))) \right), \\
& R(0,p,\theta) = R_{ges}, \\
& (N_{out}(0,p,\theta), N_p(0,p,\theta), N_r(0,p,\theta), n_p(0,p,\theta), n_r(0,p,\theta), N_{in}(0,p,\theta)) \\
& \quad = (N_{out}^0, N_p^0, N_r^0, n_p^0, n_r^0, N_{in}^0) = \theta \in \mathbb{R}^6_{\geq 0}, \\
& (a, b, k, \tilde{p}, w, z, \alpha, \beta, \gamma, \delta, \mu, \phi, \chi, R_{ges}, \delta_{Ca}) = p \in \mathbb{R}^{15}_{\geq 0}, \\
& \text{for all } t \in [0, T],
\end{aligned}
$$

again omitting arguments on the right-hand side of the equations. Also note that m has been removed from the system because of assumption 7.2.

7.2.2. *Optimization methods.* Solving the optimization problems we just formulated is quite challenging:

- We have between 15 and 21 variables. So the number of variables is rather large (for a data fitting problem).
- The interactions between the different variables are really complex.
- Rather small changes in the parameters can have a large impact on the later behavior of the model, especially if there is no stimulation during the first few seconds of the data
- Different kinds of behavior are possible for each of the models which suggests that there might be many local minima.
- In some cases it might be very hard for the optimization algorithm to get away from bad local minima. For instance, if the model has reached some local minimum where the initial response amplitude is way too low, unlearning this bad habit would require multiple parameters to be changed in a specific way.

In fact, we tried different nonlinear optimization algorithms and most of them failed completely. Finally, the L-BFGS-B algorithm (see [ZBLN97]) did the best job. But

even with this algorithm optimization sometimes failed. (For example in case of very bad starting parameters.)

So, basically we always use the L-BFGS-B algorithm for solving any of these complex optimization problems. But we apply a few additional techniques:

- Step by step optimization: We generally started by optimizing on single spike data to get the correct response shape. Then optimization is done for two frequencies simultaneously by adding the respective objective function values. This way optimization on data from one frequency does not destroy the performance for the other frequency.
- We sometimes manually adjusted parameters. This method was quite useful for finding initial parameter values and changing the shape of the response curve in more or less specific ways.
- The given data was kept at fixed values most of the time in order to reduce the number of variables.
- Random modifications: We often modified the parameters randomly after optimization and then optimized once more. This was done to avoid becoming stuck in bad local minima.

  The modifications were done by multiplying each parameter with a random number in $[1-\epsilon, 1+\epsilon]$ were ϵ was generally set to 0.01. To avoid overly big modifications in many parameters at the same time, we did not choose uniformly distributed random numbers but computed each factor according to

$$factor = 1 + (2r_1 - 1) \cdot (2r_2 - 1) \cdot \epsilon$$

  where r_1 and r_2 are two random numbers taken from a uniform distribution on $[0, 1]$.

  This technique was generally used repeatedly.

7.2.3. *Procedure.* For each model two different trials were performed:

(1) In the first trial we checked whether the chosen models can reproduce the correct response shapes and see if there is any chance to do optimization successfully for more data:
   (a) First optimization was done for single spike data ranging from time $t = 990ms$ till $t = 1030ms$:
   We started by manually adjusting the parameters until the shape of the spike was roughly reproduced and the variable behavior looked reasonable. Then we optimized using the L-BFGS-B algorithm.
   After that we again tuned some of the parameters by hand and optimized once more. This was done to leave suboptimal local minima while the manual adjustments made it more likely to end up with a better objective function value after optimization.
   For all models we repeated this step until the objective function value was smaller than 200 times the length of the data array.
   Note that in this step we changed the given data by hand but did not include these parameters into the automatic optimization procedure.
   (b) Now more data was used for optimization ($990 - 1150ms$), taking data from experiments with 10 and 100 Hz. Optimization was done for both frequencies simultaneously by summing up the objective functions of the two different frequencies, weighting the data of the 10 Hz experiment double because of the much lower number of spikes in comparison to the 100 Hz data. We optimized the model and then did 10 rounds of random parameter variation followed by optimization.

Again, only the model parameters were optimized whereas the given data was left untouched.

(c) Without optimizing on that data, the resulting model was tested on 50 Hz data ($990 - 1150ms$).

(2) The second task we designed is much more demanding. The purpose of this task is to see which effects can be reproduced and also to figure out the limits of the tested models (and our optimization approach):

(a) Single spike optimization using data from time $t = 800ms$ till $t = 1030ms$:
As starting point, the optimal parameters from the single spike scenario of the first trial have been used.
We optimized once and then did 10 rounds of random parameter variation followed by optimization. During all these runs, the model parameters and the given data have both been optimized and randomly modified for the second version of the ODE model and the DDE model. For the first version of the ODE model only the model parameters were changed simply because including the given data into the optimization procedure did not yield satisfactory results for this model.

(b) As in the first trial we now optimized on the 10 Hz ($800-2800ms$) and 100 Hz ($800-1400ms$) data simultaneously. This time both objective function values were weighted equally though because of the longer time range of the 10 Hz data.
Optimization was done once. If the objective function was still bad, the technique of random modification and successive optimization was applied up to 4 times. Here we used $\epsilon = 0.1$ for the random modification if $\epsilon = 0.01$ did not lead to significant improvements.

(c) Without further optimization, the resulting model was tested on 50 Hz data from the $800 - 2800ms$ time range.

7.3. **Implementation.** As stated above, everything was implemented in Python. Let us have a few words on the specific methods we used.

The SciPy package `scipy.integrate.odeint` was picked as ODE solver of our choice. The following parameters were used:

- In addition to the vector of derivatives of the state variables, the Jacobian matrix of this vector was given to `odeint`.[34]
- The maximal absolute stepsize was set to 1 because inputs were sometimes missed completely without this parameter.
- Asides from that, the solver was always called with default parameters.

The Python interface `scipy.optimize.fmin_l_bfgs_b` was used to run the L-BFGS-B algorithm. The parameters were set as follows:

- We set `factr` to $1e12$. (This parameter determines a stop criterion. Check the SciPy documentation for more information.)
- We let the algorithm compute the gradient of the objective function numerically and set the step size for doing this to 0.001.

7.4. **Results.** For both versions of the ODE model, the given data

$$(N_{out}^0, N_v^0, V_0, N_{in}^0) = (0, 25, 20, 50)$$

worked well in the first trial and was left unchanged during this trial.

[34]This parameter was not supplied for the optimization of model parameters and given data in the single spike scenario of the second trial. The reason for that being that it simply was not necessary to speed this optimization up or make the solution more accurate.

7.4.1. *First trial — ODE model with χ^2-based h.* For the ODE model with χ^2-based h, we obtained as optimal parameters for the single spike data:

$$\begin{aligned}(a, b, k, w, \alpha, \beta, \gamma, \delta, \mu, R_{ges}, \tau_0, \delta_{Ca}, h_{amp}, h_\delta, h_{width}, s_0, s_1)\\ \approx (0.12, 9.04, 0.072, 64.36, 0.27, 0.0064, 0.65, 0.064,\\ 0.0091, 25.76, 0.13, 9.31, 0.26, 64.36, 19.31, 1.29, 3.98)\end{aligned}$$

Optimization on the 10 and 100 Hz data changed the parameters to

$$\begin{aligned}(a, b, k, w, \alpha, \beta, \gamma, \delta, \mu, R_{ges}, \tau_0, \delta_{Ca}, h_{amp}, h_\delta, h_{width}, s_0, s_1)\\ = (0.092, 10.50, 0.025, 46.23, 0.17, 0.022, 0.44, 0.035,\\ 0.018, 18.70, 0.10, 8.56, 0.18, 46.32, 13.87, 1.85, 4.43).\end{aligned}$$

Results for this version of the ODE model are depicted in figure 16. Different effects like the time courses of the response amplitudes for the different frequencies are reproduced fairly well for this model. In particular, the generalization to the 50 Hz data was successful. Also note the nearly perfect reproduction of the single spike shape.

7.4.2. *First trial — ODE model with constant h.* For the ODE model with constant h we had as optimal parameters for the single spike data

$$\begin{aligned}(a, b, h, k, w, \alpha, \beta, \gamma, \delta, \mu, R_{ges}, \tau_0, \delta_{Ca}, s_0, s_1)\\ \approx (0.089, 13.69, 0.010, 0.030, 50.70, 0.18, 0.0075,\\ 0.49, 0.041, 0.0088, 20.28, 0.091, 8.54, 2.03, 4.05)\end{aligned}$$

and

$$\begin{aligned}(a, b, h, k, w, \alpha, \beta, \gamma, \delta, \mu, R_{ges}, \tau_0, \delta_{Ca}, s_0, s_1)\\ \approx (0.12, 12.98, 0.042, 0.035, 48.10, 0.20, 0.00046,\\ 0.46, 0.039, 0.012, 19.25, 0.096, 8.42, 1.92, 3.93)\end{aligned}$$

as optimal values after optimizing on 10 and 100 Hz data.

Figure 17 shows a summary of the results for this model. Here, the results are a little worse than for the other version of the ODE model but can still be considered good. The shapes of the responses are output quite accurately and the creation of the time course of the response amplitudes works pretty well for the 100 Hz and acceptably for the 50 Hz data. Only the second response in the 10 Hz experiment kind of breaks ranks.

7.4.3. *First trial — DDE model.* For the DDE model the following boundary conditions have been used in all steps of the first trial:

$$(N_{out}^0, N_p^0, N_r^0, n_p^0, n_r^0, N_{in}^0) = (0, 25, 200, 10, 100, 50)$$

Here, optimization on the single spike data led to the values

$$\begin{aligned}(a, b, k, \tilde{p}, w, z, \alpha, \beta, \gamma, \delta, \mu, \phi, \chi, R_{ges}, \delta_{Ca})\\ \approx (0.12, 10.00, 0.032, 15.00, 50.00, 3.00, 0.19,\\ 0.013, 0.70, 0.048, 0.022, 0.0010, 0.00039, 34.00, 9.40).\end{aligned}$$

	ODE Model (χ^2)	ODE Model (const.)	DDE Model
single spike	53	150	81
10 Hz data	589	586	757
100 Hz data	914	1676	1901
50 Hz data	1841	3083	4675

TABLE 2. Approximate objective function values for the three models in the first trial. All values have been divided by the length of the data for easier interpretation. The first row shows performances for single spike fitting after step 1, i.e. optimization on single spike data. All other rows show performances of the models after step 2, i.e. optimization on 10 and 100 Hz data. (Cf. section 7.2.3.)

After optimization on 10 and 100 Hz data we had

$$\begin{aligned}(a, b, k, \tilde{p}, w, z, \alpha, \beta, \gamma, \delta, \mu, \phi, \chi, R_{ges}, \delta_{Ca}) \\ \approx (0.16, 9.53, 0.057, 14.30, 47.67, 2.86, 0.20, \\ 0.013, 0.67, 0.061, 0.024, 0.0013, 8.24 \cdot 10^{-5}, 32.42, 8.96).\end{aligned}$$

The results for the DDE model are plotted in figure 18 and are essentially the same as for the ODE model with constant h. Interestingly, the second response from the 10 Hz experiment is too large for both of these models.

To make a more objective comparison possible, the objective function values of all models are summarized in table 2. So we see that the ODE model with a χ^2-based function h performed best on the first trial with quite impressive results.

For further analysis you might also want to consider figures 22, 23 and 24 which contain plots of the corresponding state variable behavior.

Let us now proceed with the results from the second trial.

7.4.4. *Second trial — ODE model with χ^2-based h.* For the first version of the ODE model we used the same given data as in the first trial, i.e.

$$(N_{out}^0, N_v^0, V_0, N_{in}^0) = (0, 25, 20, 50)$$

Here the the single spike optimization gave us

$$\begin{aligned}(a, b, k, w, \alpha, \beta, \gamma, \delta, \mu, R_{ges}, \tau_0, \delta_{Ca}, h_{amp}, h_\delta, h_{width}, s_0, s_1) \\ = (0.12, 9.04, 0.072, 64.36, 0.27, 0.0064, 0.65, 0.064, \\ 0.0091, 25.76, 0.13, 9.31, 0.26, 64.36, 19.31, 1.29, 3.98).\end{aligned}$$

After optimization on the 10 and 100 Hz data, the values have been changed to

$$\begin{aligned}(a, b, k, w, \alpha, \beta, \gamma, \delta, \mu, R_{ges}, \tau_0, \delta_{Ca}, h_{amp}, h_\delta, h_{width}, s_0, s_1) \\ = (0.053, 9.04, 0.21, 64.36, 0.58, 0.0064, 0.85, 0.86, \\ 0.0086, 25.76, 0.15, 9.31, 0.27, 64.36, 19.31, 1.29, 3.98).\end{aligned}$$

Again, the ODE model with χ^2-based h displayed an excellent overall performance. See figure 19 for the corresponding plots. We see that the response amplitude stays a little bit too high for the 10, 50 and 100 Hz data but there are no big deviations from the actual data.

7.4.5. *Second trial — ODE model with constant h.* For the second version of the ODE model optimization on the single spike data led to the following values:

$$\begin{aligned}(N^0_{out}, N^0_v, V_0, N^0_{in}) &\approx (0, 33.52, 26.8, 67.04)\\ (a, b, h, k, w, \alpha, \beta, \gamma, \delta, \mu, R_{ges}, \tau_0, \delta_{Ca}, s_0, s_1)&\\ \approx (0.17, 9.38, 0.0013, 0.093, 67.04, 0.27, 0.0,&\\ 0.67, 0.075, 0.0063, 26.81, 0.13, 9.39, 1.34, 4.02)&\end{aligned}$$

The model parameters were then changed by the 10 and 50 Hz optimization to

$$\begin{aligned}(a, b, h, k, w, \alpha, \beta, \gamma, \delta, \mu, R_{ges}, \tau_0, \delta_{Ca}, s_0, s_1)&\\ \approx (0.31, 9.43, 0.32, 0.19, 67.35, 0.37, 0.0,&\\ 0.68, 0.075, 0.0044, 26.94, 0.14, 9.43, 1.35, 4.04).&\end{aligned}$$

Here, the performance of the ODE model with constant h is in general slightly worse than for the first trial. The system performance is presented in figure 20. Note that the drop in response amplitude of the model is too linear. In particular, this makes the model ignore the fact that the first response should be considerably bigger than the second one in the 100 Hz experiment.

Still, overall performance of the model is still quite acceptable.

7.4.6. *Second trial — DDE model.* For the DDE model we had

$$\begin{aligned}(N^0_{out}, N^0_p, N^0_r, n^0_p, n^0_r, N^0_{in}) &\approx (0, 25.40, 203.22, 10.16, 101.61, 50.80),\\ (a, b, k, \tilde{p}, w, z, \alpha, \beta, \gamma, \delta, \mu, \phi, \chi, R_{ges}, \delta_{Ca})&\\ \approx (0.095, 10.16, 0.03, 15.24, 50.80, 3.05, 0.19,&\\ 0.013, 0.61, 0.042, 0.02, 0.0010, 0.00015, 30.48, 8.74)&\end{aligned}$$

after optimization on the single spike data and

$$\begin{aligned}(a, b, k, \tilde{p}, w, z, \alpha, \beta, \gamma, \delta, \mu, \phi, \chi, R_{ges}, \delta_{Ca})&\\ \approx (0.52, 10.12, 0.075, 15.18, 50.62, 3.04, 0.21,&\\ 0.013, 0.62, 0.056, 0.022, 0.0010, 3.39 \cdot 10^{-5}, 30.37, 8.72)&\end{aligned}$$

after optimization on 10 and 100 Hz data.

This time, optimization worked not quite as well as for the first trial as can be seen in figure 21. We see that there are some issues. For example, response amplitudes for the 100 Hz data drop faster than in the actual measurements and continue to drop until the simulation stops even if that does not happen in the experimental data. Things are even worse for the 50 Hz data where the response amplitude goes to 0 even if it should not go below one third of the initial response size. On the other hand, for the 10 Hz data, response amplitudes are generally slightly too high.

Remark (Variable behavior of the DDE model)**:** If you take a look at the state variable behavior for the DDE system you see that N_{in} grows excessively while the number of vesicles is dropping too fast. (Cf. figure 27.)

The behavior of the state variables for the other models are presented in the appendix in figures 25 and 26 respectively.

This could indicate modeling issues or mean that we are stuck in an area with unfortunate variable values.

As for the first trial, we present a summary of the objective function values for the second trial in table 3. We see that the objective function values were generally worse than in the first trial. There is, however, one interesting exception to this worsening: The first version of the ODE model performed slightly better on the 50

	ODE Model (χ^2)	ODE Model (const.)	DDE Model
single spike	56	56	99
10 Hz data	318	377	503
100 Hz data	1534	2120	4637
50 Hz data	1256	4122	9133

TABLE 3. Approximate objective function values for the three models in the second trial. All values have been divided by the length of the data for easier interpretation. The first row shows performances for single spike fitting after step 1, i.e. optimization on single spike data. All other rows show performances of the models after step 2, i.e. optimization on 10 and 100 Hz data. (Cf. section 7.2.3.)

Hz data than before. Also note that this time for none of the models the amplitude of the second response was higher than that of the first for the 10 Hz data.

Remark: Stochasticity makes the results look a bit worse than they actually are. The supposedly random variation in response amplitudes can of course not be captured by a deterministic model. To tackle this issue one could for instance use data from different experiments to compute average response data and then optimize on this data.

Also, note that results are sometimes looking bad in the plots even if they are not that bad from an optimization point of view, like completely messing up the first response for the sake of achieving a slightly better fit for many successive responses for example. After all, we used the squared Euclidean distance as objective function where all responses are considered to be equally important.

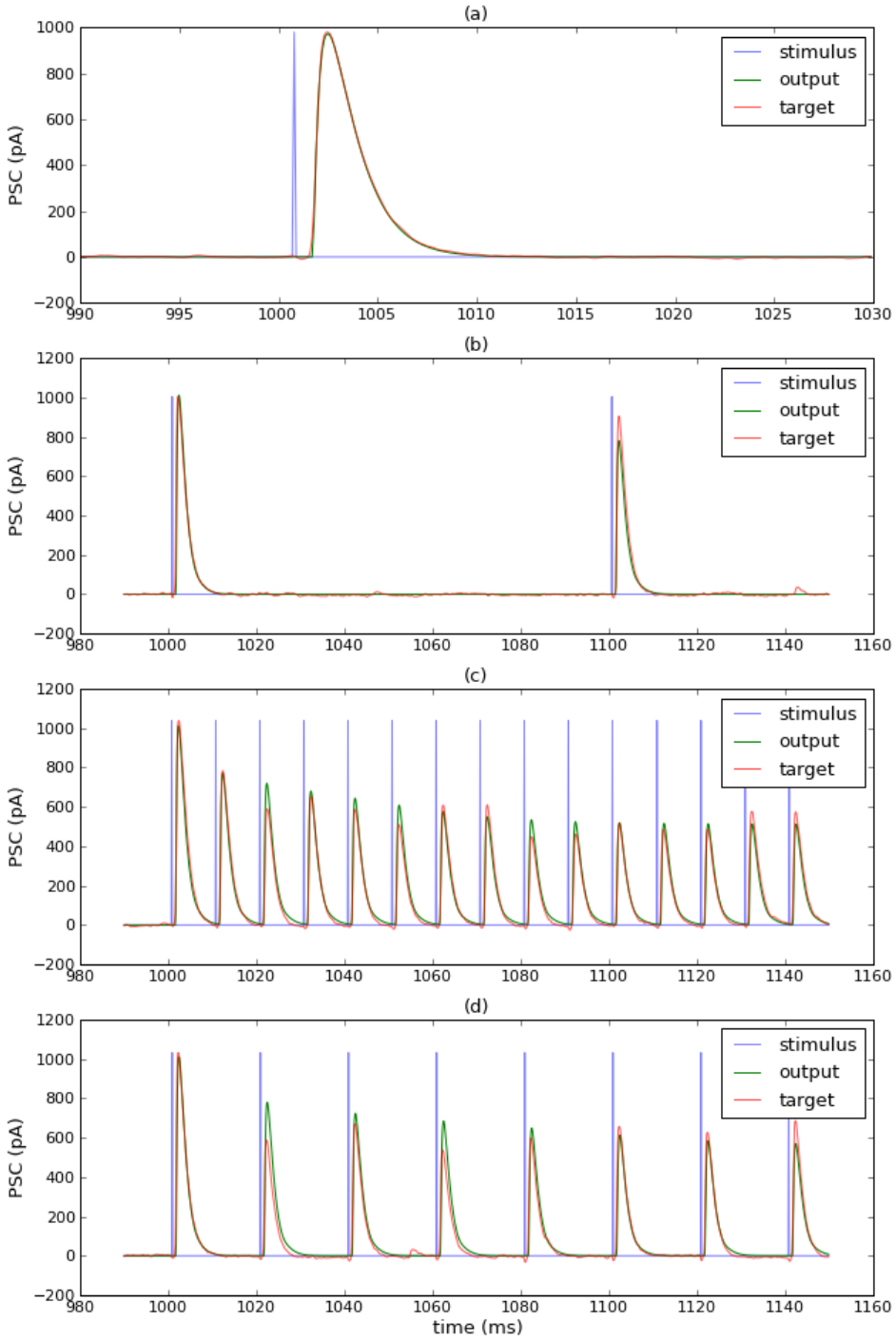

FIGURE 16. Performance of ODE model with χ^2-based function h in the first trial. (a) Performance of the model on single spike data after optimization on that data. (b) Performance of the model on 10 Hz data after optimization on 10 Hz and 100 Hz data. (c) Performance of the model on 100 Hz data after optimization on 10 Hz and 100 Hz data. (d) Performance of the model on 50 Hz data after optimization on 10 Hz and 100 Hz data.

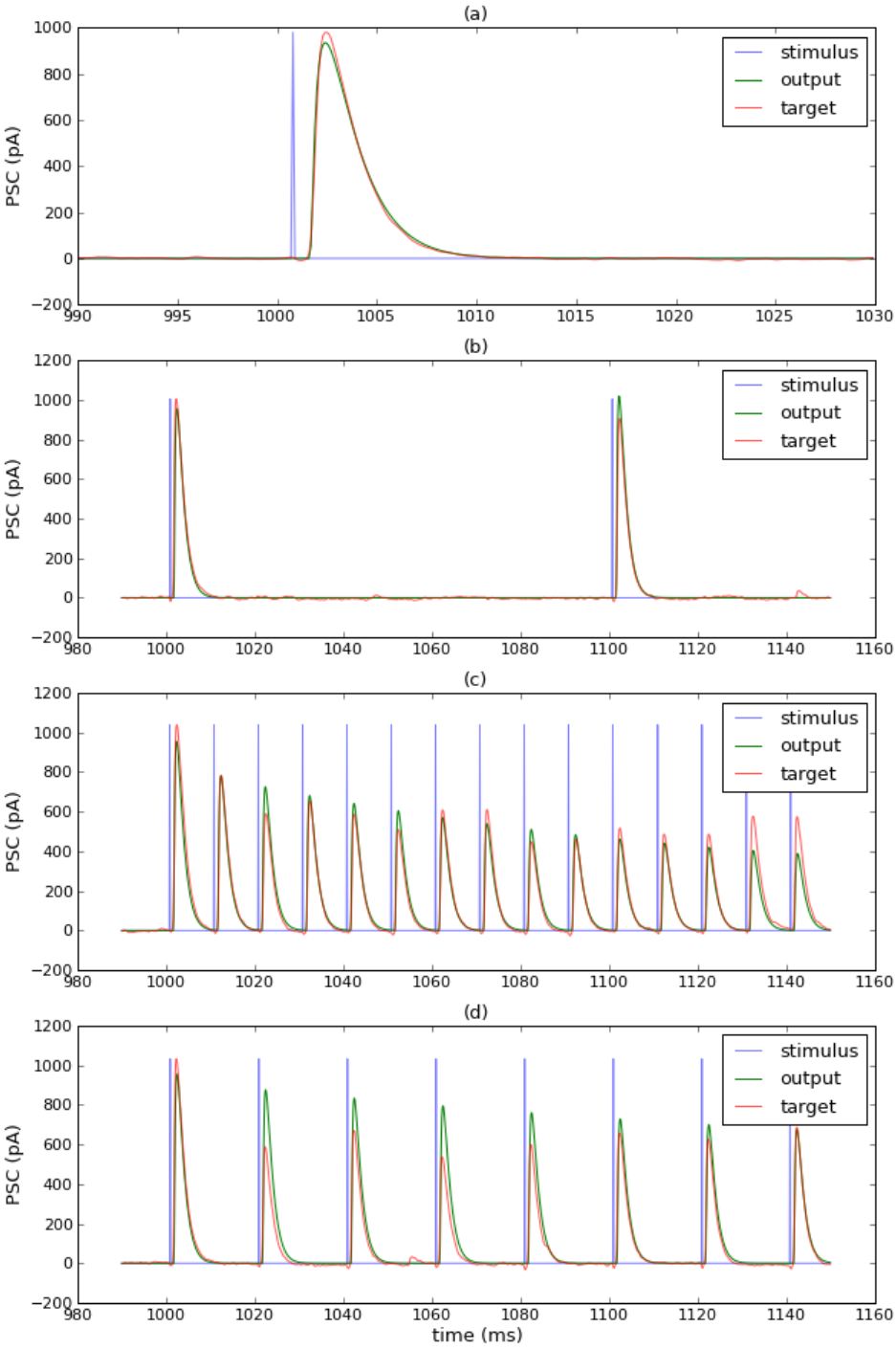

FIGURE 17. Performance of ODE model with constant function h in the first trial. (a) Performance of the model on single spike data after optimization on that data. (b) Performance of the model on 10 Hz data after optimization on 10 Hz and 100 Hz data. (c) Performance of the model on 100 Hz data after optimization on 10 Hz and 100 Hz data. (d) Performance of the model on 50 Hz data after optimization on 10 Hz and 100 Hz data.

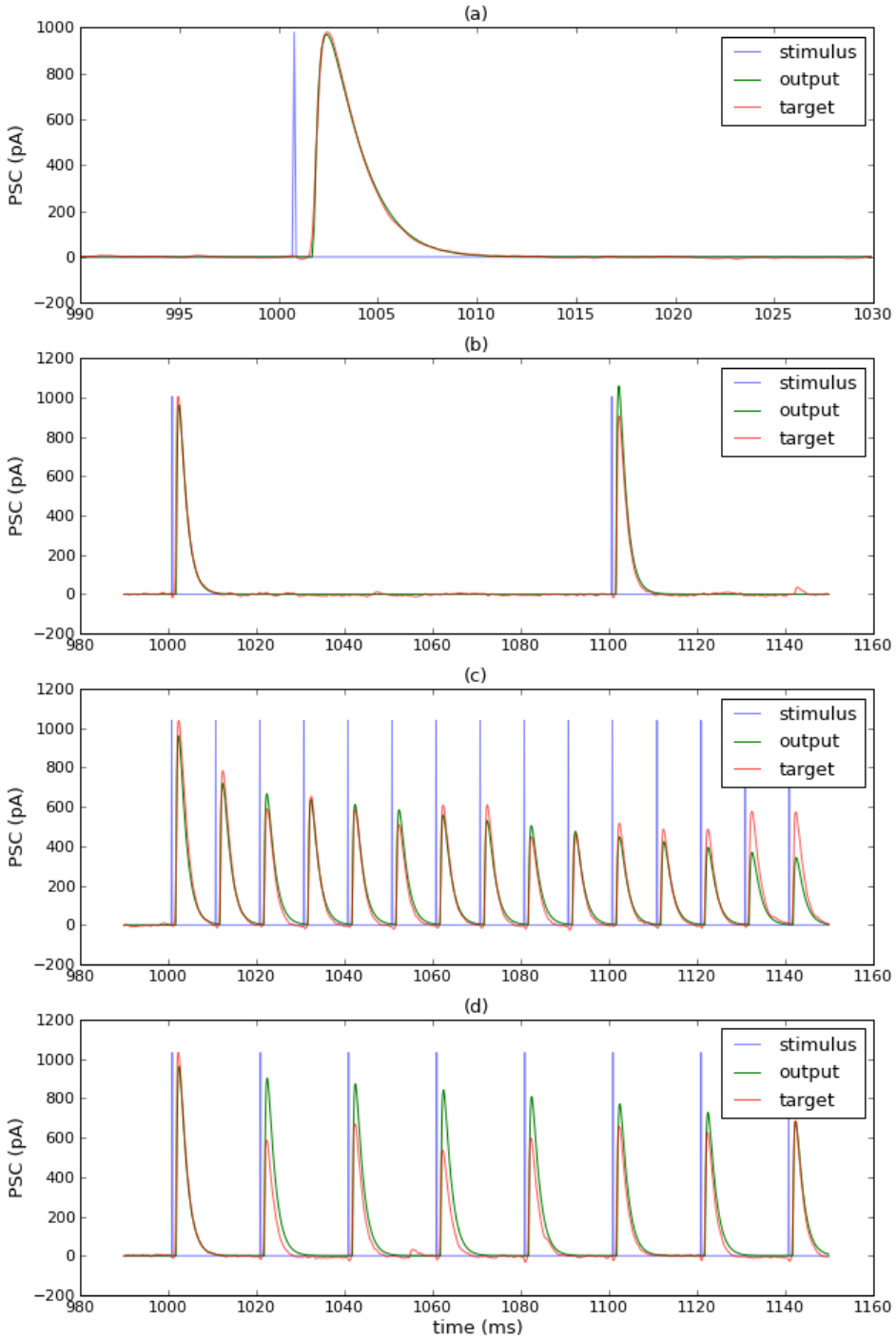

FIGURE 18. Performance of DDE model in the first trial. (a) Performance of the model on single spike data after optimization on that data. (b) Performance of the model on 10 Hz data after optimization on 10 Hz and 100 Hz data. (c) Performance of the model on 100 Hz data after optimization on 10 Hz and 100 Hz data. (d) Performance of the model on 50 Hz data after optimization on 10 Hz and 100 Hz data.

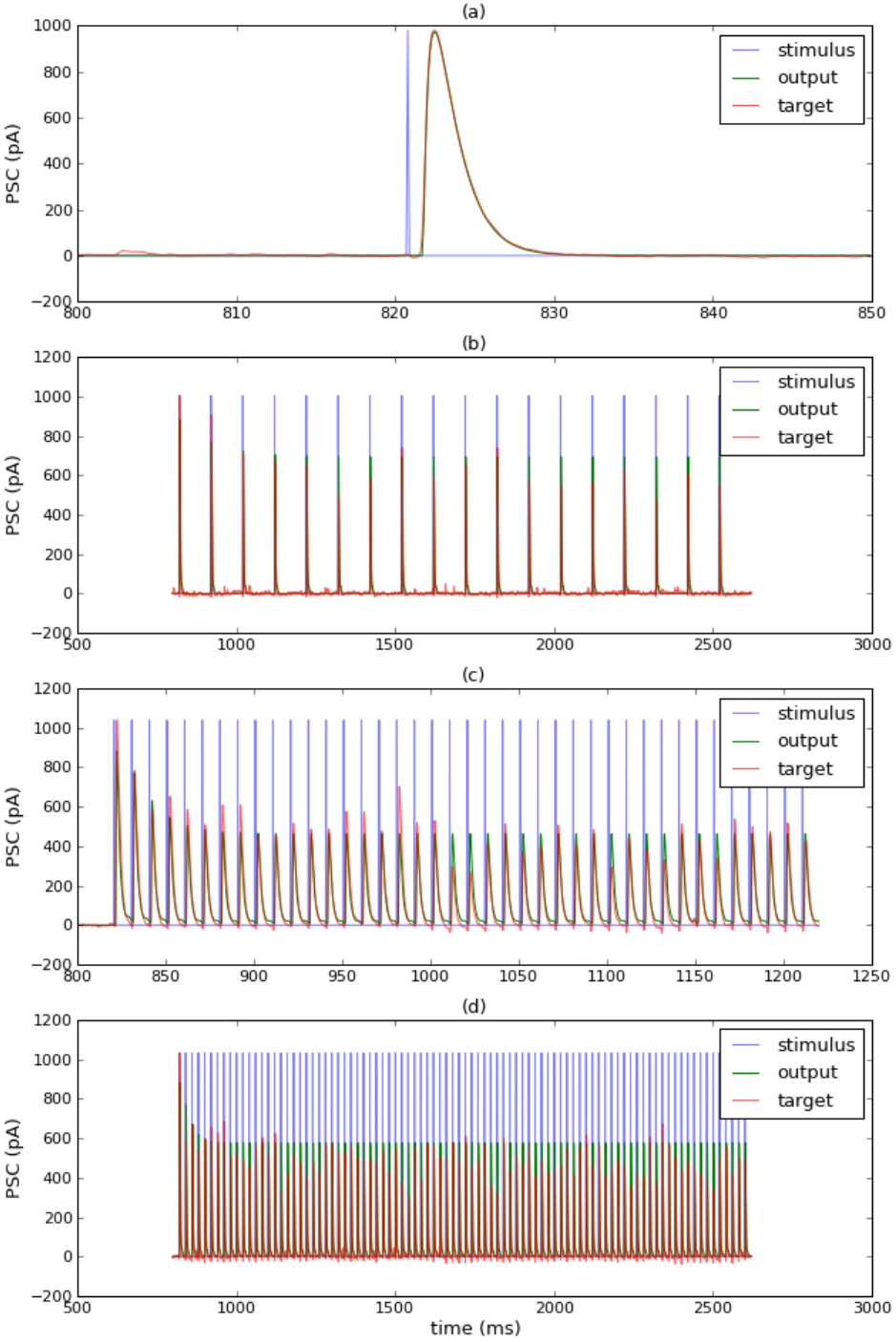

FIGURE 19. Performance of ODE model with χ^2-based function h in the second trial. (a) Performance of the model on single spike data after optimization on that data. (b) Performance of the model on 10 Hz data after optimization on 10 Hz and 100 Hz data. (c) Performance of the model on 100 Hz data after optimization on 10 Hz and 100 Hz data. (d) Performance of the model on 50 Hz data after optimization on 10 Hz and 100 Hz data.

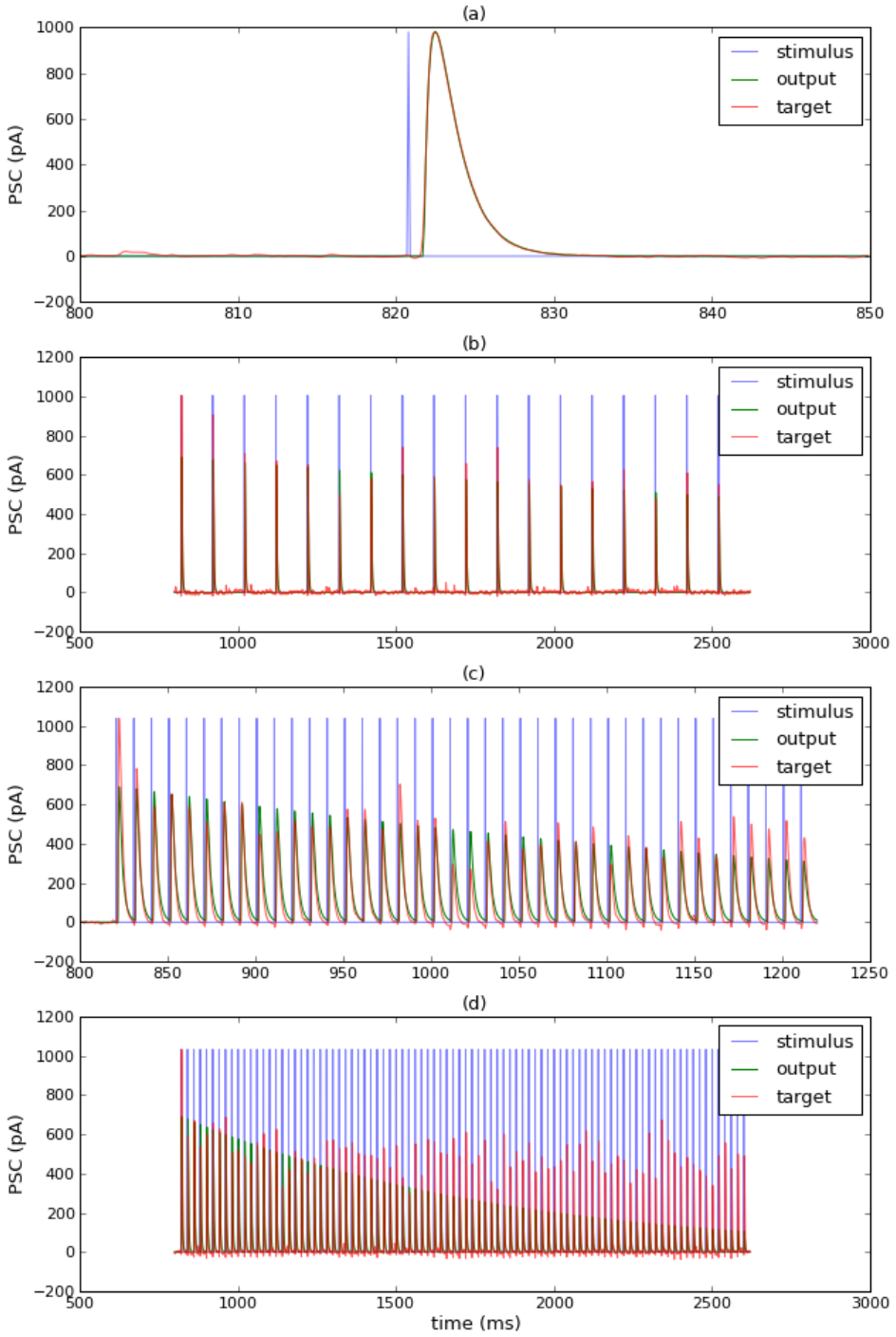

FIGURE 20. Performance of ODE model with constant function h in the second trial. (a) Performance of the model on single spike data after optimization on that data. (b) Performance of the model on 10 Hz data after optimization on 10 Hz and 100 Hz data. (c) Performance of the model on 100 Hz data after optimization on 10 Hz and 100 Hz data. (d) Performance of the model on 50 Hz data after optimization on 10 Hz and 100 Hz data.

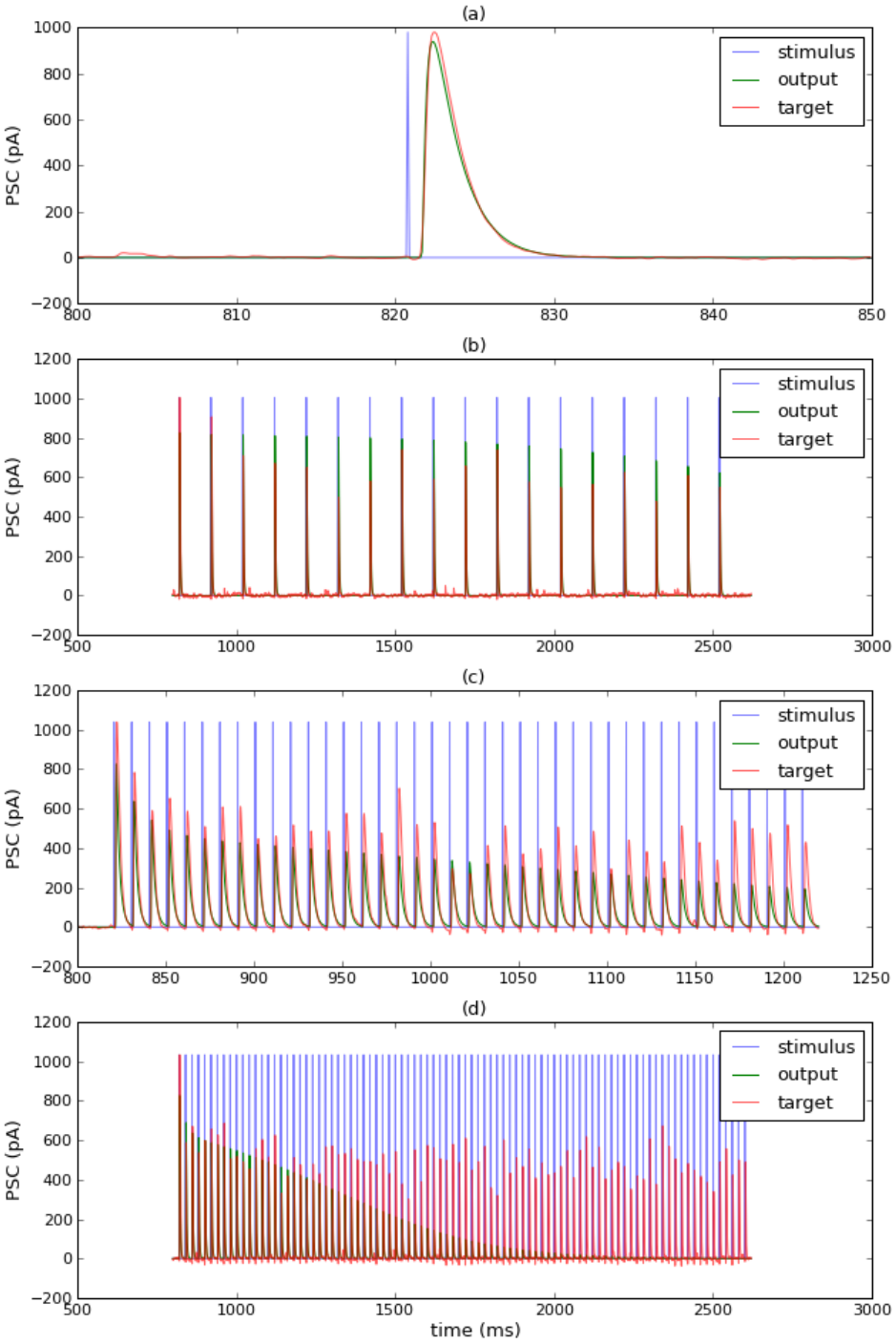

FIGURE 21. Performance of DDE model in the second trial. (a) Performance of the model on single spike data after optimization on that data. (b) Performance of the model on 10 Hz data after optimization on 10 Hz and 100 Hz data. (c) Performance of the model on 100 Hz data after optimization on 10 Hz and 100 Hz data. (d) Performance of the model on 50 Hz data after optimization on 10 Hz and 100 Hz data.

8. Discussion

Generally speaking, the test results look quite promising. Especially the ODE model with χ^2-based function h was able to capture lots of the characteristics of experimentally determined measurements of the postsynaptic current. This suggests that we chose reasonable assumptions in the creation of the original PDE model.

8.1. **The ODE models.** All in all, the ODE model performed better with a χ^2-based h than with a constant h which indicates that we chose an appropriate modeling approach for h.

For further development, note that the response amplitude is dropping too fast for constant h whereas a bigger drop would be desirable for the version with a χ^2-based function h. So a combination of these versions might lead to improvement. It would also be interesting to obtain biologically plausible values for all other parameters, optimize h as function parameter and then compare the computed optimal function to our proposal.

8.2. **The DDE model.** As already mentioned in section 7.1.2, the selected data has not been very advantageous for the DDE model. But even so, acceptable results were obtained in most test cases.

However, in some cases a few issues became apparent. These issues are linked to the behavior of the system's state variables and one should find out whether this originates in bad modeling assumptions or in unfortunate variable choices. I think that for that purpose an in-depth analysis of the system dynamics in dependency of the model parameters and given data would prove very valuable.

If adjustments to the model need to be made in order to improve the performance, one could for instance think about dropping the assumption that $\delta_m \geq 2s$ or adding an extra term for vesicle creation (for vesicles coming from the cell body for example)[35].

For that matter, also note that some other existing models (cf. [AG04] or [BK12]) use three vesicle pools. (They distinguish between immediately available vesicles, vesicles in the small pool and ones that are in the reserve pool.) So if the test results can not be improved significantly by using system dynamics analysis one could also consider adding an extra vesicle pool and see how this changes the situation.

And of course, the model should finally be implemented as DDE system and tested on longer measurements to find out if vesicle pool dynamics can be captured.

8.3. **Closing words.** We have introduced several novel mathematical models for synaptic transmission at chemical synapses. The main model of this thesis has been analyzed in detail and led us to an ODE model that has been tested successfully on experimental measurements. We have learned about limitations of the different models but also proposed some ideas for further development.

I think that this work could very well serve as basis for future research where the specific direction of this endeavor should be dictated by its particular goals.

[35] In that case you should probably also add a term for some kind of vesicle loss.

Appendix A. Notations and abbreviations

A.1. **Abbreviations.**

- a.e.: almost everywhere
- ODE: ordinary differential equation
- DDE: delay differential equation
- NT: neurotransmitter
- PDE: partial differential equation
- PSP: postsynaptic potential
- PSC: postsynaptic current (i.e. the current flowing across the membrane of the postsynaptic cell)

A.2. **Notations.**

- $[Ca](t)$: calcium concentration inside the presynaptic terminal at time t
- $const(x)$: some value that only depends on x

Appendix B. Basic results

Lemma B.1
Let p and g be real-valued functions on $[0,T]$ and $y_0 \in \mathbb{R}$. Then there exists a uniquely determined function $y : [0,T] \to \mathbb{R}$ that solves the initial value problem

$$\frac{dy}{dt} + p(t)y = g(t), \;\; y(0) = y_0.$$

Moreover, it holds that

$$y(t) = \exp\left(-\int_0^t p(\lambda)d\lambda\right)\left(\int_0^t \exp\left(\int_0^\lambda p(\epsilon)d\epsilon\right) g(\lambda)d\lambda + y_0\right).$$

for all $t \in [0,T]$.

Proof. Our approach is essentially taken from [BD01, section 2.1]. We first show that each solution is of the above form. It holds that

$$\begin{aligned}
& \frac{dy}{dt} + p(t)y = g(t) \\
\Rightarrow \quad & \frac{d(\exp\left(\int_0^t p(\lambda)d\lambda\right) y)}{dt} = \exp\left(\int_0^t p(\lambda)d\lambda\right)\frac{dy}{dt} + \exp\left(\int_0^t p(\lambda)d\lambda\right) p(t)y \\
& \qquad = \exp\left(\int_0^t p(\lambda)d\lambda\right) g(t) \\
\Rightarrow \quad & \exp\left(\int_0^t p(\lambda)d\lambda\right) y = \int_0^t \exp\left(\int_0^\lambda p(\epsilon)d\epsilon\right) g(\lambda)d\lambda + c
\end{aligned}$$

for some constant $c \in \mathbb{R}$. Now the condition $y(0) = y_0$ implies that $c = y_0$ and dividing both sides by $\exp\left(\int_0^t p(\lambda)d\lambda\right)$ gives us the above formula.

It is left to show that each such y solves the initial value problem. So let

$$y(t) = \exp\left(-\int_0^t p(\lambda)d\lambda\right)\left(\int_0^t \exp\left(\int_0^\lambda p(\epsilon)d\epsilon\right) g(\lambda)d\lambda + y_0\right).$$

for all $t \in [0,T]$. It is obvious that $y(0) = y_0$. Furthermore, it holds that

$$\begin{aligned}
\frac{dy}{dt} + p(t)y &= -p(t)y + \exp\left(-\int_0^t p(\lambda)d\lambda\right)\exp\left(\int_0^t p(\lambda)d\lambda\right) g(t) + p(t)y \\
&= g(t).
\end{aligned}$$

□

Lemma B.2
Let $a > b$, $\bar{x} \in C^1([a,b])$ monotonously increasing, $x^0 \leq \bar{x}(0)$, $f \in C^0([a,b] \times \mathbb{R})$ Lipschitz continuous w.r.t. to the second argument and x be a solution to

$$\dot{x} = f(t,x), \;\; x(a) = x^0. \tag{93}$$

If $f(t, \bar{x}(t)) \leq 0$ for all $t \in [a,b]$ then we have that $x(t) \leq \bar{x}(t)$ for all $t \in [a,b]$.

Proof. First note that $x - \bar{x}$ is a solution to

$$\frac{d(x-\bar{x})}{dt} = f(t,x) - \frac{d\bar{x}}{dt}, \;\; (x-\bar{x})(a) \leq 0.$$

Furthermore, it holds that

$$\begin{aligned}(x-\bar{x})(t)=0 \;&\Rightarrow\; x(t)=\bar{x}(t)\\ &\Rightarrow\; \dot{x}(t)=f(t,\bar{x}(t))\leq 0\\ &\Rightarrow\; \frac{d(x-\bar{x})}{dt}\leq -\frac{d\bar{x}}{dt}\leq 0\end{aligned}$$

for all $t\in[a,b]$. Hence, we might assume w.l.o.g. that $\bar{x}\equiv 0$.

Now assume that there exists some $\bar{t}\in(a,b]$ such that $x(\bar{t})>0$. We set $\hat{t}:=\max\{t\in(a,\bar{t})\mid x(t)\leq 0\}$. Then $x(\hat{t})=0$ and by definition of $\hat{t}$ it must hold that $\dot{x}(\hat{t})\geq 0$. But since $\dot{x}(\hat{t})=f(\hat{t},0)\leq 0$ we get that $\dot{x}(\hat{t})=0$.

We define

$$\tilde{x}(t):=\begin{cases}x(t) & ,t\leq\hat{t}\\ 0 & ,t>\hat{t}\end{cases}$$

Then $\tilde{x}$ solves (93) and $\tilde{x}(t)\neq x(t)$ for all $t\in(\hat{t},\bar{t}]$. This, however, is a contradiction to the Picard-Lindelöf theorem since f is Lipschitz w.r.t. x. □

Lemma B.3
Let $a>b$. For $i\in\{1,2\}$ let $x^{i,0}\in\mathbb{R}$, $f^i\in C^0([a,b]\times\mathbb{R})$ Lipschitz continuous w.r.t. the second argument and $x^i\in C^1([a,b])$ be a solution to the initial value problem

$$\begin{aligned}&\dot{x}^i=f^i(t,x^i),\;\; t\in(a,b),\\ &x^i(0)=x^{i,0}.\end{aligned}$$

If $f^1(t,x)\geq f^2(t,x)$ for all $t\in[a,b], x\in\mathbb{R}$ and $x^{1,0}\geq x^{2,0}$ then $x^1(t)\geq x^2(t)$ for all t.

Proof. For x^2-x^1 it holds that

$$\frac{d(x^2-x^1)}{dt}=\dot{x}^2-\dot{x}^1=f^2(t,x^2)-f^1(t,x^1),\;\; (x^2-x^1)(a)\geq 0.$$

It holds

$$(x^2-x^1)(t)=0\Rightarrow x^2(t)=x^1(t)\Rightarrow\frac{d(x^2-x^1)(t)}{dt}=f^2(t,x^1(t))-f^1(t,x^1(t))\geq 0.$$

So we can apply proposition B.2 to get that $x^1(t)\geq x^2(t)$ for all $t\in[a,b]$. □

Lemma B.4
For any real numbers x_1,x_2,y_1,y_2 it holds that

$$|x_1y_1-x_2y_2|\leq|x_1|\cdot|y_1-y_2|+|y_2|\cdot|x_1-x_2|.$$

Proof. Let $x_1,x_2,y_1,y_2\in\mathbb{R}$. It holds that

$$\begin{aligned}|x_1y_1-x_2y_2|&=|x_1(y_1-y_2+y_2)-x_2y_2|\\ &=|x_1(y_1-y_2)+(x_1-x_2)y_2|\\ &\leq|x_1|\cdot|y_1-y_2|+|y_2|\cdot|x_1-x_2|.\end{aligned}$$

□

Lemma B.5 (Lipschitz continuity of differentiable functions on bounded sets)
Let $a,b\in\mathbb{R}$, $a<b$ and $f:[a,b]\to\mathbb{R}$ be continuous on $[a,b]$ and differentiable on (a,b). It holds that

$$|f(a)-f(b)|\leq\sup\{|f'(x)|\mid x\in(a,b)\}|a-b|.$$

Proof. Let a, b and f be as described above. By the mean value theorem there exists at least one $x_0 \in (a, b)$ with

$$f'(x_0) = \frac{f(b) - f(a)}{b - a}.$$

Hence, we have that

$$|f(a) - f(b)| = |f'(x_0)| \cdot |a - b| \leq \sup\{|f'(x)| \mid x \in (a, b)\}|a - b|.$$

□

Lemma B.6 (Lipschitz continuity of exp on bounded sets)
For all $x, y \in \mathbb{R}$ it holds that

$$|e^x - e^y| \leq \max\{e^x, e^y\}|x - y|.$$

Proof. Immediate consequence of lemma B.5. □

Lemma B.7 (Gronwall's inequality (integral form))
Let $\xi(t)$ be a nonnegative, summable function on $[0, T]$ which satisfies for almost all t the integral inequality

$$\xi(t) \leq C_1 \int_0^t \xi(\lambda) d\lambda + C_2$$

for constants $C_1, C_2 \geq 0$. Then

$$\xi(t) \leq C_2\big(1 + C_1 t e^{C_1 t}\big)$$

for almost all $0 \leq t \leq T$.

Proof. See [Eva10, p.709]. □

Theorem B.8 (Picard-Lindelöf)
Let $t_0 \in \mathbb{R}$, $x_0 \in \mathbb{R}^n$ and

$$Q_{a,b} := \big\{(t, x) \in \mathbb{R} \times \mathbb{R}^n \mid |t - t_0| \leq a, \ \ \|x - x_0\| \leq b\big\}$$

where $a, b > 0$ are given. Furthermore, let $f : Q_{a,b} \to \mathbb{R}^n$ be continuous and

$$\|f(t, x) - f(t, y)\| \leq L\|x - y\| \quad \text{for all } (t, x), (t, y) \in Q_{a,b}$$

with constant $L \geq 0$. For any c with $0 < c \leq \min\{a, b/K\}$ where

$$K := \max_{(t,x) \in Q_{a,b}} \|f(t, x)\|$$

then there exists exactly one continuously differentiable solution to the initial value problem

$$\dot{x} = f(t, x), \quad x(t_0) = x_0, \quad (t, x) \in \mathbb{R} \times \mathbb{R}^n$$

on the interval $[t_0 - c, t_0 + c]$.

Proof. See [MV11, Satz 2.8]. □

Lemma B.9
Let the real-valued function f be continuous on $[a, b] \times [c, d]$ and define

$$F(x) := \int_c^d f(x, y) dy.$$

Furthermore, assume that $\partial f / \partial x$ exists on $[a, b] \times [c, d]$ and is continuous. Then F' exists on $[a, b]$ and it holds that

$$\frac{d}{dx} \int_c^d f(x, y) dy = \int_c^d \frac{\partial f(x, y)}{\partial x} dy.$$

Proof. See [Heu91, 113.2 Satz]. □

Lemma B.10
Let $(f_n)_{n\in\mathbb{N}}$ be a sequence of functions that are differentiable on $[a,b]$ such that $(f_n(x_0))_{n\in\mathbb{N}}$ converges for some point $x_0 \in [a,b]$. If $(f_n')_{n\in\mathbb{N}}$ converges uniformly on $[a,b]$, then $(f_n)_{n\in\mathbb{N}}$ converges uniformly on $[a,b]$ to a function f and

$$f'(x) = \lim_{n\to\infty} f_n'(x)$$

for all $a \leq x \leq b$.

Proof. This is Theorem 7.17 in [Rud76]. A proof can be found in that book. □

Appendix C. Additional figures

See next page and the following.

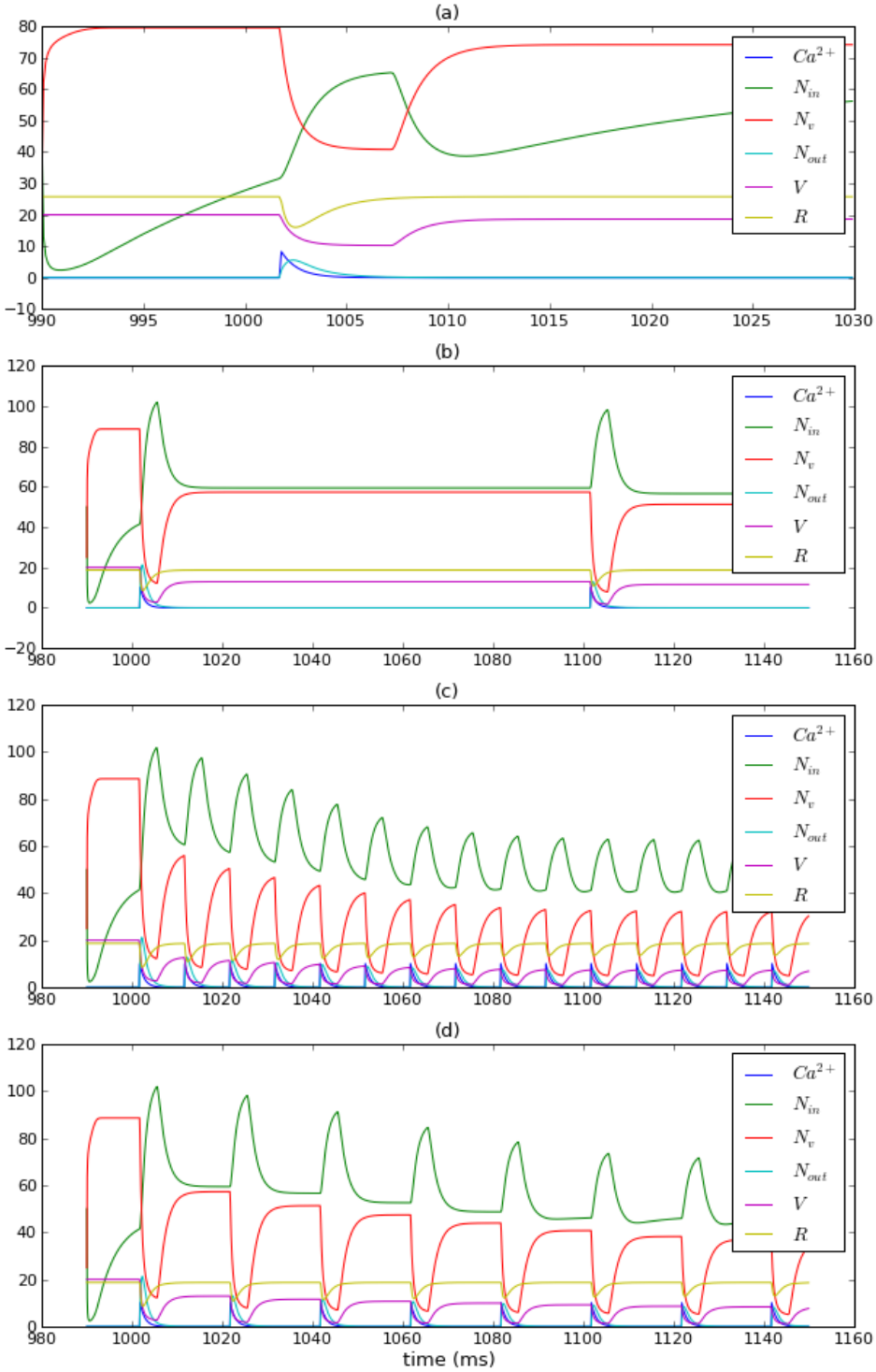

FIGURE 22. Behavior of ODE model with χ^2-based function h in the first trial. (a) Behavior of the model on single spike data after optimization on that data. (b) Behavior of the model on 10 Hz data after optimization on 10 Hz and 100 Hz data. (c) Behavior of the model on 100 Hz data after optimization on 10 Hz and 100 Hz data. (d) Behavior of the model on 50 Hz data after optimization on 10 Hz and 100 Hz data.

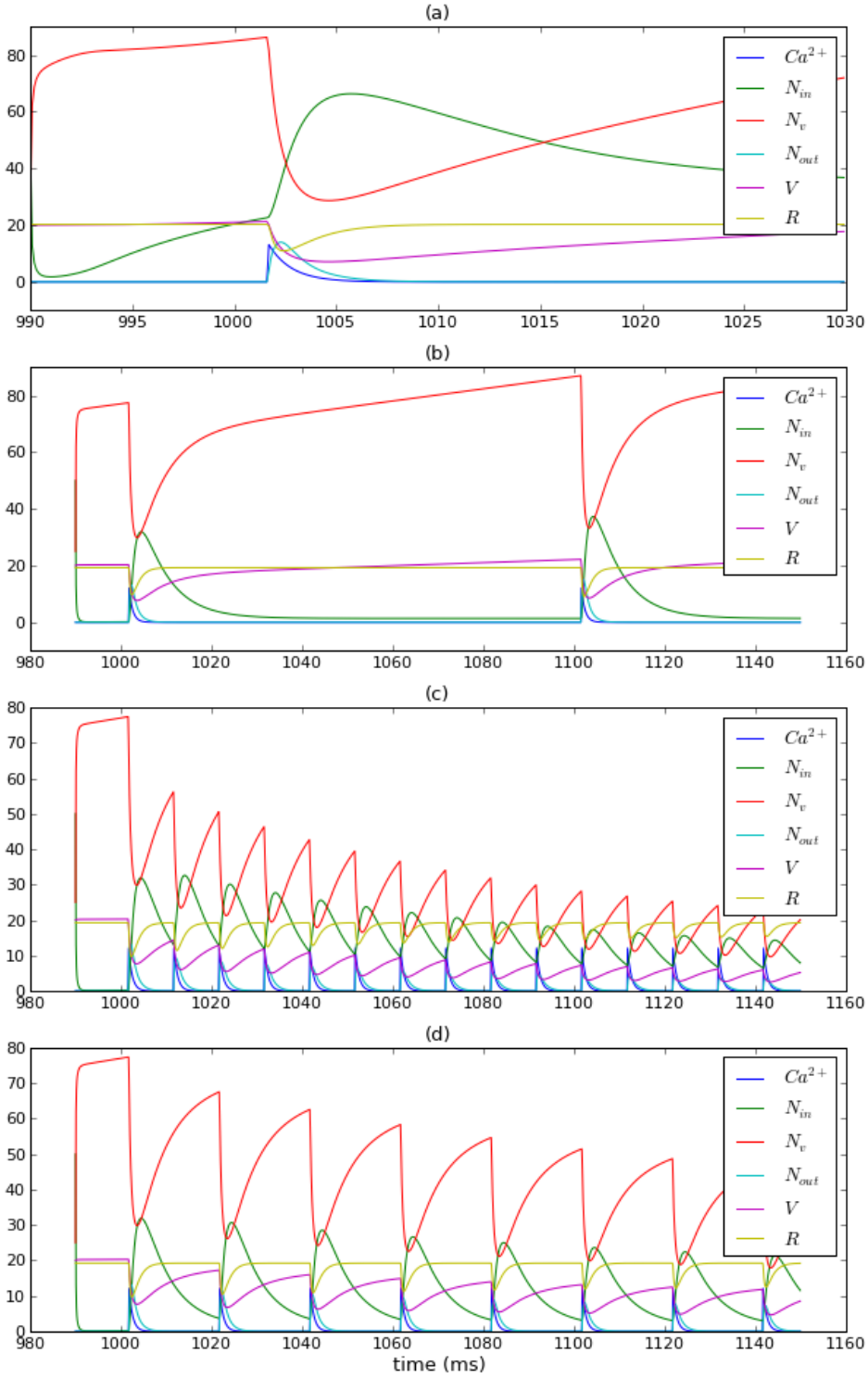

FIGURE 23. Behavior of ODE model with constant function h in the first trial. (a) Behavior of the model on single spike data after optimization on that data. (b) Behavior of the model on 10 Hz data after optimization on 10 Hz and 100 Hz data. (c) Behavior of the model on 100 Hz data after optimization on 10 Hz and 100 Hz data. (d) Behavior of the model on 50 Hz data after optimization on 10 Hz and 100 Hz data.

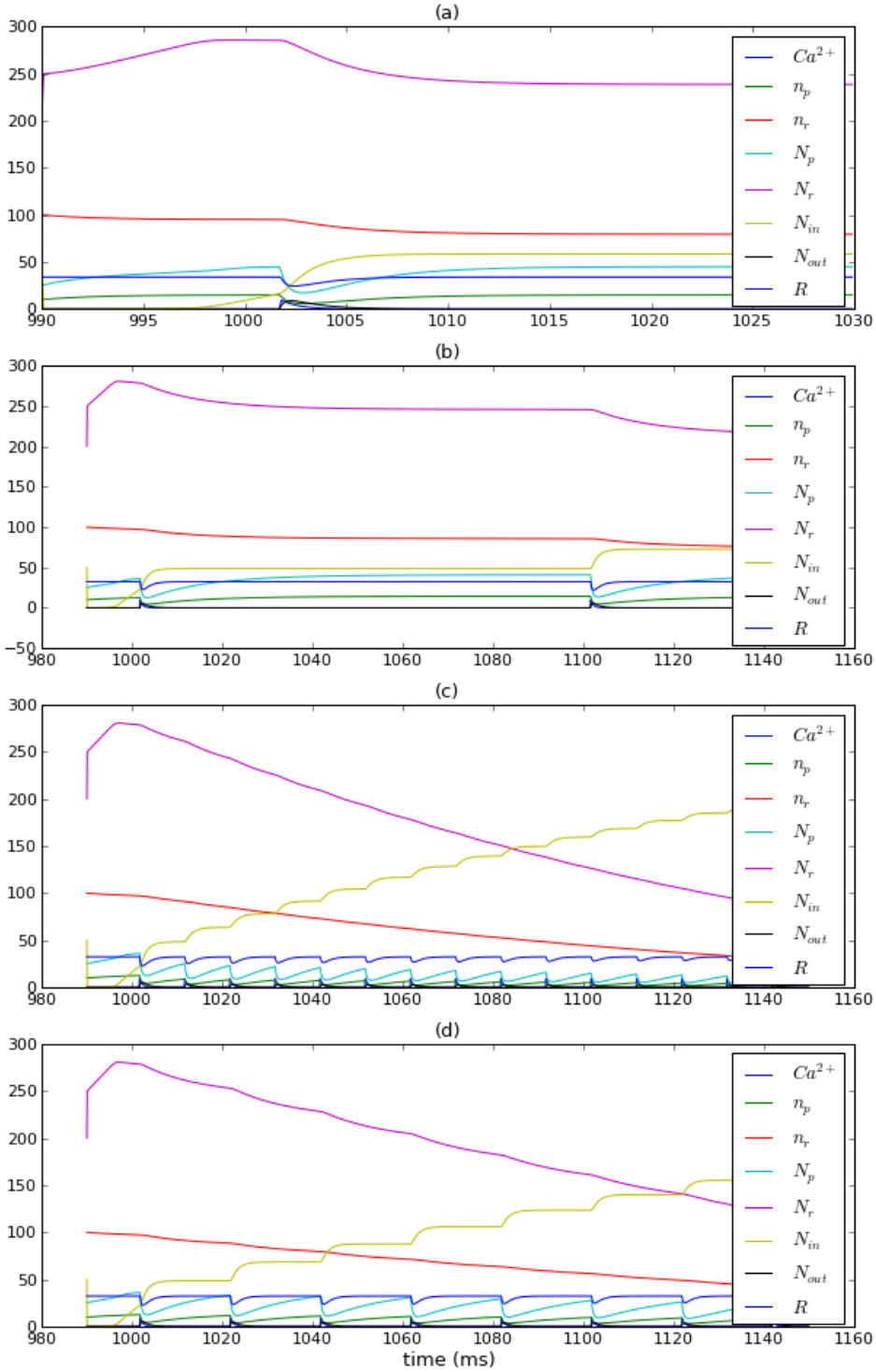

FIGURE 24. Behavior of DDE model in the first trial. (a) Behavior of the model on single spike data after optimization on that data. (b) Behavior of the model on 10 Hz data after optimization on 10 Hz and 100 Hz data. (c) Behavior of the model on 100 Hz data after optimization on 10 Hz and 100 Hz data. (d) Behavior of the model on 50 Hz data after optimization on 10 Hz and 100 Hz data.

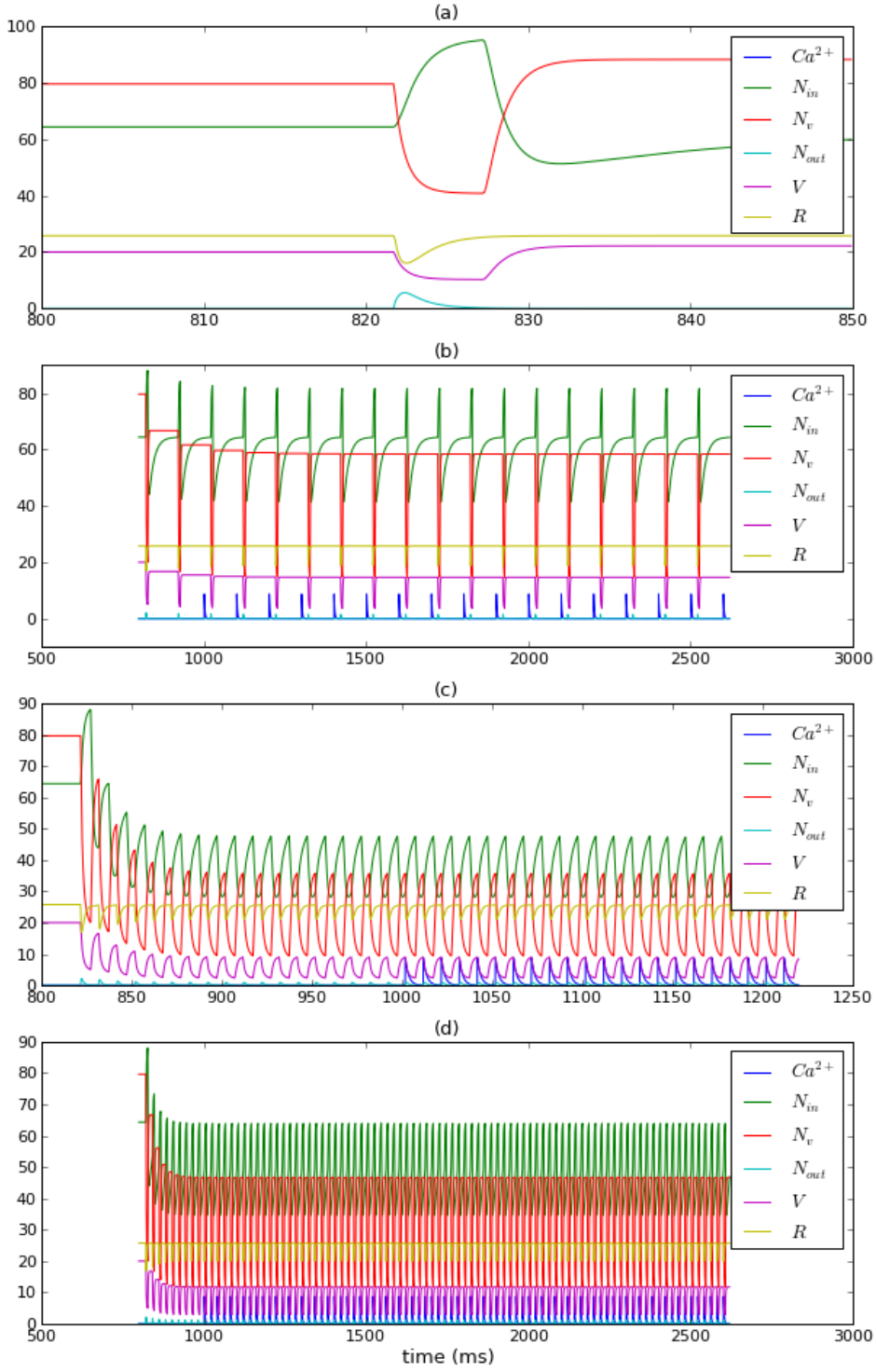

FIGURE 25. Behavior of ODE model with χ^2-based function h in the second trial. (a) Behavior of the model on single spike data after optimization on that data. (b) Behavior of the model on 10 Hz data after optimization on 10 Hz and 100 Hz data. (c) Behavior of the model on 100 Hz data after optimization on 10 Hz and 100 Hz data. (d) Behavior of the model on 50 Hz data after optimization on 10 Hz and 100 Hz data.

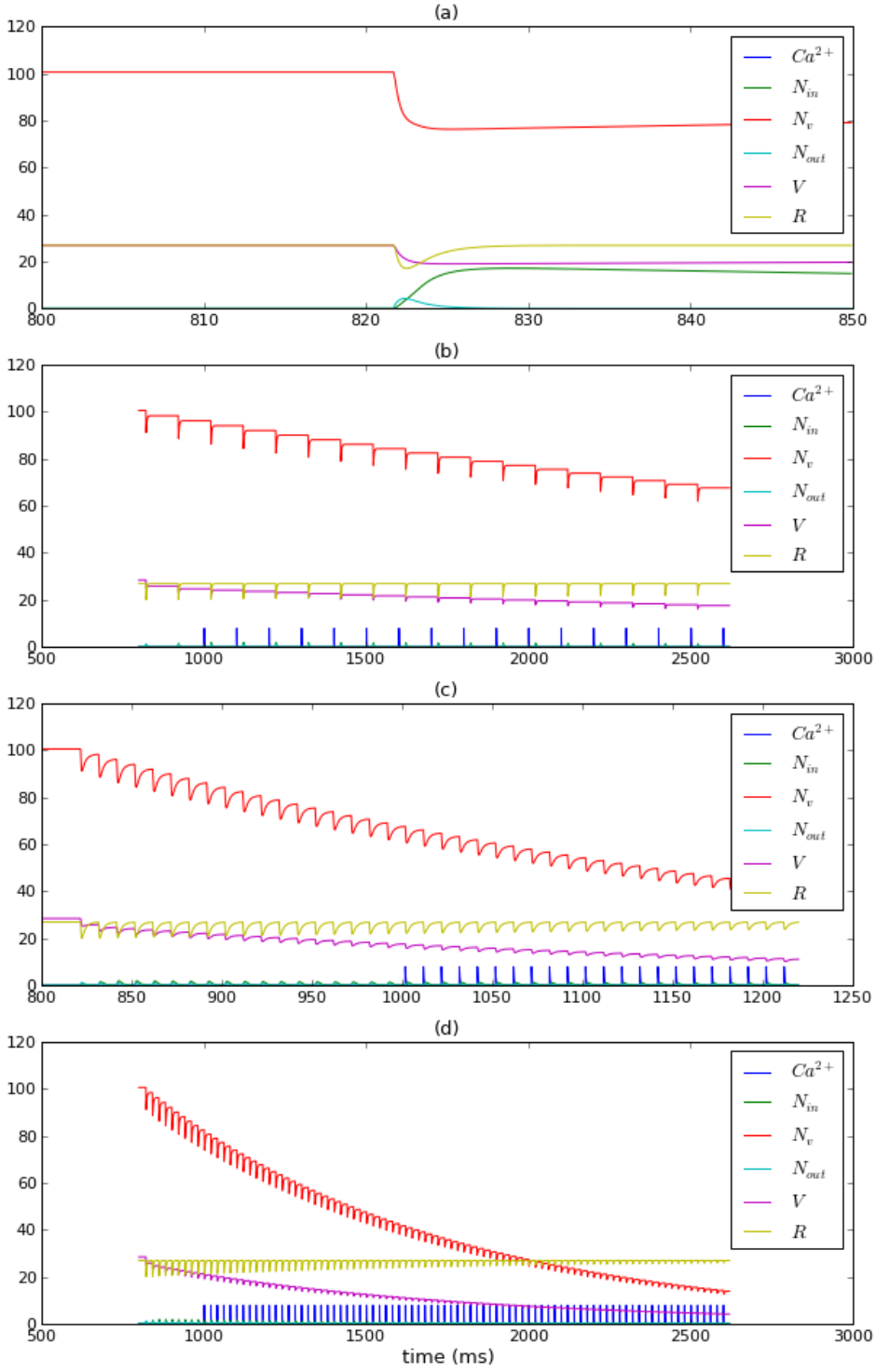

FIGURE 26. Behavior of ODE model with constant function h in the second trial. (a) Behavior of the model on single spike data after optimization on that data. (b) Behavior of the model on 10 Hz data after optimization on 10 Hz and 100 Hz data. (c) Behavior of the model on 100 Hz data after optimization on 10 Hz and 100 Hz data. (d) Behavior of the model on 50 Hz data after optimization on 10 Hz and 100 Hz data.

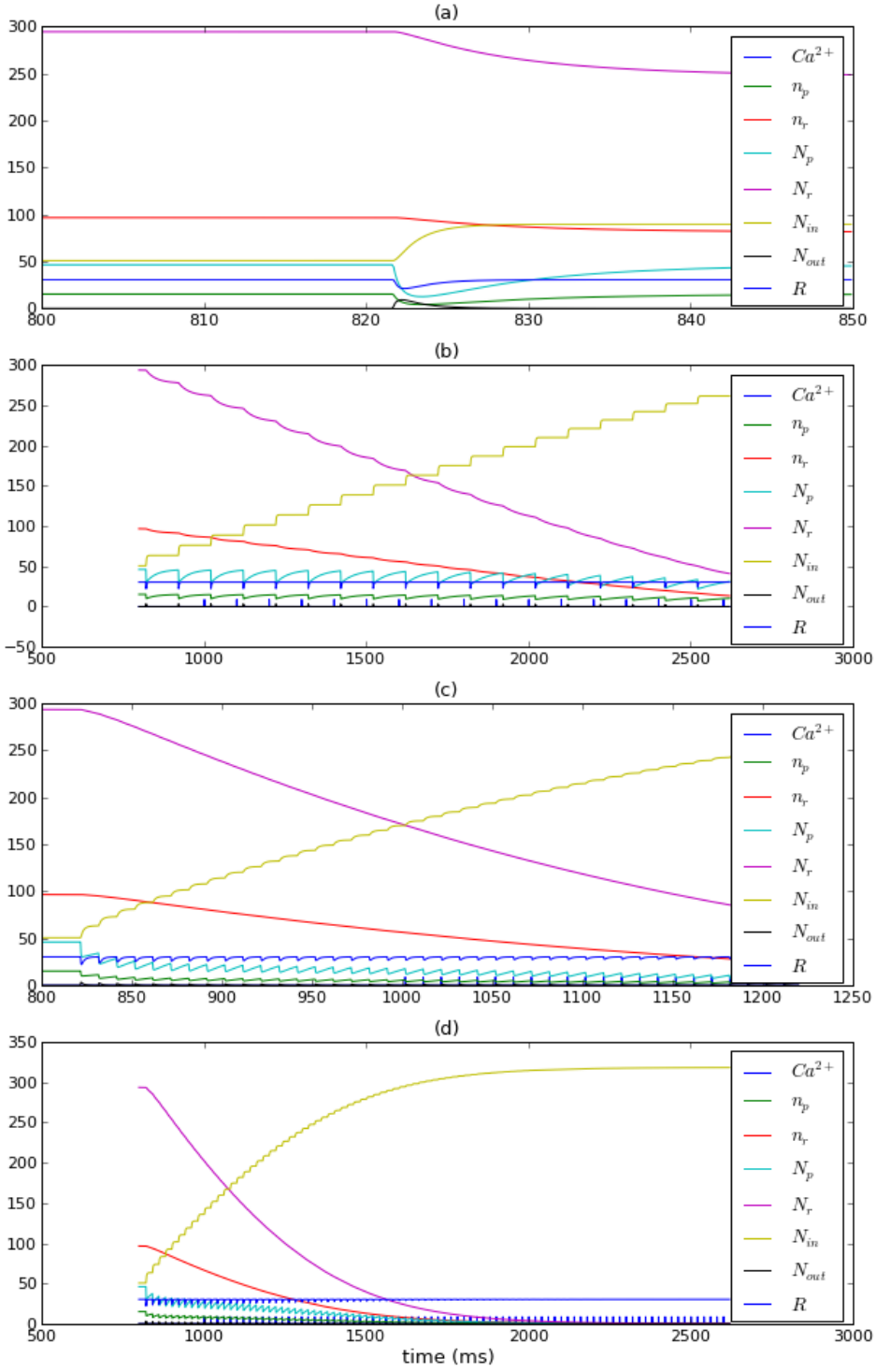

FIGURE 27. Behavior of DDE model in the second trial. (a) Behavior of the model on single spike data after optimization on that data. (b) Behavior of the model on 10 Hz data after optimization on 10 Hz and 100 Hz data. (c) Behavior of the model on 100 Hz data after optimization on 10 Hz and 100 Hz data. (d) Behavior of the model on 50 Hz data after optimization on 10 Hz and 100 Hz data.

References

[AG04] F. Aristizabal and M. I. Glavinovic. Simulation and parameter estimation of dynamics of synaptic depression. *Biological Cybernetics*, 90(1):3–18, 2004.

[AMF+13] Moritz Armbruster, Mirko Messa, Shawn M Ferguson, Pietro De Camilli, and Timothy A Ryan. Dynamin phosphorylation controls optimization of endocytosis for brief action potential bursts. *eLife*, 2, 2013.

[AT13] Pierre F. Apostolides and Laurence O. Trussell. Rapid, activity-independent turnover of vesicular transmitter content at a mixed glycine/gaba synapse. *The Journal of neuroscience: the official journal of the Society for Neuroscience*, 33(11):4768–4781, 2013.

[Bak13] Dennis Bakker. Short-term plasticity at the mntb-lso synapse: pharmacological inhibition of $GABA_A$ and $GABA_B$ receptors. Master's thesis, TU Kaiserslautern, 2013.

[BD01] William E. Boyce and Richard C. DiPrima. *Elementary Differential Equations and Boundary Value Problems*. John Wiley & Sons, Inc., seventh edition, 2001.

[BK08] Andrzej Bielecki and Piotr Kalita. Model of neurotransmitter fast transport in axon terminal of presynaptic neuron. *Journal of mathematical biology*, 56(4):559–576, 2008.

[BK12] Andrzej Bielecki and Piotr Kalita. Dynamical properties of the reaction-diffusion type model of fast synaptic transport. *J. Math. Anal. Appl.*, 393(2):329–340, 2012.

[Eva10] L.C. Evans. *Partial Differential Equations*. Graduate studies in mathematics. American Mathematical Society, second edition, 2010.

[Fis10] Alexander Fischer. Elektrophysiologische charakterisierung der entwicklungsabhängigen änderung von $GABA_A$r-, $GABA_B$r- und glyr-vermittelten strömen bei der synaptischen transmission an der mntb-lso synapse. Diploma thesis, TU Kaiserslautern, 2010.

[GKNP14] Wulfram Gerstner, Werner M. Kistler, Richard Naud, and Liam Paninski. *Neuronal Dynamics*. Cambridge University Press, 2014.

[Heu91] Harro Heuser. *Lehrbuch der Analysis Teil 2*. B. G. Teubner Stuttgart, tenth edition, 1991.

[HH52] A. L. Hodgkin and A. F. Huxley. A quantitative description of membrane current and its application to conduction and excitation in nerve. *J. Physiol.*, 117(4):500–544, 1952.

[Hun07] J. D. Hunter. Matplotlib: A 2d graphics environment. *Computing In Science & Engineering*, 9(3):90–95, 2007.

[KSJ+13] Eric R. Kandel, James H. Schwartz, Thomas M. Jessell, Steven A. Siegelbaim, and A. J. Hudspeth. *Principles of neural science*. McGraw-Hill companies, fourth edition, 2013.

[KvG09] Jun Hee Kim and Henrique von Gersdroff. Traffic jams during vesicle cycling lead to synaptic depression. *Neuron*, 63(2):143–145, 2009.

[MV11] Bernd Marx and Werner Vogt. *Dynamische Systeme*. Spektrum Akademischer Verlag, second edition, 2011.

[NS08] Erwin Neher and Takeshi Sakaba. Multiple roles of calcium ions in the regulation of neurotransmitter release. *Neuron*, 59(6):861–872, 2008.

[PAF+04] Dale Purves, George J. Augustine, David Fitzpatrick, William C. Hall, Anthony-Samuel LaMantia, James O. McNamara, and S. Mark Williams. *Neuroscience*. Sinauer Associates, Inc., third edition, 2004.

[PG07] Fernando Pérez and Brian E. Granger. IPython: a system for interactive scientific computing. *Computing in Science and Engineering*, 9(3):21–29, May 2007.

[RST11] Claire Ribrault, Ken Sekimoto, and Antoine Triller. From the stochasticity of molecular processes to the variability of synaptic transmission. *Nat Rev Neurosci*, 12(7):375–387, July 2011.

[Rud76] Walter Rudin. *Principles of mathematical analysis*. McGraw-Hill Book Co., New York, third edition, 1976. International Series in Pure and Applied Mathematics.

[Sau14] Friedrich Sauvigny. *Analysis: Grundlagen, Differentiation, Integrationstheorie, Differentialgleichungen, Variationsmethoden*. Springer Spektrum, 2014.

[SDC12] Yasunori Saheki and Pietro De Camilli. Synaptic vesicle endocytosis. *Cold Spring Harbor perspectives in biology*, 4(9), 2012.

[TZR93] LO. Trussell, S. Zhang, and IM. Raman. Desensitization of ampa receptors upon multiquantal neurotransmitter release. *Neuron*, 10:1185–1196, 1993.

[WRCP+13] Shigeki Watanabe, Benjamin R. Rost, Marcial Camacho-Pérez, M. Wayne Davis, Berit Söhl-Kielczynski, Christian Rosenmund, and Erik M. Jorgensen. Ultrafast endocytosis at mouse hippocampal synapses. *Nature*, 504(5):242–7, 2013.

[ZBLN97] Ciyou Zhu, Richard H. Byrd, Peihuang Lu, and Jorge Nocedal. Algorithm 778: L-bfgs-b: Fortran subroutines for large-scale bound-constrained optimization. *ACM Trans. Math. Softw.*, 23(4):550–560, December 1997.